UNITED STATES DEPARTMENT OF THE INTERIOR

GEOLOGICAL SURVEY

GEOTECHNICAL PROPERTIES AND FREEZE/THAW CONSOLIDATION BEHAVIOR OF SEDIMENT FROM THE BEAUFORT SEA, ALASKA

by

Homa J. Lee[1],

William J. Winters[2],

and

Edwin J. Chamberlain[3]

Open-File Report

85-612

October, 1985

[1]U.S. Geological Survey, Menlo Park, CA 94025
[2]U.S. Geological Survey, Woods Hole, MA 02543
[3]U.S. Army Cold Regions Research and Engineering Laboratory, Hanover, NH 03755

INTRODUCTION AND OBJECTIVE

Two investigations into the interaction of ice and the seafloor in the Beaufort Sea, Alaska, were made. The first (Part A) is a synthesis of publicly-obtained geotechnical information derived by testing samples from deep borings and samples of surficial sediment. This synthesis provides a previously unavailable data base on which studies of undersea permafrost, seasonal freeze/thaw cycling and ice gouging can be based.

The second investigation (Part B) is a continuation of studies by E.J. Chamberlain on the influence of freeze/thaw processes on Beaufort Sea sediment. Dense overconsolidated sediment occurs at many locations on the Beaufort shelf (Chamberlain, 1978, Reimnitz and others, 1980) and can be an advantage to offshore development. It may also present an obstacle to offshore construction. For example, irregular ice-gouged surfaces of overconsolidated sediment may exert concentrated point loads that could fracture mat foundations. Also, a continuous blanket of stiff overconsolidated silt would hinder access to deeper sands and gravels needed for artificial island construction. Chamberlain (1978) has suggested that although a number of factors may affect the consolidation properties, freeze/thaw was probably dominant in overconsolidating the sediment. One question is whether the process of freeze/thaw overconsolidation occurred only during periods of sea level lowering and subaerial exposure of parts of the Beaufort Shelf, or if it is also occurring presently during short periods of "subtle" and seasonal seafloor freezing. A second question is how do the engineering properties of Holocene sediment influenced by subtle freeze/thaw overconsolidation differ from those of heavily overconsolidated Pleistocene sediment that has been subaerially exposed? This report attempts to answer those questions and hence improve our understanding of the regional distribution of the engineering properties of sediment on the Beaufort Shelf. Isopach maps of Holocene sediment distribution (for example, Wolf and others, in preparation) could be used for estimating such regional distributions. To provide insight into these questions, freeze/thaw consolidation tests were conducted with "subtle" freezing temperatures. Results of these tests are summarized in a later section.

Additionally, the impact of freeze/thaw overconsolidation on shearing strength was studied. With common forms of overconsolidation, well defined relationships between overconsolidation ratio and shearing strength can be defined (Ladd and Foott, 1974). Previous strength studies have not been conducted with freeze/thaw overconsolidation samples and the ordinary relations may not hold. An example of the kind of unexpected behavior that may occur with freeze/thaw overconsolidation is provided by permeability measurements. Typically, overconsolidation leads to a reduction in permeability. However, freeze/thaw overconsolidation actually increases the permeability because of the development of vertical shrinkage cracks (Chamberlain and Gow, 1979). Such anomalous behavior resulting from significant structural changes may occur with shearing strength as well.

DATA INCLUDED

The data synthesis is based on four series of laboratory tests on deep boring or surficial samples:

1. Eight deep (to 65 m subbottom) borings conducted from the ice surface in the spring of 1976 and 1977 by the U.S. Army Cold Regions Research and Engineering Laboratory (CRREL). These borings were in the Prudhoe Bay area and have been given the designation "PB". All results were previously presented by Sellman and Chamberlain (1980).

2. Twenty deep (to 100 m subbottom) borings conducted from the ice surface in 1979 by Harding-Lawson Associates under contract to the Conservation Division, U.S. Geological Survey (USGS). The borings were obtained from a 100-km long stretch of coast between the Canning River and a point somewhat west of Prudhoe Bay. The borings are designated "HLA" after the contractor conducting the boring and laboratory test operations.

3. Seventeen surface samples and nineteen diver operated in-place strength tests conducted by the USGS in 1976 and before. These test results were presented previously by Reimnitz and others (1977).

4. Eighteen block samples of stiff overconsolidated silty clay obtained by the USGS in 1983. These were tested for strength and consolidation properties in 1984 at the USGS geotechnical laboratory located in Palo Alto, CA.

The new investigations of freeze/thaw overconsolidation behavior were conducted using three bulk grab samples obtained by the USGS in Prudhoe Bay in 1983. The "subtle" freeze/thaw consolidation behavior of these samples was determined by E.J. Chamberlain at CRREL in 1984. A study of the impact of freeze/thaw processes on strength behavior was conducted by the USGS in 1984 with considerable assistance from E.J. Chamberlain.

PART A:

METHODS-GEOTECHNICAL PROPERTIES SYNTHESIS

Sampling. The "PB" and "HLA" borings were conducted using conventional drilling equipment that was mounted on sleds. Samples of silts and clays that were not ice bonded were obtained with pushed Shelby tubes and are probably of fairly high quality. The early USGS surface samples (Reimnitz and others, 1977) were typically taken with a Van Veen grab sampler. These samples are probably of relatively poor quality. The 1983 USGS seafloor surface samples were taken with either a pipe dredge or a Van Veen sampler or manually cut from exposed seafloor in the swash zone. Because the sediment sampled in this program was stiff silty clay, the sediment typically broke loose as a large block sample. As a result the quality of most of these samples is fairly good.

In-place tests. The diver-operated in-place vane shear strength tests were conducted using a Moore-Dill hand held device (Dill and Moore, 1965). The bottom of the 2 cm by 2 cm vane was inserted 2 to 15 cm into the seafloor and rotated at a constant steady rate. The rotation rate was controlled so that failure occurred in about 2 minutes.

Laboratory testing. Water content and Atterberg limit determinations were obtained using ASTM standards. Rapid determinations of the vane shearing strength were obtained on shipboard using the Moore-Dill hand held device for the Reimnitz and others (1977) samples and with the hand-held Torvane (Hunt, 1984) for the 1983 block samples.

In the "HLA" and "PB" studies consolidation testing was conducted using a standard oedometer and ASTM procedures. In the USGS testing of 1983 block samples consolidation testing was conducted using the constant rate of strain method (Wissa and others, 1971) in a back-pressured triaxial cell.

The critical consolidation property obtained was the maximum past stress, σ'_{ym}. This parameter represents the equivalent maximum vertical stress that the sample has experienced and was obtained from the results of a consolidation test using the Casagrande (1936) construction. For samples that have undergone freeze/thaw overconsolidation, the maximum past stress obtained in this way may not represent the actual largest stress the sample has ever experienced. Rather, it indicates that the sample is behaving in much the same way as it would if it had experienced such a maximum past stress. Interpretation of the maximum past stress was somewhat difficult for most samples that appeared to be heavily overconsolidated. The Casagrande construction requires a plot of void ratio versus the log of vertical effective stress that proceeds from a nearly horizontal line through a sharp transition into a second linear zone. With many of these silts and clays, the second linear section did not exist. Rather, the void ratio-effective stress plots continued to curve downward throughout the test. Such behavior may result from disturbance, the silty nature of the sediment, or the freeze/thaw process itself.

Strength properties were measured using a variety of techniques. The strength of "PB" samples was obtained by triaxial testing with a consolidation stress equal to the estimated in-place overburden stress. Because final shear strength testing was conducted with no pore water flow, these tests are considered to be consolidated-undrained (CU). This type of test commonly yields a shear strength that is somewhat higher that it would have been in-place (Ladd and Lambe, 1964). The 1983 block samples were tested using the unconfined compression test. In such a test a cylindrical sample is loaded fairly rapidly without confinement or additional laboratory consolidation until a peak shearing stress is reached. Such a shearing strength is typically considered to be lower than the in-place strength. Some "HLA" samples were subjected to CU triaxial tests with consolidation stresses equal to the overburden stress. Others were tested using the unconsolidated-undrained (UU) triaxial technique. In a UU test a cylindrical sample is encased in a membrane and sheared in a pressurized triaxial chamber. Pore water drainage is never allowed to occur but the sample may densify somewhat in the pressure chamber if it is not fully saturated initially. The shearing strength measured by axially loading such a sample is often near the in place

shearing strength (Lambe and Whitman, 1969). However, such a correspondance is a result of compensating errors and cannot be relied upon.

An indirect method that often provides good estimates of in-place sediment strength is the normalized soil parameter (NSP) approach (Ladd and others, 1977). According to this approach, the undrained shear stength, s_u, of many types of sediment is uniquely determined by the overconsolidation ratio (OCR), the in-place overburden effective stress, σ'_v, and two soil constants, S and m. The governing equation is:

$$s_u = S\ \sigma'_v\ (OCR)^m \quad (1)$$

where $OCR = \sigma'_{vm}/\sigma'_v$

Although no measurements were made for these samples, the value for the exponent m is typically about 0.8 (Ladd and others, 1977). The ratio of undrained strength to consolidation stress for normal consolidation, S, can vary between 0.2 and 1.0 or more depending upon type of strength test, plasticity index, and sediment type (Lambe and Whitman, 1969, p. 452, Schwab and Lee, 1983, Andresen and others, 1979). A triaxial compression test performed to measure S on one of the 1983 block samples yielded a value of 0.5. However, for the plasticity index range encountered in the Beaufort Sea silts and silty clays (10% to 20%), Andresen and others (1979) reported S equal to 0.3. A representative value of S therefore would range between 0.3 and 0.5. We selected an intermediate value of 0.4 to insert into Eq. 1 to estimate shear strength wherever a value of σ'_{vm} was obtained from a consolidation test.

RESULTS-GEOTECHNICAL PROPERTIES SYNTHESIS

Geotechnical properties are given in the following tables and figures:

SURFICIAL SAMPLES:

DEEP BORINGS:

In the borings the typical profile is a 3 to 35-m-thick layer of fine grained silt and clay overlying coarse sand and gravel. In some borings a 0.5

to 4 m thick layer of sand is found at the surface. The sediment tested for geotechnical behavior was almost exclusively from within the upper layer of fine-grained silt and clay (Figure 36). Results are presented for a common depth so that variations in properties with subbottom depth could be excluded (Figs. 37 and 38 and Table 5). A depth of 4 m was selected because it was shallow enough that the sediment was typically silt and clay and yet deep enough that certain surface effects such as modern ice gouging would not have influenced the properties. Maximum past stress and strength at 4 m were determined from curves following the trends of data in Figures 8 through 34. These results are extrapolations for the few holes in the southwest part of the area in which the upper fine grained layer is only 3 m thick. For the strength data some consideration was given to the type of test used to obtain the shear strength. That is, UU and NSP data are typically close to the in-place value while CU data are often too high. Also, only NSP strengths based on consolidation tests rated as "good" and "medium" (Table 4) were considered. Those based on "poor" tests were excluded.

DISCUSSION -- GEOTECHNICAL PROPERTIES SYNTHESIS

The variation in surficial sediment properties as shown in Figures 3 and 4 (water content), Fig. 5 (shear strength) and Fig. 6 (maximum past stress) is almost random. Such a complex pattern of properties likely reflects a complex geologic history that includes intense ice gouging, infilling of depressions with reworked sediment, possible freeze/thaw cycles, and exposure of older, compact sediment by erosion. Although the processes cannot be separated, at least the typical ranges of these properties can be specified. For example, surface shearing strength seldom exceeds 50 kPa and is seldom lower than 2 kPa. Water content, corrected for salt, ranges between about 15% and 60% of dry weight, and maximum past stress varies between 20 kPa and 650 kPa with one anomalous value of 2,000 kPa.

In relating the geotechnical properties to each other, Table 2 shows the unconfined compression test and Torvane readings to be roughly equal to each other for about two-thirds of the block samples (UC value typically about 15% higher). For the remaining one-third, the values differ by up to a factor of 3. In these cases different sediment types within the same block may have been tested or greatly differing amounts of disturbance introduced in preparing for each test. In general, either type of test appears suitable for a rapid, approximate measure of undrained shearing strength.

The variation of the log of shear strength and log of maximum past stress with water content for the block samples exhibits some scatter, but a trend is indicated by linear regressions (Fig. 40a). The lines are sub-parallel, with the ratio of strength to maximum past stress at the same water content ranging between 0.02 and 0.45 (average of 0.15). The ratio of strength to consolidation stress for normal consolidation, S, is between 0.3 and 0.5 as discussed previously. Therefore, on the average, over half the sediment strength has been lost in removing the maximum past stress and exposing this sediment to the seafloor.

Properties measured on the deep boring samples vary somewhat more consistently. Perhaps most consistent is the variation in the thickness of the upper fine grained layer (Fig. 36). A steady thickening with distance offshore is readily apparent and is consistent with the existence of a series

of offshore thickening sediment wedges reported by Dinter (in publication). A slight thickening to the east may exist as well.

Undrained shear strength at 4 m varies between 26 and 200 kPa with perhaps some increase with distance offshore. These strengths are greater by a factor of 4 to 10 than the strengths of surficial samples. The maximum past stress at 4 m varies between 30 and 400 kPa with some tendency toward higher values at greater distances offshore. These values are comparable to or slightly lower than those for the surficial sediment.

The variation of the log of shear strength and log of maximum past stress with water content at the 4 m level for the boring samples is shown in Fig. 40b. Again, results are scattered but sub-parallel lines roughly fitting the data could be drawn. The ratio of strength to maximum past stress at the same water content varies between 0.17 and 0.90 with an average of 0.37. On the average, therefore, there is little loss of strength from an assumed normally consolidated ratio of 0.3 to 0.5.

Figure 41 shows linear regressions of strength and maximum past stress versus water content for block samples and for the 4 m level in borings. Given the scatter in the original data, the lines for maximum past stress are very similar. The difference between the strength values is significant, however, and amounts to a factor of more than 2. Because the maximum past stresses for the surface samples cover the same range and follow the same water content correlation as do the results for the deeper boring samples, we suggest that a common intensity of environmental factors was responsible for causing the observed maximum past stresses. Such factors could include a previous existence of overburden or overconsolidation by freeze/thaw cycling. The much lower surface strength suggests intense mechanical disturbance of the overconsolidated sediment at the seafloor. Ice gouging is a likely principal agent in creating this disturbance.

Chamberlain (1978) suggested that freeze/thaw is the dominant factor in overconsolidating the sediment. Our geotechnical synthesis can provide insight into whether the freeze/thaw process of overconsolidation was only significant during periods of sea level lowering or if it is active today during shallow seasonal freezing of the seafloor. In the first case, complete freezing of the seafloor would occur during subaerial exposure. Such severe freezing, followed by thawing during a sea level rise, would likely have a maximum effect on the consolidation properties. Chamberlain (1981) has shown that severe freeze/thaw cycling ultimately reduces the water content of sediment to its plastic limit. Therefore, high levels of overconsolidation and a water content near the plastic limit are probably indicative of a sediment that has been subaerially exposed and frozen severely. An estimated pre-Holocene age for the sediment would also support subaerial exposure. However, such age determinations are approximate owing to extensive reworking of sediment by ice gouging.

Shallow freezing of the modern seafloor could influence the sediment in one of two ways. First, if this subtle freeze/thaw process began after a Holocene sediment profile had developed, we might expect a crust of moderately overconsolidated sediment to overlie normally consolidated sediment. Crusts do exist on the Beaufort shelf (Ladd and others, 1985, Boring PB-8, Fig 34) but are far from universal. For example, the previous comparison of boring

and block sediment properties (Fig. 41) showed nearly identical levels of overconsolidation at the seafloor surface as at 4m subbottom depth.

Second, seasonal freeze/thaw processes could occur more or less continuously as the sediment column was being deposited. In this case, we might expect a fairly uniform level of overconsolidation to develop with subbottom depth. Because the freeze/thaw process would be subtle, however, the water content would probably not be lowered as far as the plastic limit.

Table 5 provides information regarding the extent to which seasonal freeze/thaw processes are significant in the area investigated. One column lists an estimate of the thickness of the Holocene sediment determined by P.A. Smith of the USGS (Smith, 1985, and personal communication, 1985). Another column describes the relative proximity of water content at 4 m subbottom depth to the plastic limit, liquid limit, or midrange between the two limits. Of the borings for which the relative water content is available, 13 out of 24 of the ages at 4 m are older than Holocene. Of these 13 borings, 11 have water contents near the plastic limit. Therefore, about half (54%) of the sediment at 4 m is older than Holocene and has been subaerially exposed and frozen. In this older sediment, most water contents have been reduced to the plastic limit, as would be expected from severe freeze/thaw cycling.

Of the 11 borings that contain Holocene sediment to 4 m or greater, only 1 has a water content as low as the plastic limit at 4 m. That boring (HLA-4) has only 4 m of Holocene sediment and may be anomalous. Of the remaining 8 borings, 5 have water contents near the liquid limit at 4 m and are probably normally consolidated. Five borings have water contents midrange between the plastic and liquid limits and are moderately overconsolidated. These 5 borings, representing 21% of the available data, may indeed show the influence of seasonal freeze/thaw cycling of the modern seafloor.

SUMMARY OF PART A

The regional variation of physical properties of surficial sediment shows an almost random pattern within which only rough ranges of values can be specified. An extremely dynamic environment, coupled with a complex geologic history, is likely the cause of such a great and chaotic variation.

In comparing fairly deep (4 m) and surficial sediment, a common range of maximum past stress is apparent. A common intensity of environmental factors causing the maximum past stress is probably the cause of this correspondence. However, the range of strength for the surface sediment is significantly lower than that for the deeper sediment. Intense mechanical disturbance resulting from ice gouging probably reduced the strength of the surface sediment.

About 50% of the sediment at 4 m was probably overconsolidated when it was subaerially exposed and frozen and thawed during the Pleistocene. Roughly 30% is Holocene in age and normally consolidated. The remaining 20% is apparently Holocene in age and moderately overconsolidated. This latter 20% of the sediment at 4 m could well have been overconsolidated by Holocene, subaqueous freeze/thaw processes.

PART B:

STUDIES OF FREEZE/THAW OVERCONSOLIDATION--"SUBTLE" FREEZING

Background. The term "subtle freezing in saline soil" implies nucleation and ice crystal growth in seawater sediment at temperatures within 1°C below the bulk freezing point of the pore water. This study evolved from earlier observations of overconsolidated sediment in the Beaufort Sea (Chamberlain and others, 1978, and Sellman and Chamberlain, 1980). The phenomenon of overconsolidation by freezing and thawing has been observed by numerous researchers studying the consolidation properties of soils. Generally, the overconsolidation has been attributed to the negative pore water pressures generated in the region of freezing. This causes a flow of water from the adjacent unfrozen zone to feed the growing ice lenses and results in an increase in the effective stress on the adjacent unfrozen material. As a result, the soil particles are reoriented and consolidated into a more compact structure. As the water content in the unfrozen region adjacent to the zone of ice segregation is depleted, the hydraulic conductivity falls. At some critical water content, the unfrozen zone can no longer provide water at the rate required by the driving suction forces. The desiccated zone is then quickly engulfed by in-place freezing and a new zone of ice segregation is established on the opposite side of the desiccated zone. The process continues as long as the net heat flow outward is positive and water is available for freezing. The resulting structure in cross-section may appear banded as in the example shown in Figure 42A. Vertical, as well as horizontal, ice features can result if the sediment is predominantly a plastic clay. The vertical features visible in the horizontal cross-section of Figures 42B and 42C are ice filled shrinkage cracks that resulted from the desiccation of the unfrozen material during the ice segregation process. The clay bounded by the ice features is overconsolidated.

Figure 43 (taken from an earlier study of Beaufort Sea sediment, Chamberlain, 1978) illustrates the overconsolidation process in terms of effective stress, the difference between total applied stress, σ, and pore water pressure, u. A clay slurry is normally consolidated (point a) and frozen unidirectionally with water free to flow to and from the unfrozen part. The large negative pore water pressures that develop in the freezing zone cause the effective stress in the adjacent unfrozen material to increase and the void ratio to decrease. In terms of total applied stress and bulk sediment properties, the sediment will have heaved to point b. In terms of effective stress and properties of discrete "bands" of clay, the sediment will have consolidated to point b' along the virgin consolidation curve. Upon thawing, the discrete "bands" of clay may swell and the final condition upon equilibrium of pore water tension will be at point c. In geotechnical engineering terminology, the sediment is overconsolidated. The density is greater than the density that would result solely from the existing applied total stress.

Previously published (Chamberlain, 1978) results of laboratory freeze/thaw consolidation tests on a sediment from Prudhoe Bay show that freezing and thawing of a sediment slurry can produce overconsolidation levels comparable to those encountered with natural heavily overconsolidated sediment (Fig. 44). However, these tests were conducted with large temperature differentials that would not be considered "subtle."

Causes of Beaufort Sea Sediment Freezing. Earlier studies of subsea permafrost concluded that freezing and thawing was a major mechanism in causing the overconsolidation of this sediment. For the older sediment that was exposed to the cold arctic air and frozen during the sea level lowering of the Pleistocene epoch, this explanation appears to be justified. However, to determine whether the younger Holocene sediment would become overconsolidated by this mechanism, a further evaluation of freezing and thawing processes was necessary.

In water less than two meters deep, sea floor sediment can be coupled to cold temperatures by the downward growth of the winter ice sheet. This commonly occurs in the Beaufort Sea (Sellmann, personal communication), and as a result, the 2-m water depth marks the seaward limit of shallow ice-bonded permafrost. In deeper water, there are two other possible methods of coupling the seabed sediment to the cold arctic air mass and, as a result, inducing freezing; grounding of ice keels and transgression of barrier islands.

The probability of the first occurring for sufficiently long periods of time is uncertain because of the transient nature of ice keel groundings. However, there is evidence of freezing of seabed sediment beneath barrier islands. In fact, the highly overconsolidated sediment immediately seaward of Reindeer Island appears to be linked to the recent passage of this barrier island over this area (Sellmann and Chamberlain, 1980).

As there are numerous other barrier islands along the coast of the Beaufort Sea that are actively transgressing seabed sediment, this process could explain the frequent occurrence of very highly overconsolidated sediment.

However, none of these mechanisms for inducing freezing and thawing of seabed sediment appears to be viable explanations for the widespread occurrence of more lightly overconsolidated Holocene sedients in the Beaufort Sea.

Subtle Freezing and Thawing Observations. Sellmann and Chamberlain (1980) concluded that there is one other mechanism for seabed sediment freezing. That is the subtle freezing of sediment resulting from seasonal variations in seawater salinity and temperature. This explanation focuses on observations of temperature and salinity data in the region immediately above and below the top of the sediment. During an earlier testing program, CRREL personnel very carefully sampled this region for temperature and salinity. Freezing point calculations were made from the salinity data for pore water extracted from sediment and for seawater taken from the water column immediately above the sediment. When the freezing point data were plotted versus the observed temperature data, the results indicated that the temperatures in the top of the sediment were below the pore water freezing points for all seven of the sites investigated (Fig. 45). The difference between the calculated freezing points and the observed tempertures ranged from approximately one degree Celsius at site PB-1 to one tenth of a degree Celsius at site PB-7. The depth of sediment affected ranged from approximtely 2 m at site PB-8 to a few centimeters at site PB-7. This data supports the possibility that seasonal freezing of seabed sediment occurs. However, no ice was observed in the core samples taken from the apparently seasonally frozen regions, and thus, there was no direct evidence of freezing in the cores obtained.

There have been, however, observations of ice in and on seabed sediment covered by water and not coupled to cold temperatures by either ice or soil material. For example, Reimnitz (personal communication, 1983) reported feeling ice crystals break in his hand in soft sediment during a dive near the west dock in Prudhoe Bay. He also reported seeing "anchor ice" on top of sediment further offshore.

Subtle Freezing and Thawing Processes. Seasonal freezing in water depths greater than 2 m can be explained as follows: Pore water in soils, and particularly in saline soils, does not freeze completely upon nucleation. Water begins to freeze in regions of lowest salinity and highest free energy, generally in the center of pores within the soil structure. It progressively freezes as the temperature falls. As freezing progresses, brine concentrations increase in the unfrozen water films separating the ice from the mineral solids, thus, further reducing the freezing temperature of the remaining unfrozen water. For the one degree range of freezing temperatures observed for the data illustrated in Figure 45, ice bonding, thus, might not be strong and ice also might not be visible. Furthermore, any ice present would probably melt in the period of time required for core retrieval and examination.

The temperature of the seawater immediately above the sediment can be lower than the freezing point of the pore water in the sediment because of the brine exclusion process that occurs during the freezing of the winter ice sheet. During the winter as the ice cover grows, cold brines are released to the water column below. The colder saline water sinks to the seafloor. This results in a convective mixing of the seawater and cooling of the seabed during the period of ice formation. Current flow and tidal action also cause a mixing of seawater to make it more homogeneous. In all cases observed in the CRREL program, which was not conducted during the maximum freeze period, the water column was isothermal and the temperature within 0.15°C of the freezing point of the water.

The salinity of the pore water in the sediment cannot change as rapidly by circulation and convection as it does in the water column because of the very small pore water paths. Diffusion controls whether pore water salinity gains equilibrium with the seawater salinity. The salinity in the pore water, therefore, lags the salinity in the seawater, and thus, the freezing point of the pore water can be above the temperature of the seawater during the period of ice sheet growth. By using the heat sink of the overlying sea water, ice formation in seabed sediment can occur.

Laboratory Subtle Freezing Tests. To study if very subtle freezing affects the consolidation characteristics of saline sediment, laboratory freezing tests were conducted on sediment obtained with a grab sampler from Prudhoe Bay, Alaska. Two types of sediment (Table 6) were evaluated, one a silty sand to sandy silt (Sediment 3) and the other a fine sand (Sediment 2). These sediments were mixed with sea water to produce slurries and were consolidated and frozen in the apparatus shown in Figure 46.

The apparatus contains a consolidation chamber 6.25 cm in diameter by 20 cm in height. Drainage is accomplished through stainless steel porous plates located in the base and piston of the device. A thermoelectric cooling device in the base allowed bottom up freezing. An ethylene glycol solution

circulated from a temperture controlled refrigerated bath provided the reference temperature for the thermoelectric device.

Two types of tests were conducted on each of the two sediment types. The first was a normal consolidation test with load doubling increments. This test was chosen to determine the "normal" consolidation curve under increasing loads.

The second test, performed on aliquot subsamples, included both consolidation and freeze/thaw cycling. The samples were first consolidated under a very light stress (2.63 kPa) in order to simulate natural conditions in very shallow sediment. These were then subjected to several freeze/thaw cycles. The samples were frozen from the bottom up in order to minimize side friction problems. In this way, the unfrozen material heaved upward during freezing. The light (2.63 kPa) stress was reapplied after each cycle, but the piston was raised before each freeze so that no surcharge was applied during freezing. The temperature drop across the sample was adjusted to be approxi-mately 1°C and the minimum temperature allowed was no greater than 1°C below the freezing point of the pore water. The freezing point of the pore water was determined by suspending a known amount of the test material in a known amount of distilled water and determining the electrical conductance of the dilute solution remaining after 24 hours of settlement. The conductance of the pore water solution was then back calculated and the salinity and freezing point determined using the method reported by Bennett (1976) and G.F.N. Cox (personal communication).

With this freezing method, the material was subjected to the subtle freezing that the Beaufort Sea sediment appears to be undergoing. The principal difference between laboratory and field freezing conditions was an accelerated rate of freeze/thaw cycling imposed in the laboratory.

Results of Subtle Freezing Tests. Figure 47 shows the results for Sediment 2. The upper half of the figure shows the freeze/thaw cycling and the lower half the consolidation. It can be seen that each freeze/thaw cycle causes a progressive settlement of the sample through the 4th cycle. Figure 48 shows that the reduction in water content is non-linearly related to the number of freeze/thaw cycles.

Figure 49 compares the freeze/thaw consolidation data with the "normal" consolidation curve. Because of subtle differences in the physical properties of the two aliquot subsamples of Sediment 2, the slurries did not consolidate to the same water content upon the application of the initial load of 2.63 kPa. The subsample which was normally consolidated equilibrated at about 36% water content, but the freeze/thaw-consolidated sample equilibrated at about 42%. For purposes of comparison, then, a curve (b) originating at 42% water content and 2.63 kPa was drawn parallel to the normally consolidated curve (a). It can be seen that freeze/thaw cycling progressively caused a reduction in water content and that this reduction in water content was the equivalent of applying an external stress of approximtely 230 kPa after 4 cycles of freeze/thaw cycling. Had the freeze/thaw cycling continued, there is little doubt that the consolidation would have continued to much higher equivalent external stresses. Additional tests with a greater number of freeze/thaw cycles are needed to be certain of the trend. However, it is known that the

practical limit of freeze/thaw consolidation in freshwater clay sediment is the plastic limit water content (Chamberlain, 1981).

Figure 50 shows the results for the more silty Sediment 3. Again, it can be seen that consolidation progresses with freeze/thaw cycling. Figure 51 shows the results for freeze/thaw cycling on Sediment 3 superimposed on the plot for a normal consolidation (a). As for Sediment 2, a curve (b) has been drawn parallel to the "normal" consolidation curve passing through the point corresponding to 0 freeze/thaw cycles and 2.63 kPa. It can be seen that application of 5 freeze/thaw cycles was equivalent to applying an external load of 12 kPa. As was observed for sediment 2, an insufficient number of freeze/thaw cycles was applied to determine the lower limit of consolidation.

Discussion of Subtle Freezing Tests. The laboratory freezing tests show almost conclusively that subtle freezing can cause the densification of saline sediment. However, the limits of densification were not observed. Additional tests need to be conducted to determine the limits. Rate of freezing and temperature gradient effects also need to be studied as both will vary under natural conditions according to water depth and sediment temperatures. Furthermore, there needs to be an evaluation of long-term consolidation effects in subtly frozen sediment where, because of only partial freezing, water remains partially mobile and flow is not shut off by a continuous ice-mineral barrier.

INFLUENCE OF FREEZE/THAW ON SEDIMENT STRENGTH

Both "subtle" and more pronounced freeze/thaw cycling were shown to induce a state of overconsolidation in Beaufort Sea sediment. With conventional overconsolidation processes, i.e. removal of overburden or even desiccation, there is often a predictable buildup in strength related to the degree of overconsolidation. Therefore, in order to develop a model of strength development in relation to geologic processes, in this case freeze/thaw cycling of the seafloor, we conducted an experiment to determine whether a predictable increase would result from this unconventional mechanism of overconsolidation.

This experiment involved comparing the triaxial (CU) shearing strengths of Prudhoe Bay sediment. Three types of sediment were tested: Sediment 1 (silty sand), Sediment 2 (fine sand), and Sediment 3 (silty sand to sandy silt, Table 6). All samples were taken with a grab sampler in 1983 and are the same as the samples used in the "subtle" freeze/thaw experiment discussed previously. From each of the three bulk sediment samples, two sets of two to four samples each were prepared for triaxial testing. Each set was treated exactly the same way except one set was frozen and the other was not. The frozen samples were frozen under controlled conditions and then thawed under a consolidation stress. Both sets were ultimately consolidated under the same stress and sheared without drainage. The goal of the testing was to obtain the ratio of strengths of samples with one freeze/thaw cycle to those without.

The seventeen frozen samples were prepared at CRREL in a split sleeve gang mold cylindrical openings (height of 88.9 mm, diameter of 35.6 mm). Each sample consisted of six layers and was emplaced through standing water and rodded to expel air bubbles. The samples were frozen from the top down at a rate of 25 mm/day. Upon completion of freezing, the samples were removed from the molds, placed in membranes and sealed to prevent sublimation. They were

stored at -7°C until they were shipped to the USGS laboratory in Palo Alto, California. A special shipping method was used so that the samples would not thaw during shipment nor would they be super chilled by the dry ice normally used in such shipments. By trial and error, it was found that, if the samples were isolated by a one inch thickness of polystyrene insulation from the dry ice, the temperature within the sample box would range between -2 and -10°C during a 72 hour shipping period. The samples were received in Palo Alto, California, in a frozen state.

The unfrozen samples were prepared at the USGS in a membrane supported by a split cylindrical mold. The size and placement techniques were identical to those used at CRREL with the frozen samples. The unfrozen control specimens were consolidated one-dimensionally in the split molds under an axial stress of about 40 kPa. The membrane-encased frozen samples were placed in split molds and thawed one-dimensionally under an axial stress of 40 kPa.

After one-dimensional consolidation, both types of specimens were removed from their molds and consolidated isotropically in a triaxial cell to 40 kPa. Both types of specimens were then sheared without drainage to obtain an undrained shearing strength.

The results of these triaxial tests are given in Table 7. At least two and as many as four tests were run on each sediment type/treatment combination. The reproducibility for tests run on similarly prepared samples is excellent. The ratio of strength for samples having undergone freeze/thaw to that of those that have not appears to depend on sediment type. For the more sandy Sediments 1 and 2 the ratio is 0.35 to 0.40 indicating that the samples that were not frozen are much stronger. For the more silty Sediment 3 the ratio is 2.74 indicating much stronger sediment after freeze/thaw.

The strength differences correlate with differences in the water content after consolidation and during shear. For the two sandier Sediments 1 and 2, the water contents after consolidation of freeze/thaw specimens are higher than those of control specimens. For the more silty Sediment 3, the opposite is true. The data follow a consistent trend with higher strengths corresponding to lower water contents. The differences in water content may be related to changes in sediment type and response to freeze/thaw cycling. Chamberlain and Blouin (1978) found that sandy sediment often expands during freeze/thaw cycling and reconsolidation although more silty or clayey sediment commonly densifies. Our water contents after consolidation, therefore, support their findings.

Our water contents before consolidation do not correlate as well with sediment type. For Sediments 1 and 2 the trend is basically the same as for the water content after consolidation. The sandy sediment is looser after a freeze/thaw cycle while the silty sediment is denser. For Sediment 1, however, the water content before consolidation is the same for both freeze/thaw and control samples. The reason for the greater subsequent decrease in water content for the control samples is not clear.

In summary, the freeze/thaw process appears to have a pronounced influence on sediment strength. Our tests show up to a factor of 3 difference between the strengths of samples that have been frozen and thawed and those that have not. Sandy sediment appears to be weakened by freeze/thaw cycling

while silty sediment appears strengthened. The results are not totally conclusive, however, given ambiguous changes in water content for one of our sediment types (Sediment 1).

ACKNOWLEDGEMENTS

We would like to thank Erk Reimnitz, Scott Graves, Ed Kempema, and Peter Barnes for obtaining samples in the Beaufort Sea in 1983. We would also like to thank Rob Kayen and Dick Roberts for laboratory testing support at the USGS and CRREL, respectively.

This report was prepared under Agreement No. DE-A121-AC052005 for the Morgantown Energy Technology Center, U.S. Department of Energy.

REFERENCES

Andresen, A., Berre, T., Kleven, A., and Lune, T., 1979, Procedures used to obtain soil parameters for foundation engineering in the North Sea, Marine Geotechnology, v. 3, no. 3, p. 201-266.

Bennett, A.S., 1976, Conversion of in situ measurements of conductivity to salinity, Deep-Sea Research, v. 23, no. 2, p. 157-165.

Casagrande, A., 1936, The determination of the pre-consolidation load and its practical significance, Proceedings, First International Conference on Soil Mechanics and Foundation Engineering, Cambridge, Mass., p.60-64.

Chamberlain, E.J., 1978, Overconsolidated sediments in the Beaufort Sea, The Northern Engineer, v. 10, n. 3, p. 24-29.

Chamberlain, E.J., 1981, Overconsolidation effects of ground freezing, Engineering Geology, v. 18, p. 97-110.

Chamberlain, E.J. and Blouin, S.E., 1978, Densification by freezing and thawing of fine material dredged from waterways, Proceedings, Third International Conference on Permafrost, v. 1, p. 623-628.

Chamberlain, E.J. and Gow, A.J., 1979, Effect of freezing and thawing on the permeability and structure of soils, Engineering Geology, v. 13, p. 73-92.

Chamberlain, E.J., Sellmann, P.V., Blouin, S.E., Hopkins, D.M., and Lewellen, R.I., 1978, Engineering problems of subsea permafrost in the Prudhoe Bay region of the Beaufort Sea, Proceedings, Third International Conference on Permafrost, v. 1, p. 629-635.

Dinter, D.A., in publication, Quaternary sedimentation of the Alaskan Beaufort shelf: influence of regional tectonics, fluctuating sea levels, and glacial sediment sources, Tectonophysics.

Dill, R.F., and Moore, D.G., 1965, A diver-held vane-shear apparatus, Marine Geology, v. 3, p. 323-327.

Hunt, R.E., 1984, Geotechnical Engineering Investigation Manual, McGraw-Hill Book Co., New York, 983 p.

Ladd, C.C. and Foott, R., 1974, New design procedure for stability of soft clays, Journal of the Geotechnical Engineering Division, ASCE, July, p. 763-786.

Ladd, C.C., Foott, R., Ishihara, K., Schlosser, F., and Poulos, H.G., 1977, Stress-deformation and strength characteristics, Proceedings, 9th International Conference on Soil Mechanics and Foundation Engineering, v. 2, p. 421-494.

Ladd, C.C. and Lambe, C.C., 1964, The strength of "undisturbed" clay determined from undrained tests, Laboratory Shear Testing of Soils, American Society for Testing and Materials, Special Technical Publication 361, p. 342-372.

Ladd, C.C., Weaver, J.S., Germaine, J.T., and Sauls, D.P., 1985, Strength-deformation properties of Arctic silt, Proceedings, Civil Engineering in the Arctic Offshore, American Society of Civil Engineers, San Francisco, p. 820-829.

Lambe, T.W. and Whitman, R.V., 1969, Soil Mechanics, Wiley, New York, 553 p.

Reimnitz, E., Kempema, E., Ross, R., and Minkler, P., 1980, Overconsolidated surficial deposits on the Beaufort Sea shelf, U.S. Geological Survey, Open File Report No. 80-2010, 37 p.

Reimnitz, E., Maurer, D., Barnes, P., and Toimil, L., 1977, Some physical properties of shelf surface sediments, Beaufort Sea, Alaska, U.S. Geological Survey, Open File Report No. 77-416.

Schwab, W.C. and Lee, H.J., 1983, Geotechnical analyses of submarine landslides in glacial marine sediment, northeast Gulf of Alaska, in Glacial-Marine Sedimentation, Molnia, B.F., ed., Plenum Publishing, p. 145-184.

Sellmann, P.V. and Chamberlain, E.J., 1980, Permafrost beneath the Beaufort Sea: Near Prudhoe Bay, Alaska, Jour. Energy Resources Technology, v. 102, p. 35-48.

Smith, P.A., 1985, Late Quaternary geology of the Beaufort Sea inner shelf near Prudhoe Bay, in Bartsch-Winkler, Susan and Reed, K.M., 1985, The United States Geological Survey in Alaska: accomplishments during 1983, U.S. Geological Survey Circular 945, p. 100-103.

Wissa, A.E., Christian, J.T., Davis, E.H., and Heiberg, S., 1971, Consolidation at constant rate of strain, Journal of the Soil Mechanics and Foundation Engineering Division, ASCE, October, p. 1393-1413.

Wolf, S.C., Reimnitz, Erk, and Barnes, P.W., in preparation, Pleistocene and Holocene seismic stratigraphy between the Canning River and Prudhoe Bay, U.S. Geological Survey Open-File Report.

Table 1. Geotechnical properties of surface sediment samples.

Station no. and core type[1]	Geographical Coordinates	Water depth (m)	Sediment description	Water contents (% dry wt.)	Vane shear strengths[2] (kPa)	Maximum past stress (kPa)	Shear strength from unconfined compression test (kPa)
Values from Reimnitz and others, 1977:							
1V	71°10.9'N 148°34.0'W	307	mud		0(2), 2.2(5)		
2V	71° 6.2'N 148°42.0'W	43	pebbly, sandy mud		1.4(2), 9.2(5)		
3V	70°49.6'N 148°31.0'W	33	sandy mud		1.4(2), 13.8(5)		
4V	70°41.6'N 148°30.0'W	27	mud and gravelly sand		0.7(2), 7.0(5)		
5V	70°26.1'N 148°29.3'W	7	silty sand		7.7-9.2(6)		
6V	70°25.3'N 148°38.2'W	7	silty sand		7.7(2)		
7V	70°18.9'N 148°20.3'W	3	silty clay, clay		>18.4(8)		
8V	70°31.4'N 147°33.0'W	26	sandy mud		<0.7(2), 4.9(5)		
9V	70°58.3'N 146°30.1'W	364	mud		0(2), 2.6(5), 4.6(10)		
10V	70°40.0'N 146°40.0'W	47	muddy sand		3.0(2)		
11V	70°21.4'N 146°36.0'W	26	muddy sand		0(2), >18.4(5)		
12V	70°19.6'N 146°30.0'W	17	clay		13.8(2), 13.8(5)		
13V	70°13.2'N 145°31.0'W	25	muddy sand		6.1(2), 9.2(5), 13.8(10)		
14V	70°23.4'N 145°34.0'W	37	sandy, gravelly mud		0.7(2), 15.3(5)		
15V	70°44.8'N 145°31.0'W	87	mud		1.5(2), 5.2(5)		

Table 1. Geotechnical properties of surface sediment samples (continued).

Station no. and core type[1]	Geographical Coordinates	Water depth (m)	Sediment description	Water contents (% dry wt.)	Vane shear strengths[2] (kPa)	Maximum past stress (kPa)	Shear strength from unconfined compression test (kPa)
16V	70°54.1'N 145°20.0'W	300	mud		3.0(2), 5.2(5)		
17V	70° 2.3'N 145°32.0'W	1062	mud and clay		0(2), 9.2(5), >18.4(10)		
1I	70°35.6'N 149°27.1'W	12	mud		10.7(5), 17.6(10)		
2I	70°33.2'N 149°11.0'W	12	muddy sand		9.5(2)		
3I	70°33.1'N 149°11.5'W	5	sand		1.6(2)		
4I	70°28.4'N 148°27.2'W	5	muddy sand		2.3(2), 4.8(15)		
5I	70°26.9'N 148°37.5'W	6	mud and muddy sandy gravel		>9.5(2), >9.5(15)		
6I	70°26.9'N 148°30.5'W	9	---		0-2.3(2), >9.5(2), 7.1(2)		
7I	70°28.1'N 148°24.0'W	9	mud		7.1(2), 4.8(2), 4.8(2) 2.3(2), 4.8(2), 9.5(15)		
8I	70°24.2'N 148°31.5'W	3	muddy sand		7.1(2), 4.8(15)		
9I	70°19.8'N 148°23.5'W	3	muddy sand		3.7(8)		
10I	70°24.0'N 148°17.3'W	3	muddy sand		7.9(2), >9.5(15)		
11I	70°24.9'N 148° 1.0'W	7	muddy sand		>9.5(2)		
12I	70°19.5'N 147°51.5'W	3	muddy sand, mud		>9.5(2), 9.5(3)		
13I	70°17.2'N 147°42.8'W	2	muddy sand		7.5(2), >9.5(15)		

Table 1. Geotechnical properties of surface sediment samples (continued).

Station no. and core type[1]	Geographical Coordinates	Water depth (m)	Sediment description	Water contents (% dry wt.)	Vane shear strengths[2] (kPa)	Maximum past stress (kPa)	Shear strength from unconfined compression test (kPa)
14I	70°12.8'N 147°41.0'W	2	muddy sand		7.9(6.5)		
15I	70°23.3'N 147°28.7'W	2	muddy sand		4.8(2), <2.3(2), 9.5(2) 7.1(2), 7.1(10)		
16I	70°18.2'N 147°10.7'W	6	mud and muddy sand		2.3(2), >9.5(2)		
17I	70°14.7'N 147°10.5'W	6	sandy mud		>9.5(2)		
18I	70°10.3'N 147° 1.0'W	5	sandy mud		>9.5(2)		
19I	70°10.8'N 146° 3.4'W	3	sandy mud		>9.5(2)		
1983 Block samples:							
5S	70°29.9'N 149° 5.5'W	---	silty mud	29.5, 22.5, 22.9, 22.6, 22.6, 25.3, 24.5 (ave.=24.3)	14.4, 14.4, 15.4, 23.0 (ave=16.8)	630, 1000, 350 (ave=660)	35
6D	70°35.9'N 151°36.4'W	5	clay and silty clay	36.2, 50.8 57.3, 44.2, 44.8, 42.5, 44.5 (ave=45.7)	13.4, 7.2, 9.6, 13.9, 5.8, 4.8, 10.6, 9.6 (ave=9.4)	39, 53, 70, 68 (ave=58)	11
6aD	same as 6D	5	clay and silty clay	46.5	9.6, 17.3, 16.3, 19.2, 20.2, 11.5, 13.4, 11.5, 18.2, 16.3 (ave=15.4)		
7D	70°29.5'N 148°17.0'W	8	silty clay	25.0, 24.9, 24.9, 21.9 23.6, 23.2 22.2 (ave= 20.1)	13.7, 15.4, 28.8, 31.0, 37.4, 23.0, 39.4, 19.2, 27.8, 33.6, 24.0, 17.3, (ave=25.9)	305, 120, 1230, 500 (ave=540)	30
8D	70°29.3'N 148°12.2'W	?	clayey silt and silty sand	26.8, 22.7, 22.7, 24.2, 23.4 (ave= 24.0)	15.4, 22.1, 21.1 16.3, 7.7, 19.2, 15.4, 8.6, 10.6, 20.2, 10.6, 24.0, (ave=15.9)	600, 400 (ave=500)	18

Table 1. Geotechnical properties of surface sediment samples (continued).

Station no. and core type[1]	Geographical Coordinates	Water depth (m)	Sediment description	Water contents (% dry wt.)	Vane shear strengths[2] (kPa)	Maximum past stress (kPa)	Shear strength from unconfined compression test (kPa)
9S	70°16.4'N 147°47.5'W	---	silty clay	16.4	31.7, 38.4, 41.3, 48.0, 51.8, 91.2, 93.1, 72.0, 42.2 (ave=56.6)		
10D	70°34.3'N 149°34.7'W	8	clay to sand	39.4, 53.2, 54.2 (ave= 48.9)	28.8, 28.8, 28.8, 36.5, 38.4, 24.0, 38.4 (ave=32.0)		14
11D	70°32.9'N 150° 7.7'W	7	silty mud	26.2, 33.3, 33.3, 26.1, 24.0 (ave= 28.6)	19.2, 19.2, 19.2, 17.2, 35.5, 38.4, 35.5 (ave=26.3)	280, 120 (ave=200)	30
12D	70°33.8'N 149°30.5'W	8	sand with sandy silt and silty clay	57.6, 54.0 58.4, 47.5, 53.0 (ave= 54.1)	43.2, 35.5, 28.8 46.0, 9.6, 13.4, (ave=29.4)	21, 20 (ave=20)	9
13D	70°18.2'N 147°47.9'W	5	silt to sand				
14D	70°23.2'N 147°54.1'W	?	sandy mud	27.8, 26.0 (ave=26.9)	28.8, 43.2, 32.6 24.0, 17.2, 25.9 (ave=28.6)		24
15D	70°20.2'N 147°19.2'W	5	pebbly mud	31.1			
16G	70°17.7'N 146°53.7'W	6	mud	12.6, 17.5 (ave=15.0)		2000	
17D	70° 8.5'N 145°44.8'W	<5	mud with sand and pebbles on the surface	17.6, 21.2, 21.7, 20.4, (ave=20.2)	57.6, 40.3, 56.6, 45.1 (ave=49.9)	220	56
18S	70° 8.1'N 145°44.5'W	---	mud	44.8	7.2, 9.6, 10.6, 10.6 (ave=9.5)		
23S	70°48.5'N 154° 0.3'W	---	mud	24.1			
24S	70°48.5'N 154° 0.3'W	---	mud	20.7			

Table 1. Geotechnical properties of surface sediment samples (continued).

Station no. and core type[1]	Geographical Coordinates	Water depth (m)	Sediment description	Water contents (% dry wt.)	Vane shear strengths[2] (kPa)	Maximum past stress (kPa)	Shear strength from unconfined compression test (kPa)
26D	71°13.5'N 155°30.5'W	5	mud	33.4			

1 V-Van Veen grab sampler
I-In-place vane shear test
D-Pipe dredge sample
S-Sample taken manually from swash zone
G-Gravity core

2 Values in parentheses, for the Reimnitz and others (1977) data, indicate depth in sediment in cm. If no value is given in parentheses, the tests were performed on a smoothed surface with a Torvane. Strengths listed as "0" reflect values too low to be read, less than about 0.5 kPa.

Table 2. Relations between average properties of block samples.

Block sample no.	Ave. water content (%)	Shear strength from unconfined compression test, S_{uUC} (kPa)	Ave. Torvane shear strength, S_{uTV} (kPa)	Ave. maximum past stress, σ'_{vm} (kPa)	S_{uUC}/S_{uTV}	S_{uUC}/σ'_{vm}
5S	24.3	35	17	660	2.08	0.05
6D	45.7	11	9	58	1.17	0.19
7D	20.1	30	26	540	1.16	0.05
8D	24.0	18	16	500	1.13	0.04
10D	48.9	14	32	---	0.44	---
11D	28.6	30	26	200	1.14	0.15
12D	54.1	9	29	20	0.32	0.46
14D	26.9	24	29	---	0.84	---
17D	20.2	56	50	220	1.12	0.25
						(ave=0.17)

Table 3. Locations of borings.

Boring Number	Coordinates	Water Depth (m)
HLA-1	70°24.8'N 148°13.3'W	5.0
HLA-2	70°27.1'N 148°26.8'W	7.0
HLA-3	70°31.9'N 148°53.9'W	13.5
HLA-4	70°30.3'N 148°22.7'W	8.5
HLA-5	70°30.7'N 148°37.9'W	12.8
HLA-6	70°29.6'N 148° 7.7'W	11.1
HLA-7	70°27.2'N 148° 5.3'W	7.7
HLA-8	70°30.0'N 147°53.4'W	14.0
HLA-9	70°22.8'N 147°52.7'W	5.3
HLA-10	70°27.1'N 147°48.5'W	6.5
HLA-11	70°23.0'N 147°41.0'W	7.5
HLA-12	70°26.7'N 147°30.4'W	15.2
HLA-13	70°18.9'N 147°38.8'W	5.6
HLA-14	70°16.6'N 147°23.7'W	6.6
HLA-15	70°13.3'N 147° 0.3'W	5.5

Table 3. Locations of borings (continued).

Boring Number	Coordinates	Water Depth (m)
HLA-16	70°16.2'N 146°42.7'W	9.2
HLA-17	70°16.1'N 146°27.5'W	14.5
HLA-18	70°12.6'N 146° 2.6'W	11.3
HLA-19	70°18.8'N 146°58.1'W	10.5
HLA-20	70°22.0'N 147°14.6'W	11.3

Table 4. Geotechnical properties of boring samples.

Boring Number	Subbottom Depth (m)	Water Content (%)	Liquid Limit (%)	Plastic Limit[1] (%)	Plasticity Index (%)	In-Place Overburden Stress (kPa)	Triaxial Consol. Stress[2] (kPa)	Triaxial Test Shear Strength (kPa)	Maximum Past Stress[3] (kPa)	Quality of Consol. Test[4]	OCR[5]	NSP Estimated Shear Strength[6] (kPa)
HLA-1	0.4	36.4		NP		4			81	G	20	18
	1.4	25.3				13	UU	36				
	4.5	39.6	39	29	10	38			115	G	3	37
	5.8	28.8				50	96	101				
	5.8	29.9				50	48	62				
	6.8	32.6				59	UU	17				
	8.1	41.2	28	27	1	70			88	G	1.2	34
HLA-2	1.0	27.6				10	48	55				
	1.0	27.5				10	96	111				
	5.0	39.4	40	29	11	42			134	M	3	43
HLA-3	1.2	18.5		NP		13						
	2.2	24.1	34	26	8	24	35	67				
	9.0	28.2				28						
HLA-4	2.3	21.8				24						
	4.1	18.9				44	35	268				
	5.8	26.5	42	28	14	60	UU	47	287	G	5	84
	6.9	23.0				70	72	122				
	6.9	31.3				70	144	108				
	7.8	19.3	28	20	8	80			100	M	1.3	40
	11.3	32.9	55	30	25	111	UU	73	239	P		
HLA-5	2.4	34.0	40	27	13	21	UU	35	100	M	5	30
	3.2	31.4				28	72	57				
HLA-6	0.6	38.4	51	29	22	5	UU	5				
	1.5	26.2				14	72	216				
	2.0	23.7	38	24	14	19	35	153				
	2.7	29.2	27	24	3	26			359	G	14	84
	4.7	36.3				42	UU	31				
	6.7	45.6	46	27	19	57	UU	23				
	8.2	41.1				69						
	10.2	36.6				86						
	11.9	23.4	30	20	10	103						
	15.7	16.7				146	UU	113				
	17.4	28.9	29	25	4	162			335	G	2	117

Table 4. Geotechnical properties of boring samples (continued).

Boring Number	Subbottom Depth (m)	Water Content (%)	Liquid Limit (%)	Plastic Limit[1] (%)	Plasticity Index (%)	In-Place Overburden Stress (kPa)	Triaxial Consol. Stress[2] (kPa)	Triaxial Test Shear Strength (kPa)	Maximum Past Stress[3] (kPa)	Quality of Consol. Test[4]	OCR[5]	NSP Estimated Shear Strength[6] (kPa)
HLA-7	0.5	27.0	40	22	18	5	UU	66				
	2.1	37.1	43	25	18	18			187	G	10	47
	2.3	28.9				20	35	53				
	2.3	28.4				20	72	53				
	7.7	51.1	56	29	27	58	UU	17				
	12.5	28.0	45	24	21	103	UU	117	359	P		
	14.3	27.5				120	UU	94				
HLA-8	2.1	29.7	46	28	18	20	UU	64				
	5.5	33.6	36	24	12	49	UU	57				
	6.4	38.6				57	48	58				
	6.4	35.4				57	96	91				
	6.9	36.6	43	24	19	60			215	G	4	67
	13.0	22.6				124	96	192				
	13.4	25.6	38	24	14	128			249	P		
	22.1		42	25	17							
HLA-9	0.8	21.6	36	19	17	8						
	2.0	20.8	38	24	14	21	UU	137	374	M	18	84
	4.1	24.0	36	22	14	43			216	M	5	62
	4.9	22.0				51	UU	38				
	7.9	23.8	37	23	14	81			86	G	1.1	34
	11.0	22.5	40	22	18	113						
HLA-10	0.6	20.3				7						
	0.8	16.7				8						
	3.4	36.5	53	29	25	30			168	G	6	48
	3.5	37.7				31	38	62				
	3.5	37.8				31	72	43				
	4.7	32.3				42	72	129				
	6.7	23.3	33	21	12	62	UU	105	359	M	6	101
	19.1	19.4	34	23	11	196	UU	206	192	P		
	21.3	23.7	35	22	13	219	UU	83	378	M	1.7	134
HLA-11	4.0	21.5	25	19	6	42	UU	68	431	P		
	7.3	20.0				77	72	287				
	7.3	20.7				77	144	321				
	8.7	23.2	32	21	11	92			406	P		
	12.2	19.0	35	22	13	127	UU	315	335	P		
	21.6	23.9	47	24	23	225	UU	126				

Table 4. Geotechnical properties of boring samples (continued).

Boring Number	Subbottom Depth (m)	Water Content (%)	Liquid Limit (%)	Plastic Limit[1] (%)	Plasticity Index (%)	In-Place Overburden Stress (kPa)	Triaxial Consol. Stress[2] (kPa)	Triaxial Test Shear Strength (kPa)	Maximum Past Stress[3] (kPa)	Quality of Consol. Test[4]	OCR[5]	NSP Estimated Shear Strength[6] (kPa)
HLA-12	1.4	19.7	36	21	15	15			168	M	11	42
	1.5	24.4	31	21	10	16	UU	295				
	3.7	21.8				39	UU	157				
	6.4	23.4	45	26	19	67	UU	113	335	M	5	97
	8.4	24.8	47	26	21	86	UU	35				
	10.4		44	26	18							
	16.6		47	25	22							
	22.7		42	25	17							
HLA-13	1.1	17.8				12	72	268				
	1.1	18.1				12	120	268				
	1.8	18.8	32	19	13	20			134	G	7	37
	2.9	20.9				31	UU	198				
	5.6	26.7	41	23	18	58	UU	79	383	M	7	105
HLA-14	2.3	61.0	66	32	34	14	UU	18	77	G	6	22
	4.0	43.4	58	34	24	27	UU	16				
HLA-15	1.8	28.0				17	UU	24				
	5.0	83.2	57	31	26	34			35	G	1.0	14
	5.5	66.4				37	48	21				
	5.5	60.1				37	96	36				
	8.4	41.8	55	41	14	59	UU	43				
HLA-16	0.9	22.1				9						
	2.4	14.8	25	19	6	28			125	G	4	37
	2.7	13.2				31	36	>479				
	2.7	13.7				31	72	>479				
	5.5	23.5	30	22	8	59	UU	70	134	G	2	45
	9.7	22.4	27	22	5	102	192	>287	240	P		
	14.6	17.8	32	21	11	157			431	P		
	14.6	18.8				157	144	>263				
	14.6	19.8				157	240	230				
	19.1		39	27	12							
	20.6	27.3	40	24	16	214	UU	84	335	P		
	22.1		38	27	11							
HLA-17	0.9	20.0	37	25	12	10	UU	185	379	M	38	73
	2.3	21.0	34	24	10	24	UU	162	455	P		
	5.3	23.2	35	21	14	55			359	G	7	98
	11.0	23.4	42	21	21	113			527	P		
	15.7	18.6	34	23	11	165	UU	99				
	25.2	22.3	41	23	18	262	UU	266				

Table 4. Geotechnical properties of boring samples (continued).

Boring Number	Subbottom Depth (m)	Water Content (%)	Liquid Limit (%)	Plastic Limit[1] (%)	Plasticity Index (%)	In-Place Overburden Stress (kPa)	Triaxial Consol. Stress[2] (kPa)	Triaxial Test Shear Strength (kPa)	Maximum Past Stress[3] (kPa)	Quality of Consol. Test[4]	OCR[5]	NSP Estimated Shear Strength[6] (kPa)
HLA-18	0.0	26.4	35	26	9	0						
	1.8	19.4				20	37	>297				
	1.8	17.2				20	72	>335				
	2.0	19.3		NP		21			227	P		
	4.3	21.5	35	23	12	46	UU	190	55	P		
	6.6	27.8	33	24	9	67			393	M	6	110
	6.7	23.5				69	120	215				
	6.7	25.0				69	58	132				
	9.2		32	24	8							
	11.1	24.5	35	23	12	113			275	M	2	92
	14.2			NP								
HLA-19	0.6	34.8	52	27	25	5	UU	123				
	1.3	37.4	52	26	26	11	UU	48	503	M	46	94
	6.5	22.0				65						
	8.4	36.5	42	32	10	81	UU	48	335	M	4	100
	9.6	39.8				86						
	11.9	39.2				104						
	15.8	19.5	31	21	10	147	UU	199	132	P		
	23.2	20.9	40	22	18	225	UU	122	479	P		
HLA-20	1.2	24.6				12	36	144				
	1.2	23.8				12	72	192				
	1.5	25.6	39	26	13	15			383	G	26	80
	5.0	28.7	47	28	19	48	UU	46				
	8.4		38	25	13							
	17.8		36	21	15							
PB-1	1.5	47.2	41	29	12	9	CU	30				
	2.3	41.1	43	31	12	16	CU	45				
	4.1	16.3		NP		36	CU	134				
	5.2	15.0		NP		48						
	5.5	7.4		NP		54						
PB-2	0.3	21.4		NP		3						
	1.1	17.9		NP		11	CU	85				
	1.9	19.9	37	21	16	19	CU	93				
	3.3	22.7	38	20	18	32	CU	221				
	3.9	24.4	41	22	19	40	CU	160	840	M	21	183
	5.4	19.1	37	17	20	54	CU	229	500	G	9	125
	6.9	19.1	34	18	16	72	CU	270	570	G	8	152
	8.4	18.3	41	20	21	87	CU	252				

Table 4. Geotechnical properties of boring samples (continued).

Boring Number	Subbottom Depth (m)	Water Content (%)	Liquid Limit (%)	Plastic Limit[1] (%)	Plasticity Index (%)	In-Place Overburden Stress (kPa)	Triaxial Consol. Stress[2] (kPa)	Triaxial Test Shear Strength (kPa)	Maximum Past Stress[3] (kPa)	Quality of Consol. Test[4]	OCR[5]	NSP Estimated Shear Strength[6] (kPa)
PB-3	0.1	30.6		NP		0						
	0.3	29.5		NP		3						
	0.8	19.0		NP		8	CU	66				
	1.8	22.9	28	25	3	18	CU	106				
	2.7	30.6	33	24	9	25	CU	70				
	3.4	34.0	38	27	11	32	CU	25				
	3.7	37.8	41	27	14	34	CU	28				
	4.6	42.9	45	26	19	41	CU	25				
PB-5	0.1	37.6				1			620	M	620	68
	0.3	37.6				3						
	1.5	25.1		NP		14						
	1.7	30.7		NP		17						
	2.2	35.2		NP		20	CU	39				
	4.6	29.3		NP		41	CU	76				
	5.0	31.2		NP		45						
	6.5	37.3	37	27	10	57	CU	45				
	7.3	20.2		NP		64						
	7.9	19.8		NP		70						
PB-6	1.4	17.3		NP		13	CU	45				
	2.1	13.5				23			1250	M	54	223
	3.4	5.9		NP		38						
	4.9	14.7				55						
	5.9	3.4				73						
	9.3	25.5				104			620	G	5	151
PB-7	2.2	38.3				18			400	G	22	85
	63.8	31.0				560			850	G	1.5	470
PB-8	0.4	23.0				4			1100	G	275	143
	1.1	22.8	23	19	4	11	CU	71				
	1.8	20.1				18			820	G	46	154
	2.3	23.3	28	22	6	24	CU	89				
	2.7	19.9				28			680	G	24	142
	3.2	22.8	35	23	12	31			450	G	15	108
	3.6	20.7				38	CU	89				
	4.5	19.9	30	22	8	47			530	G	11	128
	4.7	21.3	24	18	6	49	CU	54				
	5.5	22.8	26	18	8	57	CU	65				
	5.9	35.7				59			175	G	3	57
	6.0	33.4	34	22	12	61	CU	36				
	6.3	40.1	60	35	25	63			330	G	5	91

Table 4. Geotechnical properties of boring samples (continued).

Boring Number	Subbottom Depth (m)	Water Content (%)	Liquid Limit (%)	Plastic Limit[1] (%)	Plasticity Index (%)	In-Place Overburden Stress (kPa)	Triaxial Consol. Stress[2] (kPa)	Triaxial Test Shear Strength (kPa)	Maximum Past Stress[3] (kPa)	Quality of Consol. Test[4]	OCR[5]	NSP Estimated Shear Strength[6] (kPa)
PB-8	6.9	32.6				68			250	G	4	82
	7.4	39.6	40	26	14	72	CU	26				
	8.2	39.2	58	36	22	79			300	G	4	96
	8.8	34.4	43	27	16	84	CU	59				
	9.4	30.3				89			550	G	6	149
	10.1	30.0	43	27	16	95	CU	98				
	11.3	29.9	41	28	13	105	CU	69				
	12.0	24.1				113			350	G	3	109

[1] NP-Non-plastic

[2] UU-Unconsolidated-undrained---sample enclosed in membrane and pressurized without drainage prior to shear; sheared without drainage.
CU or numerical value-consolidated-undrained---sample enclosed in membrane and stressed to a given level with drainage before shear (CU implies consolidation stress roughly equal to in-place overburden stress, numerical value for other stress levels); sample sheared without drainage.

[3] All maximum past stresses determined using Casagrande (1936) construction.

[4] G-good; well defined virgin compression curve with remainder of curve smooth.
M-medium; poorly defined virgin compression curve with remainder of curve smooth.
P-poor; poorly defined virgin compression curve; remainder of data cannot be approximated with a smooth curve.

[5] OCR-overconsolidation ratio; ratio of maximum past stress to in-place overburden stress; not tabulated for "P" tests.

[6] Shear strength estimated from the maximum past stress and in-place overburden stress using the normalized soil parameter approach; not tabulated for "P" tests.

Table 5. Relations between properties of boring samples representative of 4 m subbottom depth.

Boring no.	Water content (%)	Shear strength, s_u (kPa)	Shear strength excluding NSP[1] estimates, s_u^* (kPa)	Maximum past stress, σ'_{vm} (kPa)	Plasticity index (%)	s_u^*/σ'_{vm}	Water content near plastic limit (PL), liquid limit (LL), or midrange (mid)	Holocene sediment thickness[2] (m)
HLA-1	30	40	35	100	5-10	0.35	LL	7
HLA-2	35	45	---	135	12	----	LL	6
HLA-3	25	70	65	---	7	---	PL	1-3
HLA-4	22	260	260	290	16	0.90	PL	4
HLA-5	33	40	30	100	13	0.30	mid	0.5
HLA-6	34	80	30	350	12-18	0.09	?	2
HLA-7	33	60	60	100	21	0.60	mid	6
HLA-8	32	60	60	210	18	0.29	mid	5
HLA-9	21	40	70	215	15	0.19	PL	0
HLA-10	28	80	80	270	12-25	0.30	PL	3-4
HLA-11	22	150	150	---	13	----	PL	0-1
HLA-12	22	125	155	250	18	0.62	<PL	0
HLA-13	23	85	120	270	15	0.44	PL	0-1
HLA-14	44	19	15	80	29	0.19	mid to LL	5
HLA-15	60	25	25	35	20	0.71	>LL	7
HLA-16	21	60	---	130	10	----	PL	1
HLA-17	22	115	150	370	24	0.41	PL	0.5
HLA-18	21	200	200	400	10	0.50	PL	1
HLA-19	30	80	50	420	10-25	0.12	mid	0.5
HLA-20	26	65	50	390	15	0.13	PL	0
PB-1	45	30	30	---	12	----	LL	4
PB-2	21	180	180	650	19	0.28	PL	2[3]
PB-3	35	50	50	---	11	----	mid to LL	5
PB-5	30	50	50	---	10	----	LL	7
PB-6	17	80	45	---	--	----	--	3
PB-7	39	130	180	400	--	0.45	--	3
PB-8	22	110	70	500	7	0.14 (ave=0.37)	PL to mid	6[3]

[1] NSP estimates of shear strength are obtained from maximum past stresses using the normalized soil parameter method (Eq. 1)

[2] Smith (1985) and personal communication, P.A. Smith, USGS (1985). Range of values indicates uncertainty. Borings HLA-1, HLA-2, PB-3, and PB-5 contain deltaic sediment at 4 m that is probably early Holocene.

[3] Borings PB-2 and PB-8 may have 9 m and 12 m, respectively, of Holocene sediment (personal communication, D.A. Dinter, USGS, 1985).

Table 6. Index properties of sediment used in subtle freeze/thaw consolidation tests and influence of freeze/thaw on sediment strength tests.

Sediment no.	% sand[1]	% silt[1]	% clay[1]	Liquid limit (%)	Plastic limit (%)[2]
1	63.0	30.5	6.5		
	63.1	30.3	6.6		
	69.7	27.8	2.4	26	NP
2	87.9	9.3	2.8		
	83.8	13.5	2.6		
	88.8	10.2	1.0	25	NP
3	51.4	37.2	11.3		
	46.9	41.9	11.2		
	43.9	50.0	6.0	26	NP

[1] Grain size analyses were performed on 3 subsamples of each sediment.

2 NP=non-plastic

Table 7. Results of triaxial tests to determine influence of one freeze/thaw cycle on shear strength.

Sediment number	Freeze/thaw or control	Water content before consol. (%)	Water content after consol. & during shear (%)	Shear strength, S_u (kPa)	Ave S_u (F/T)/ave S_u (control)
1 (Sand/silt/clay)	F/T	35.1, 35.7 } 35.4 (ave)	31.0, 30.8 } 30.9 (ave)	52.0, 45.5 } 48.7 (ave)	0.40
	control	36	27.2, 26.3, 27.4 } 27.0 (ave)	139.8, 115.9, 107.1 } 120.9 (ave)	
2 (Fine silty sand)	F/T	41.5, 42.6 } 42.0 (ave)	31.4, 34.7 } 33.0 (ave)	113.0, 106.7 } 109.8 (ave)	0.35
	control	33	31.0, 29.2, 27.5 } 29.2 (ave)	298.4, 281.0, 372.4 } 317.3 (ave)	
3 (Clayey silt)	F/T	33.8, 33.9, 35.4, 36.6 } 34.9 (ave)	30.3, 30.7, 30.8, 31.5 } 30.8 (ave)	91.5, 88.7, 84.5, 76.3 } 85.3 (ave)	2.74
	control	38 to 45	37.3, 37.1, 37.4 } 37.3 (ave)	29.7, 34.2, 29.3 } 31.1 (ave)	

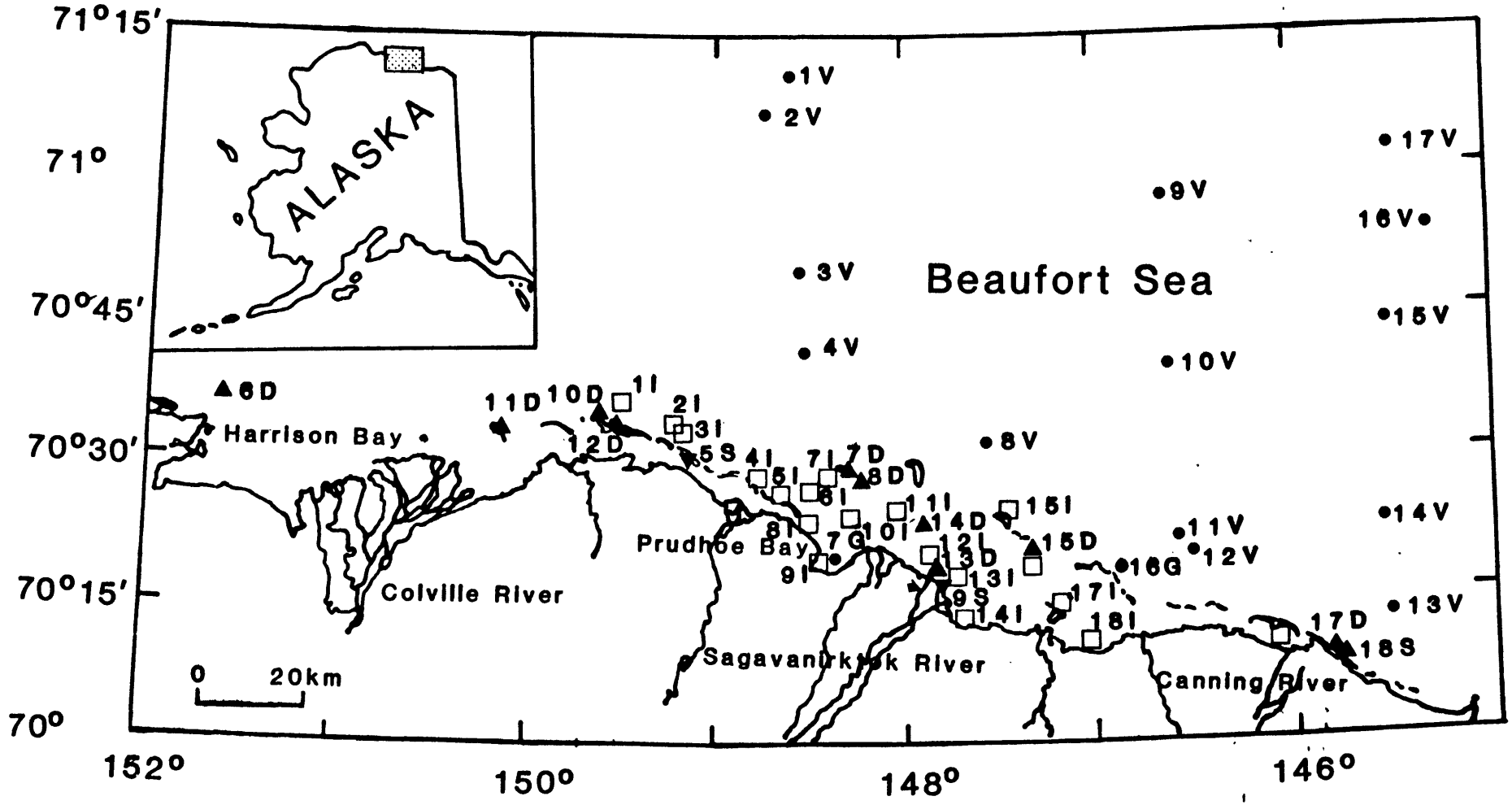

Figure 1. Locations of surficial samples east of Cape Halcott (● , "V" = Van Veen grab sample; ▼, "S" = hand cut block sample from the "swash" zone; ▲ , "D" = dredge sample; □, "I" = in situ vane shear test; ● , "G" = gravity core.

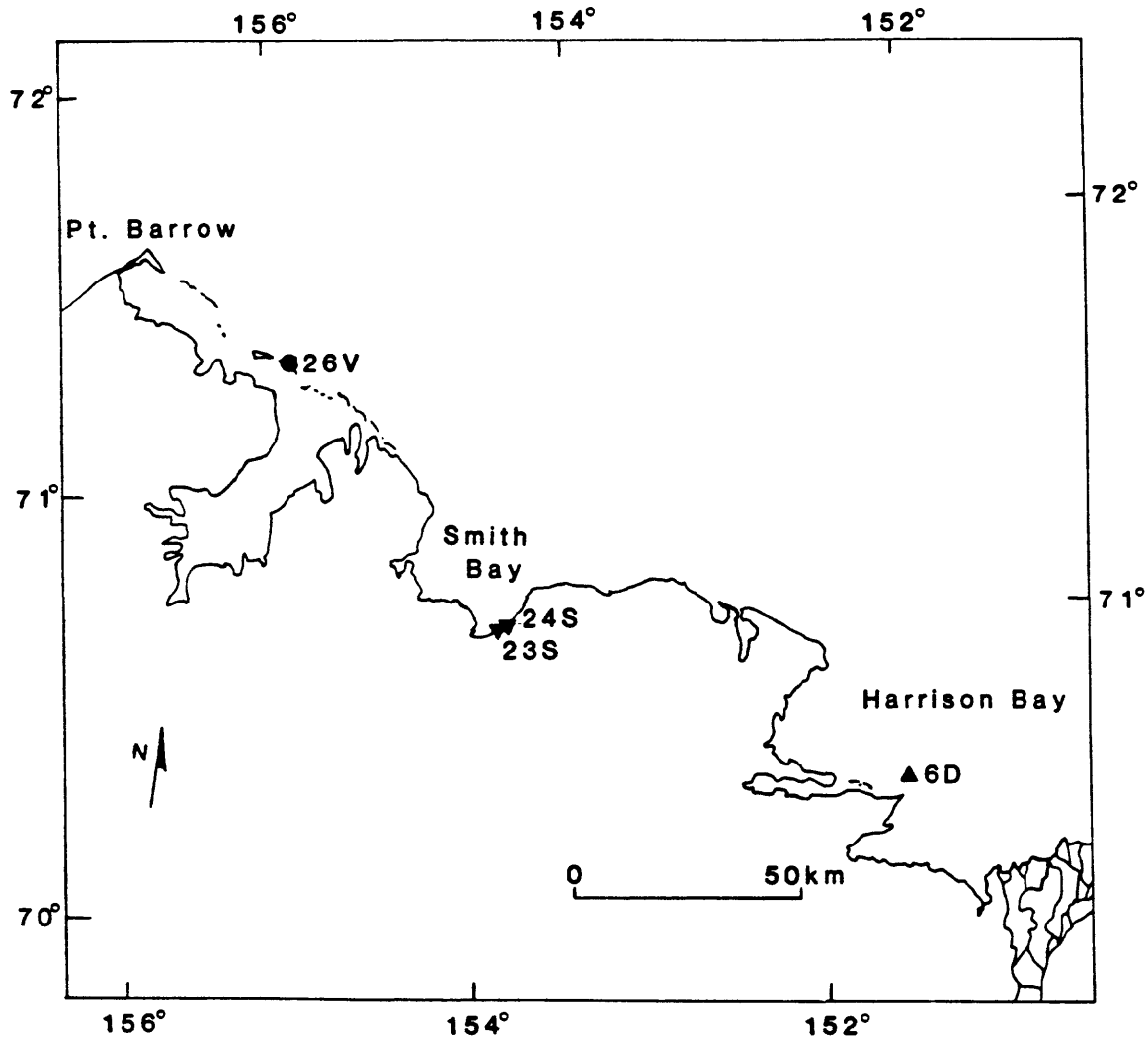

Figure 2. Locations of surficial samples west of the Colville River (● , "V" = Van Veen grab sample; ▼ , "S" = hand cut block sample from the "swash" zone; ▲ , "D" = dredge sample).

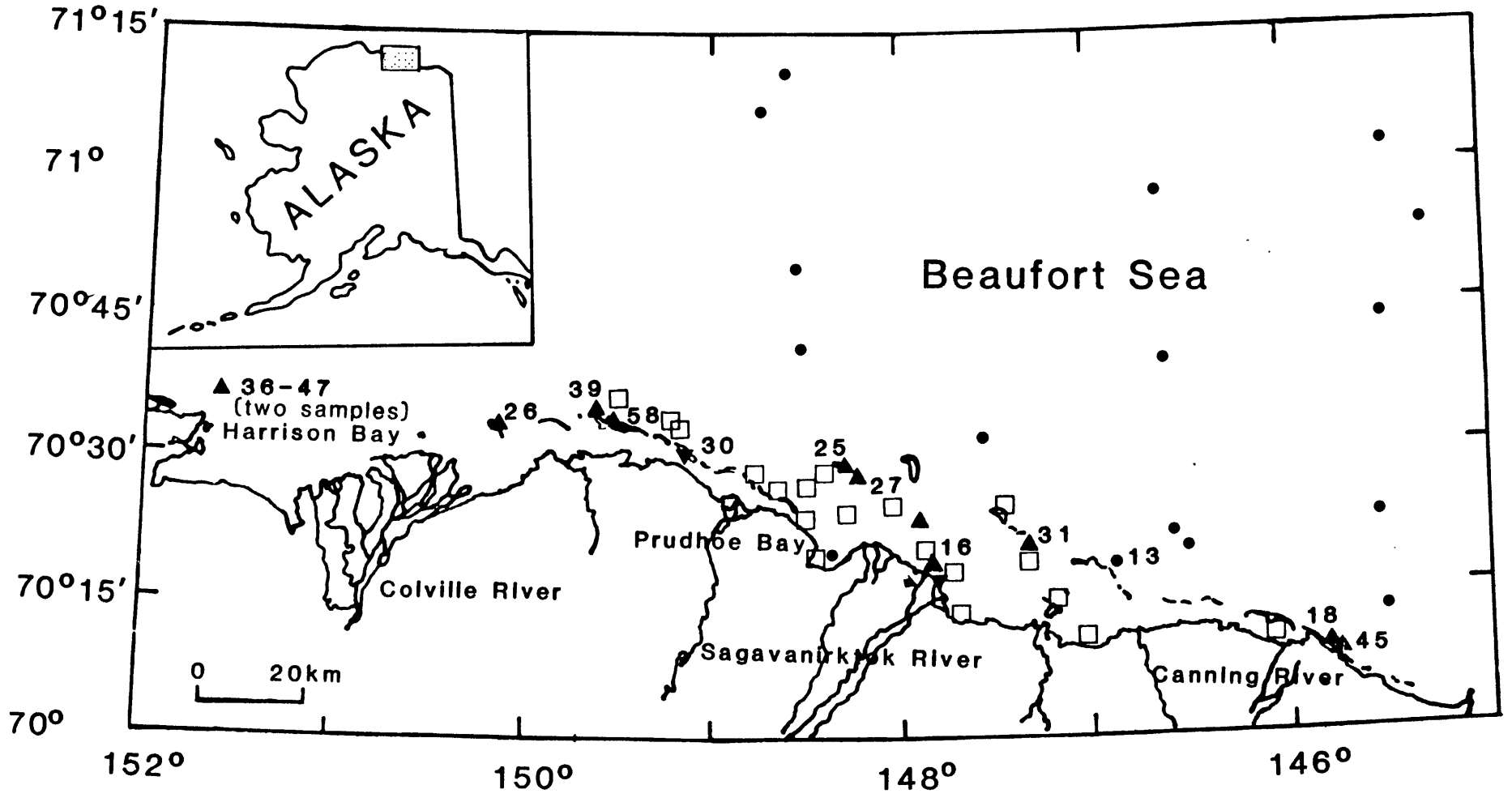

Figure 3. Average water contents of surficial samples east of Cape Halcott. See Figure 1 for meaning of sample type symbols.

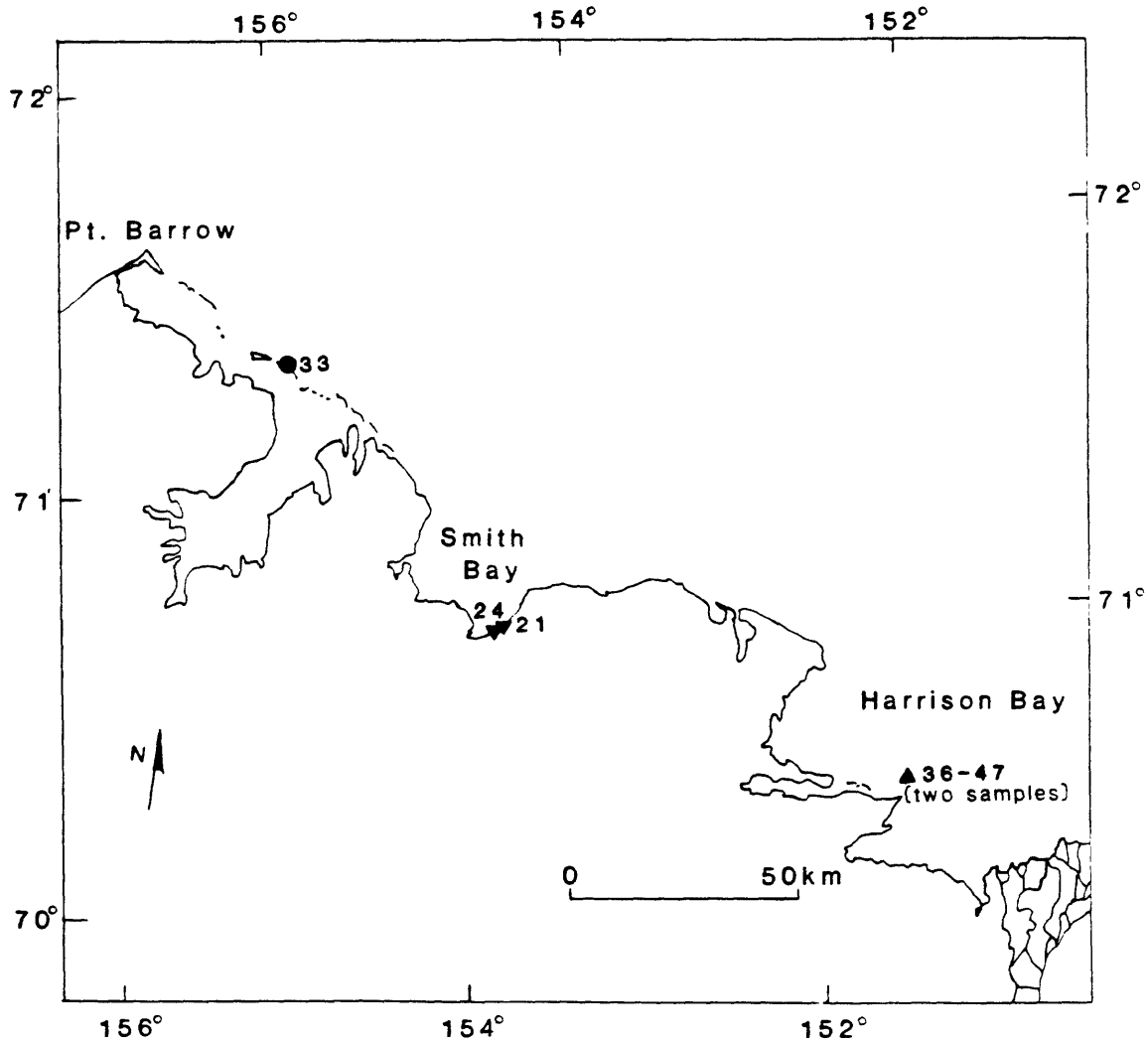

Figure 4. Average water contents of surficial samples west of the Colville River. See Figure 2 for meaning of sample type symbols.

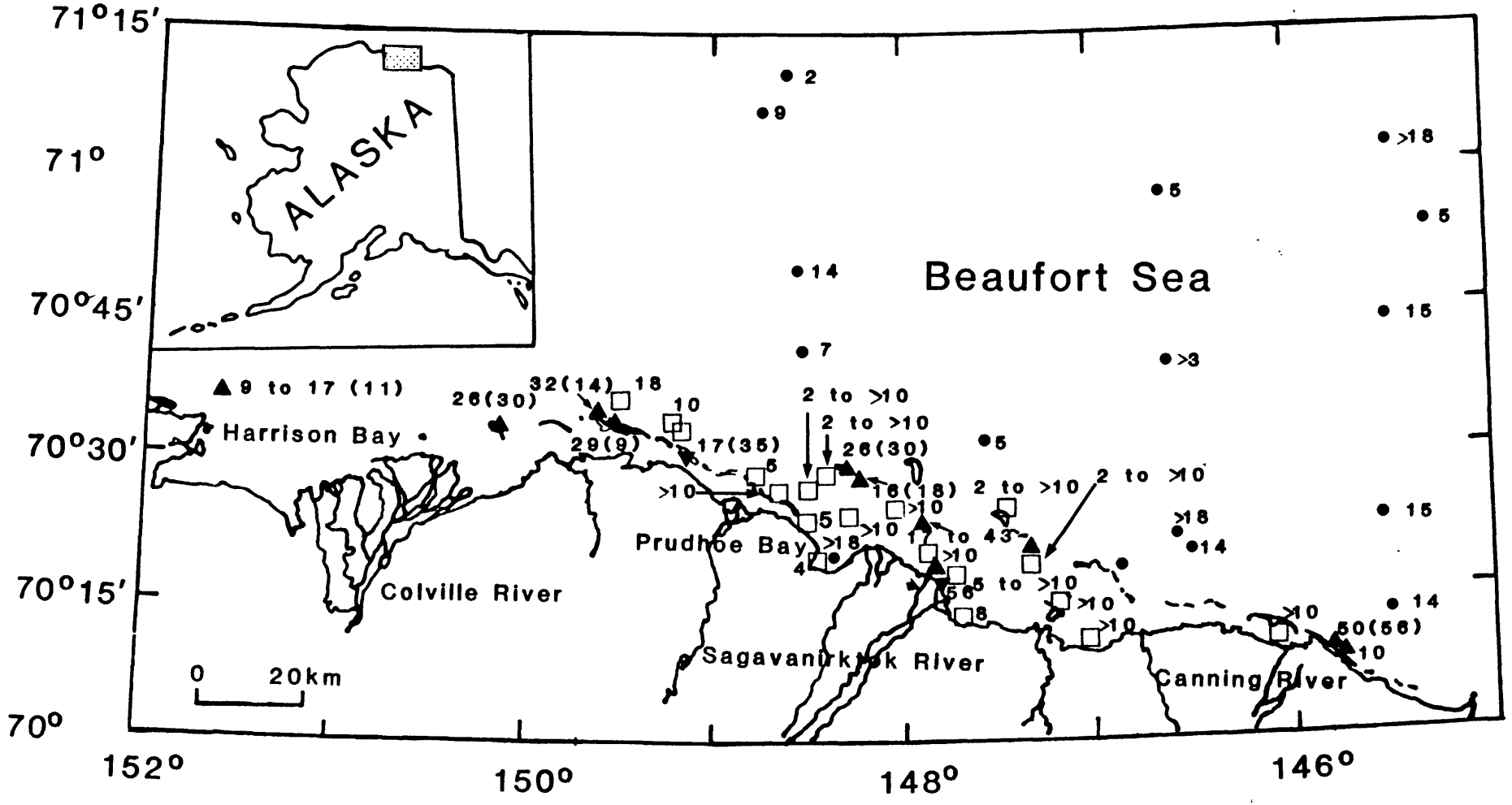

Figure 5. Average undrained shear strength (in kPa) of surface samples east of Cape Halcott. Values in parentheses are from unconfined compression tests. Remainder are from vane shear tests.

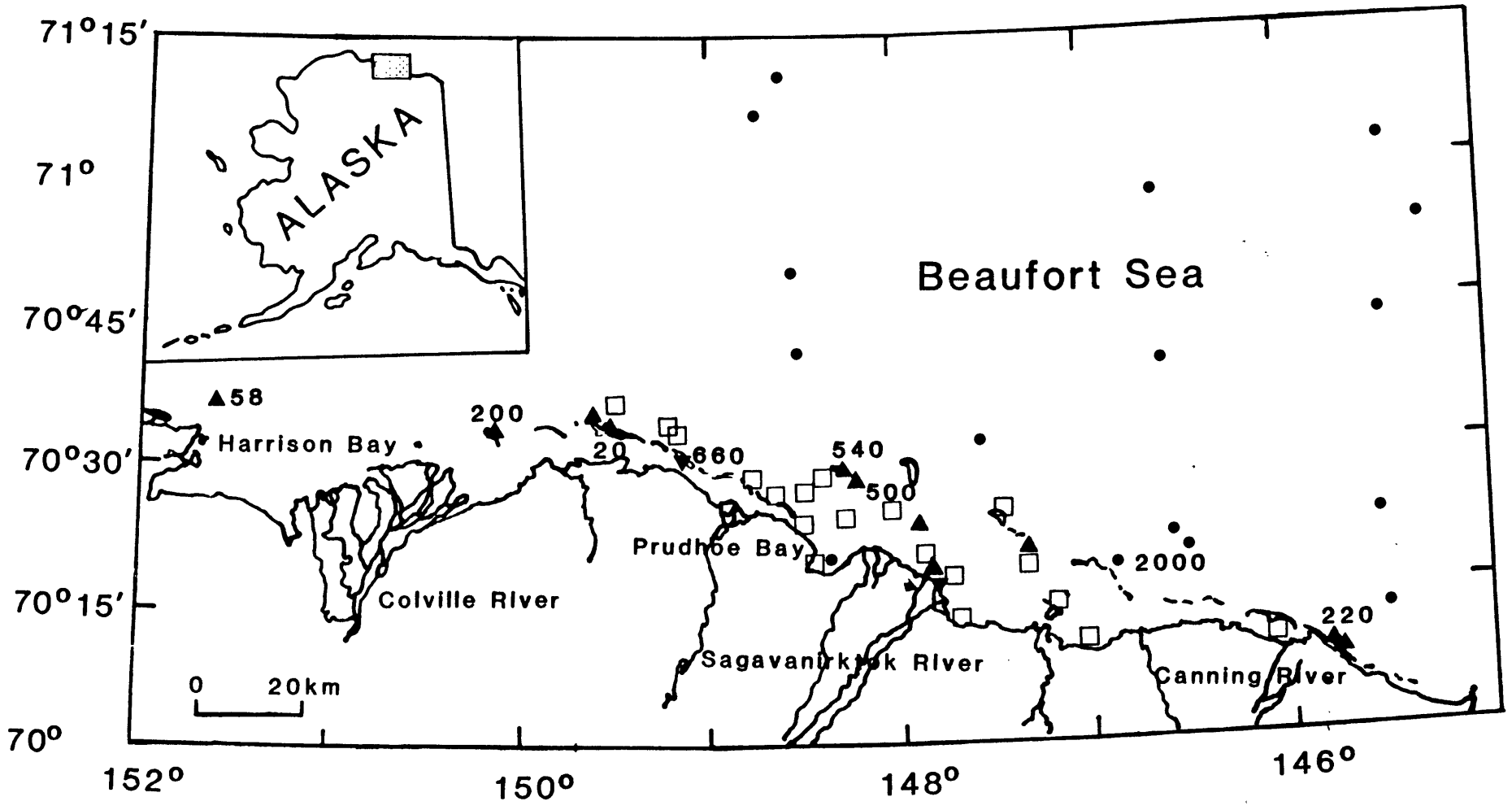

Figure 6. Average maximum past stress (in kPa) of surface samples east of Cape Halkett.

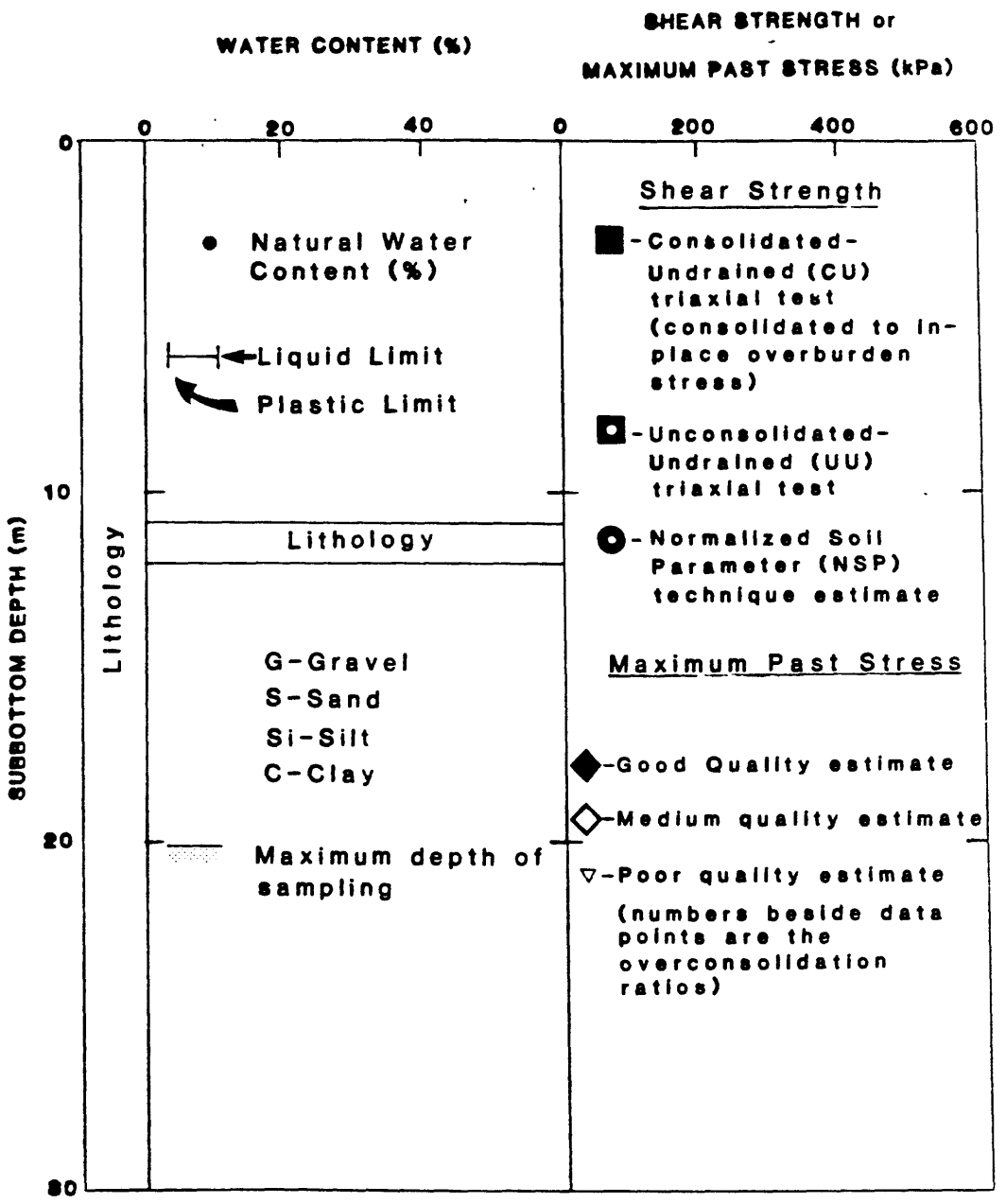

Figure 7. Legend for symbols used in boring profiles shown in Figures 8 through 34.

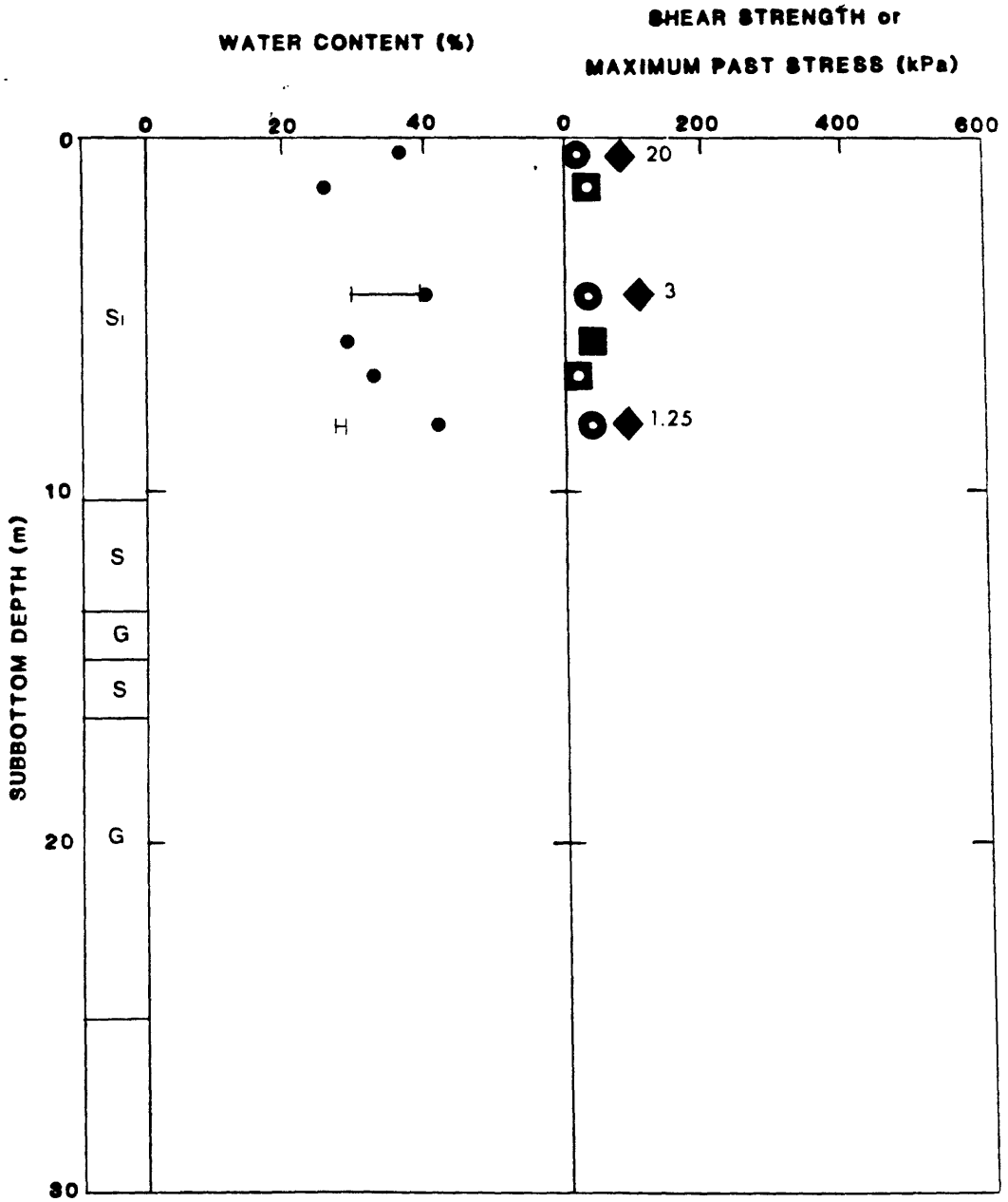

Figure 8. Physical properties and lithology profile for Boring HLA-1. See Figure 7 for legend.

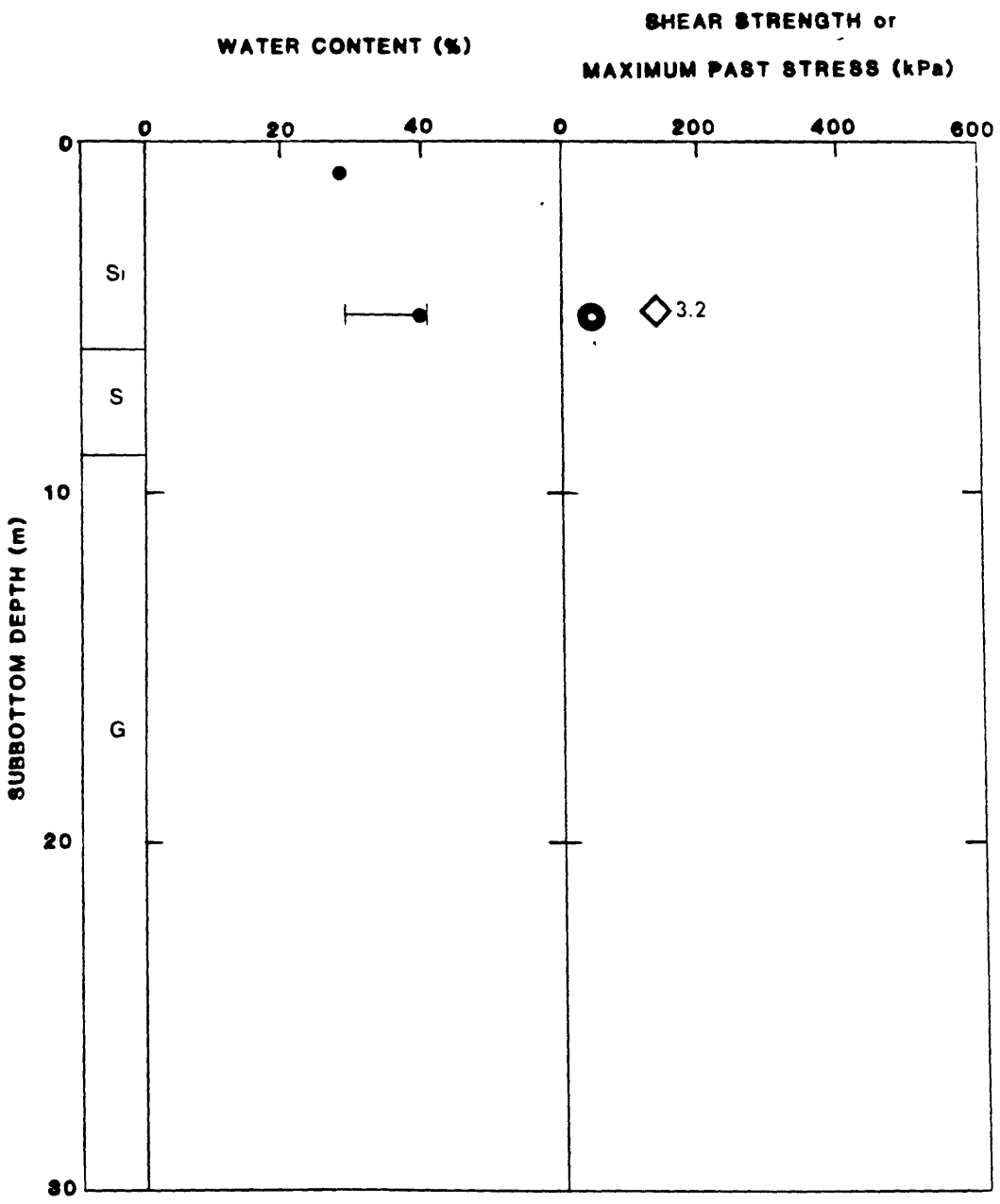

Figure 9. Physical properties and lithology profile for Boring HLA-2. See Figure 7 for legend.

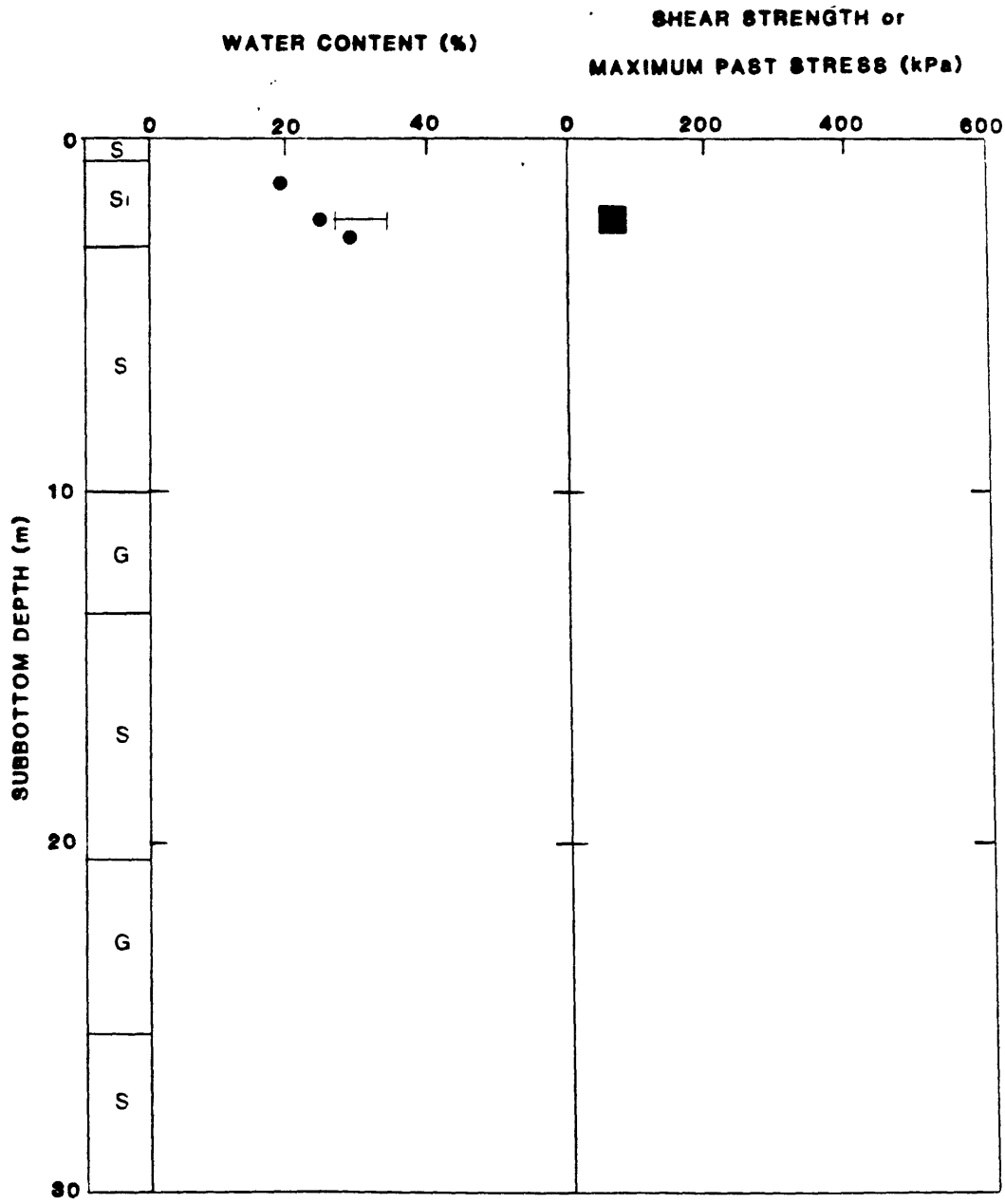

Figure 10. Physical properties and lithology profile for Boring HLA-3. See Figure 7 for legend.

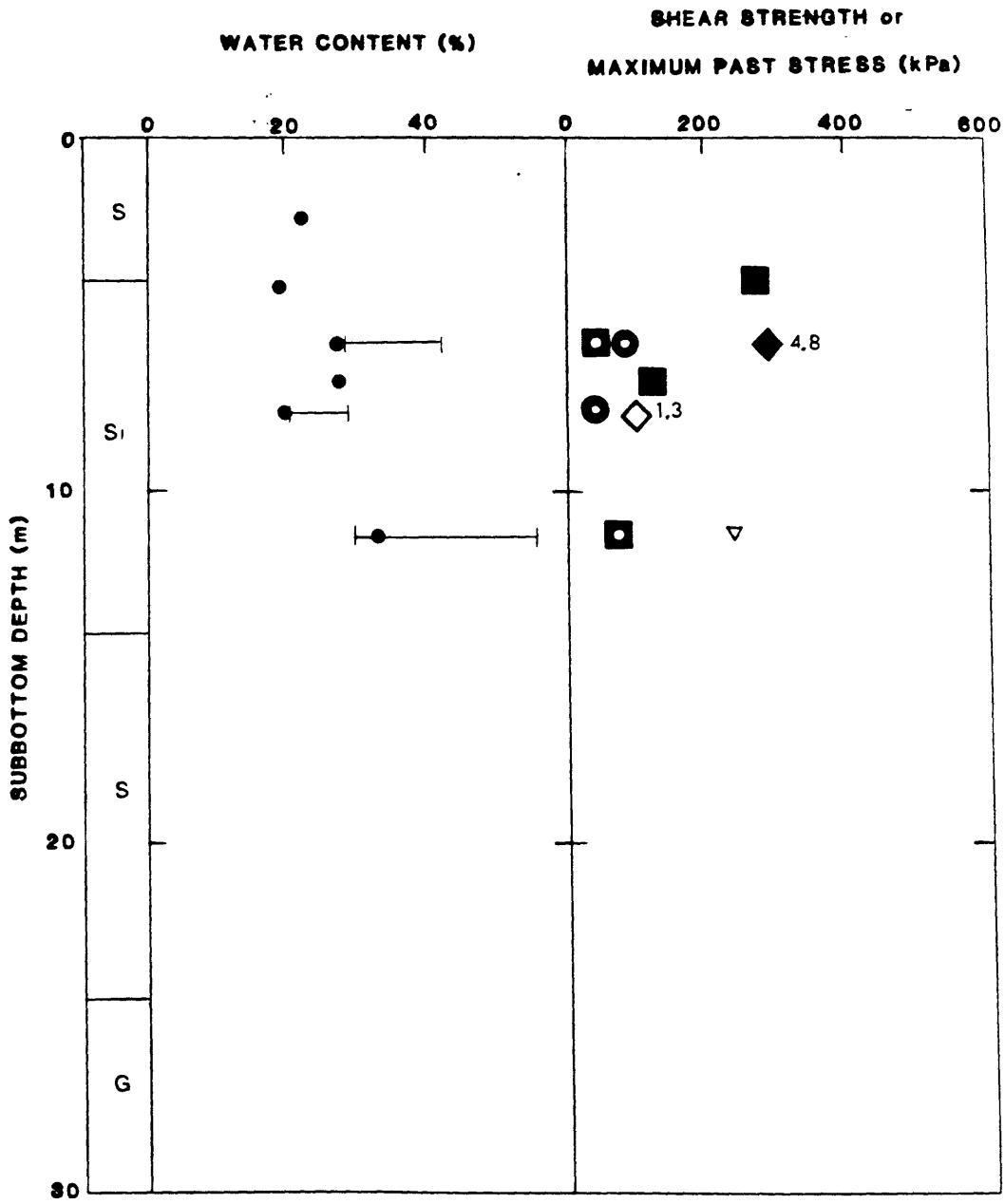

Figure 11. Physical properties and lithology profile for Boring HLA-4. See Figure 7 for legend.

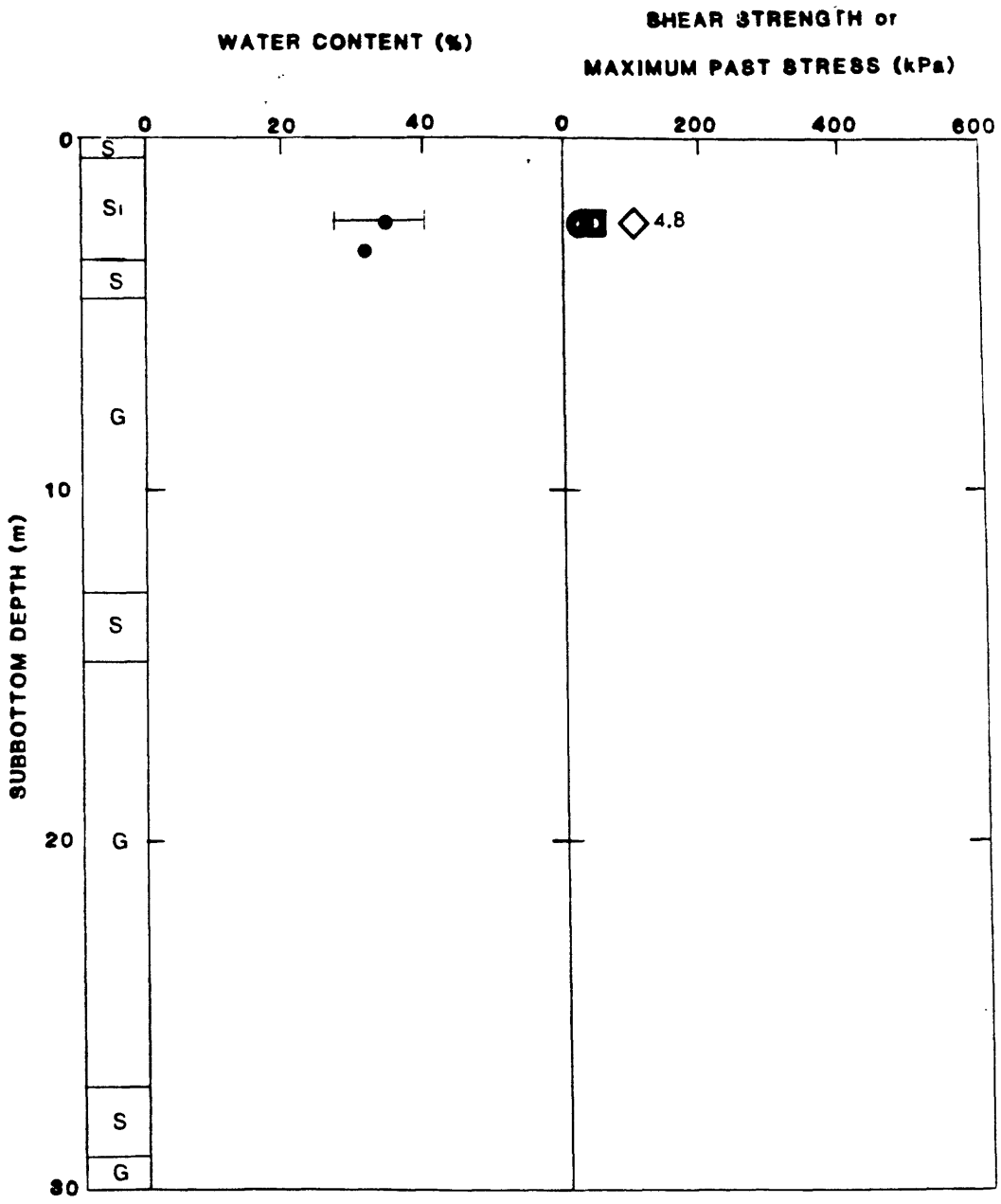

Figure 12. Physical properties and lithology profile for Boring HLA-5. See Figure 7 for legend.

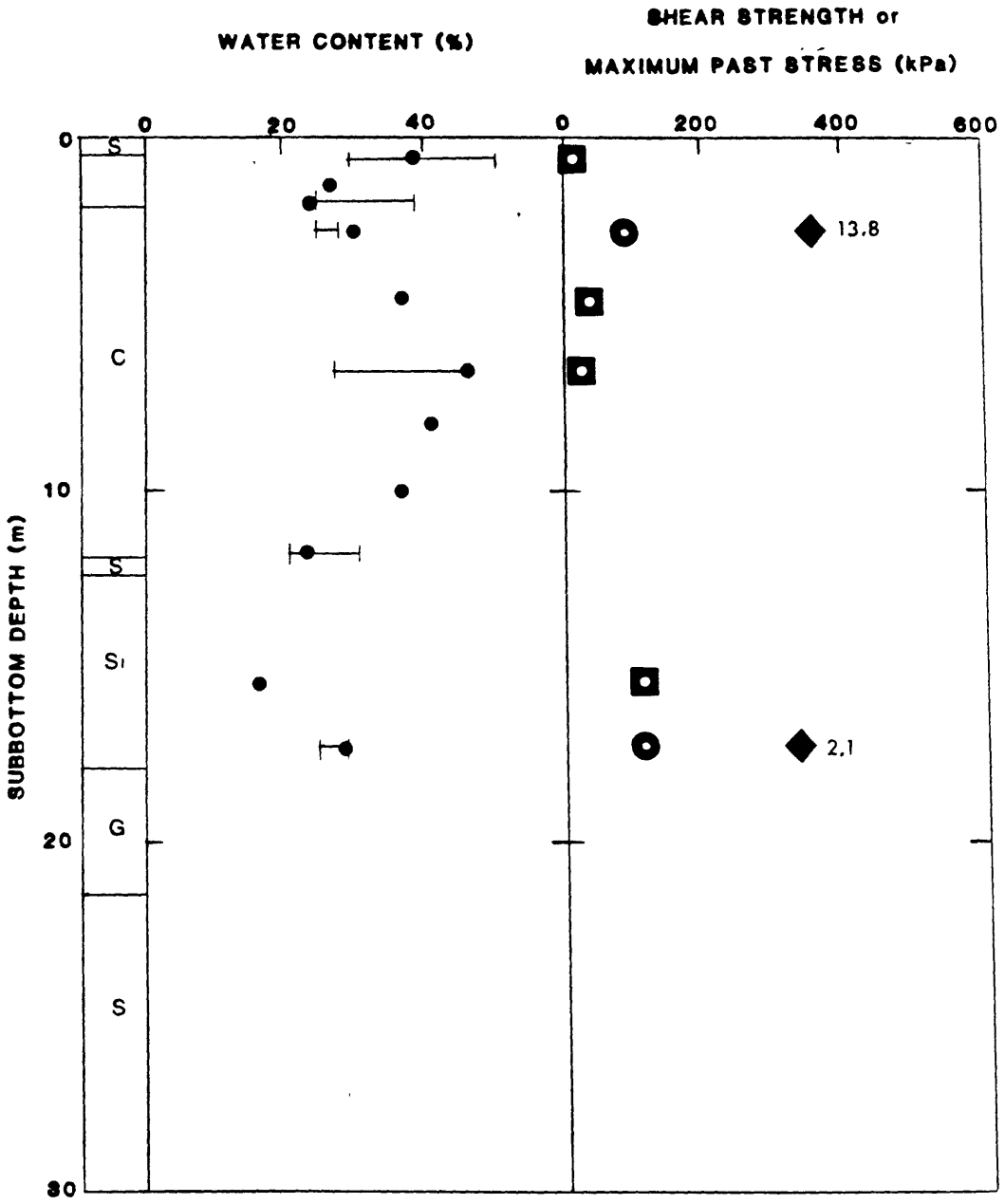

Figure 13. Physical properties and lithology profile for Boring HLA-6. See Figure 7 for legend.

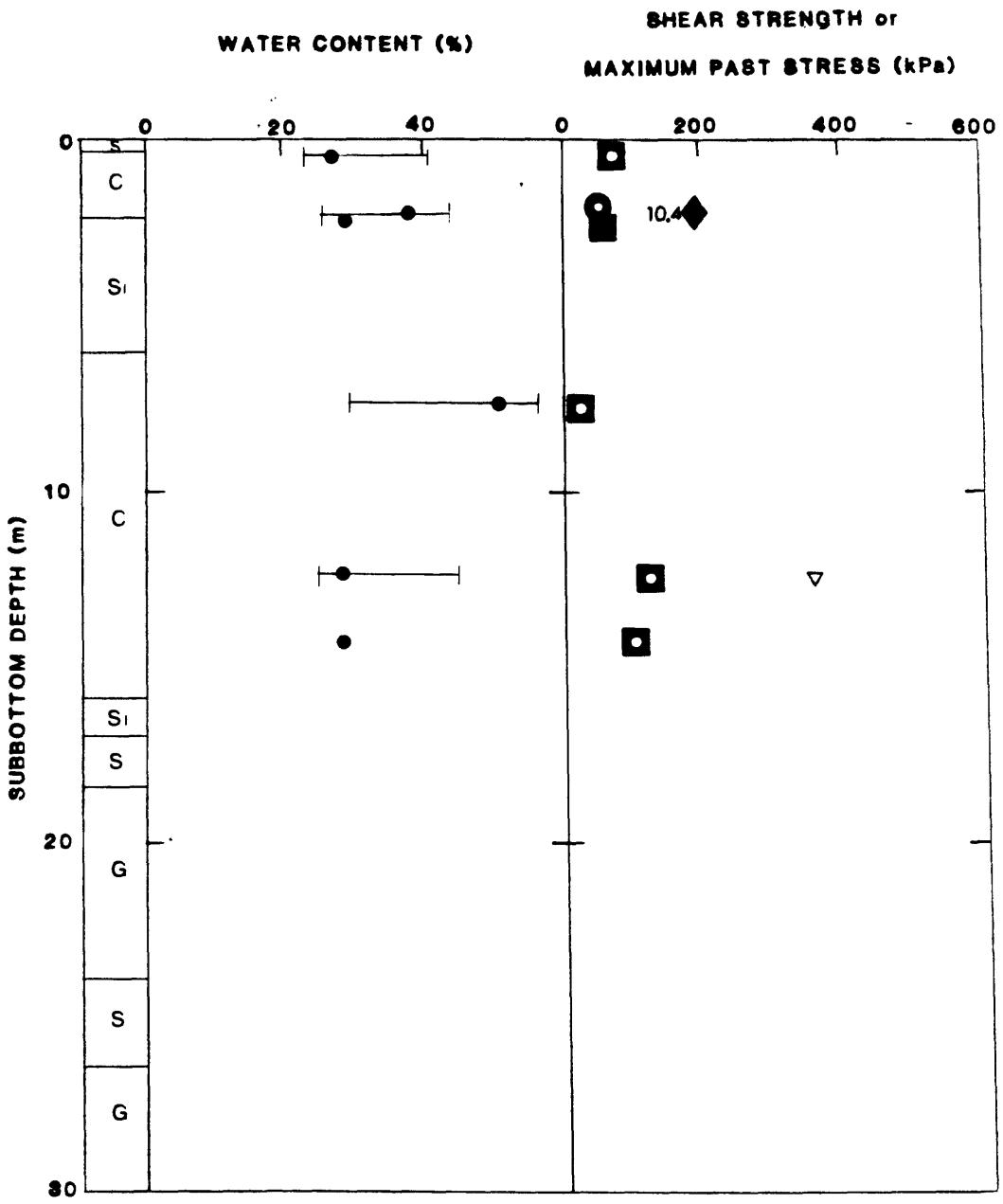

Figure 14. Physical properties and lithology profile for Boring HLA-7. See Figure 7 for legend.

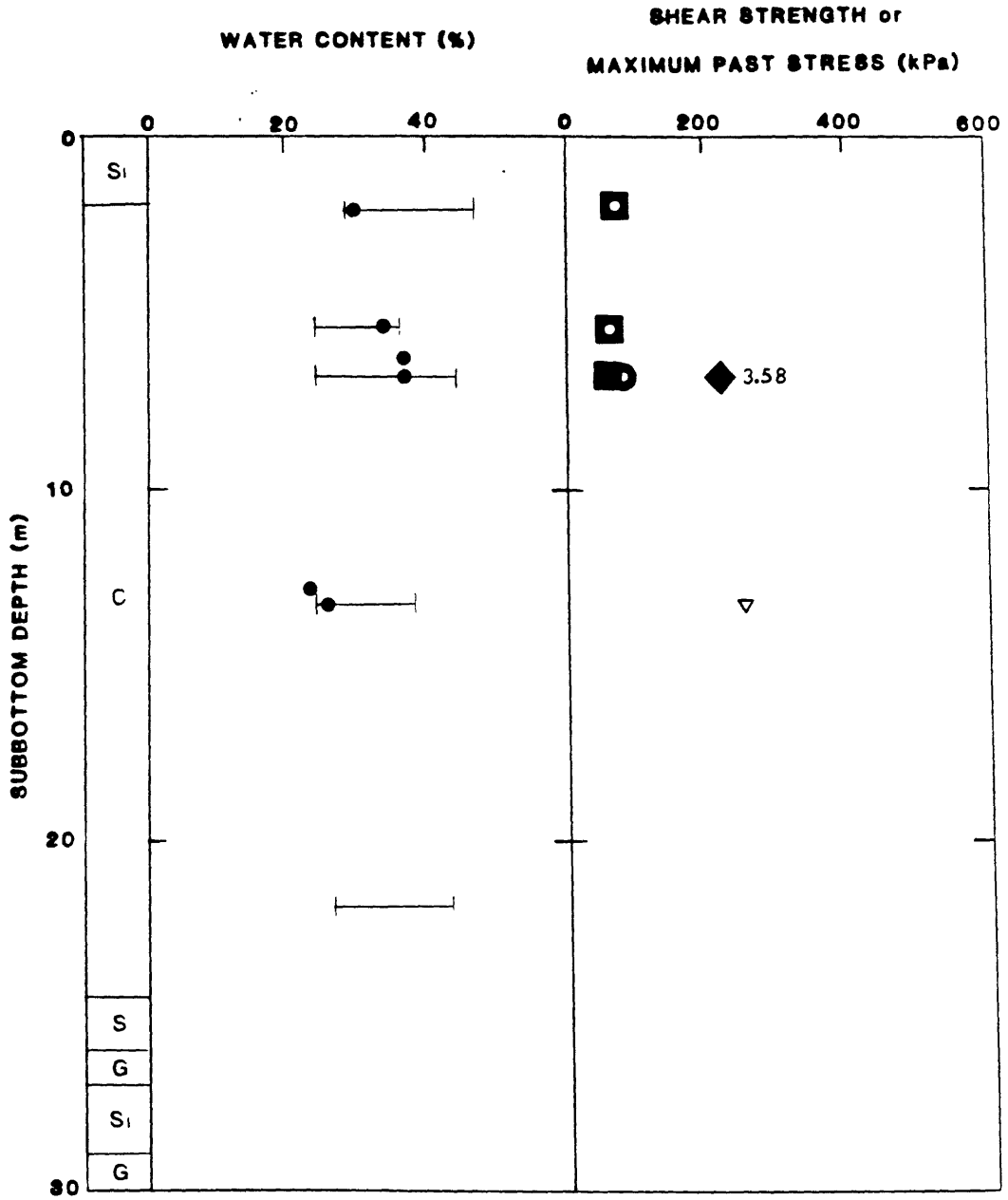

Figure 15. Physical properties and lithology profile for Boring HLA-8. See Figure 7 for legend.

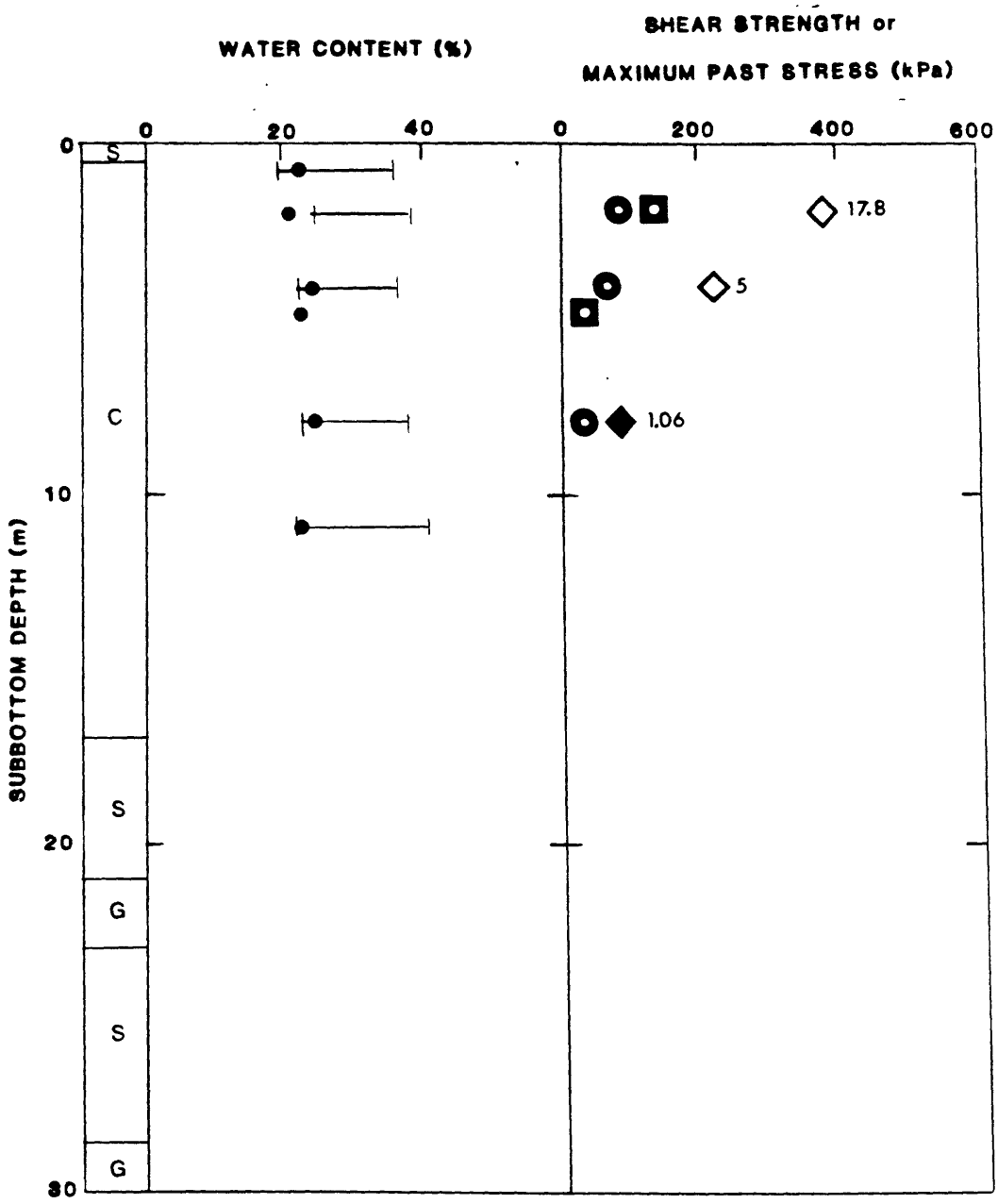

Figure 16. Physical properties and lithology profile for Boring HLA-9. See Figure 7 for legend.

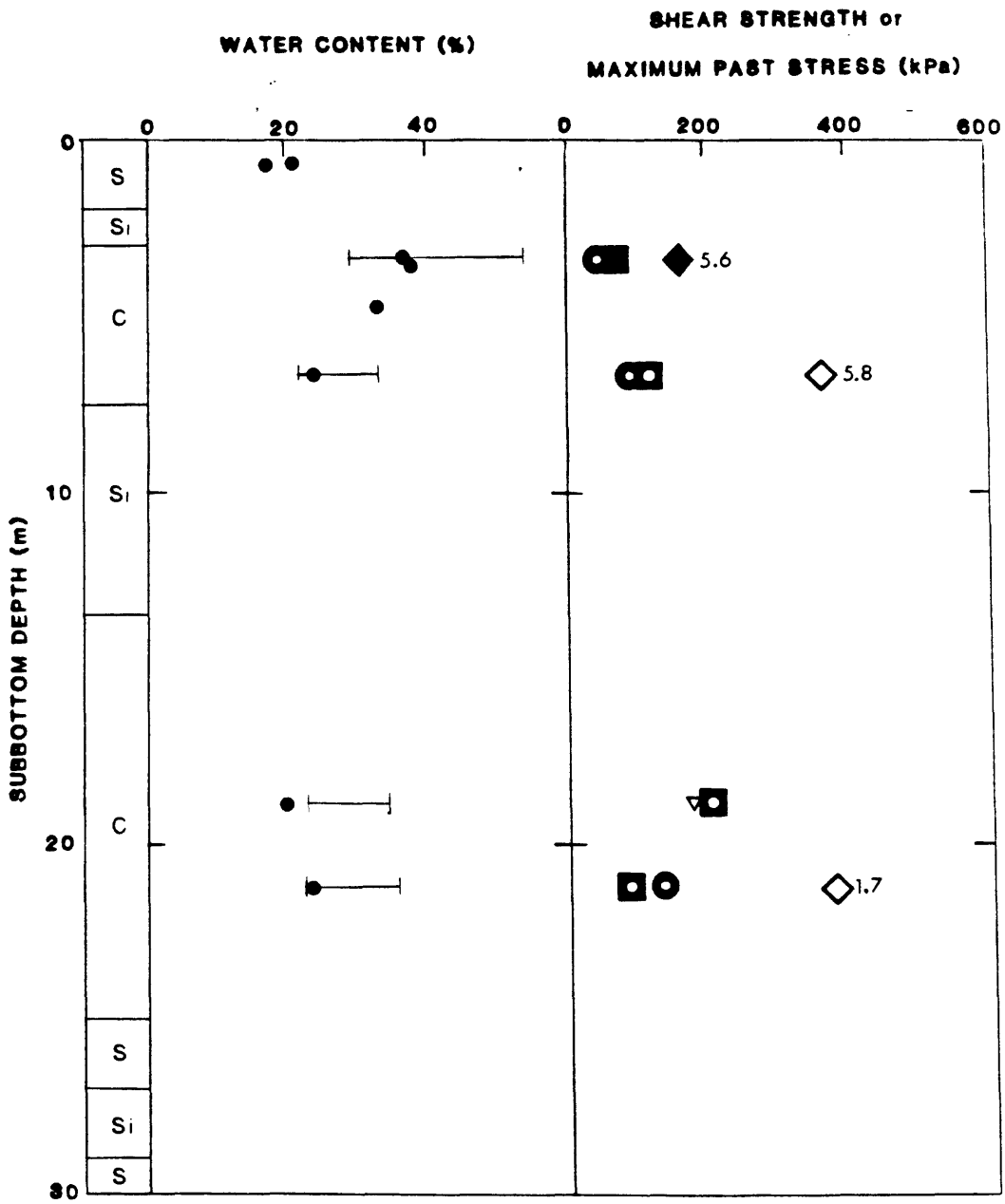

Figure 17. Physical properties and lithology profile for Boring HLA-10. See Figure 7 for legend.

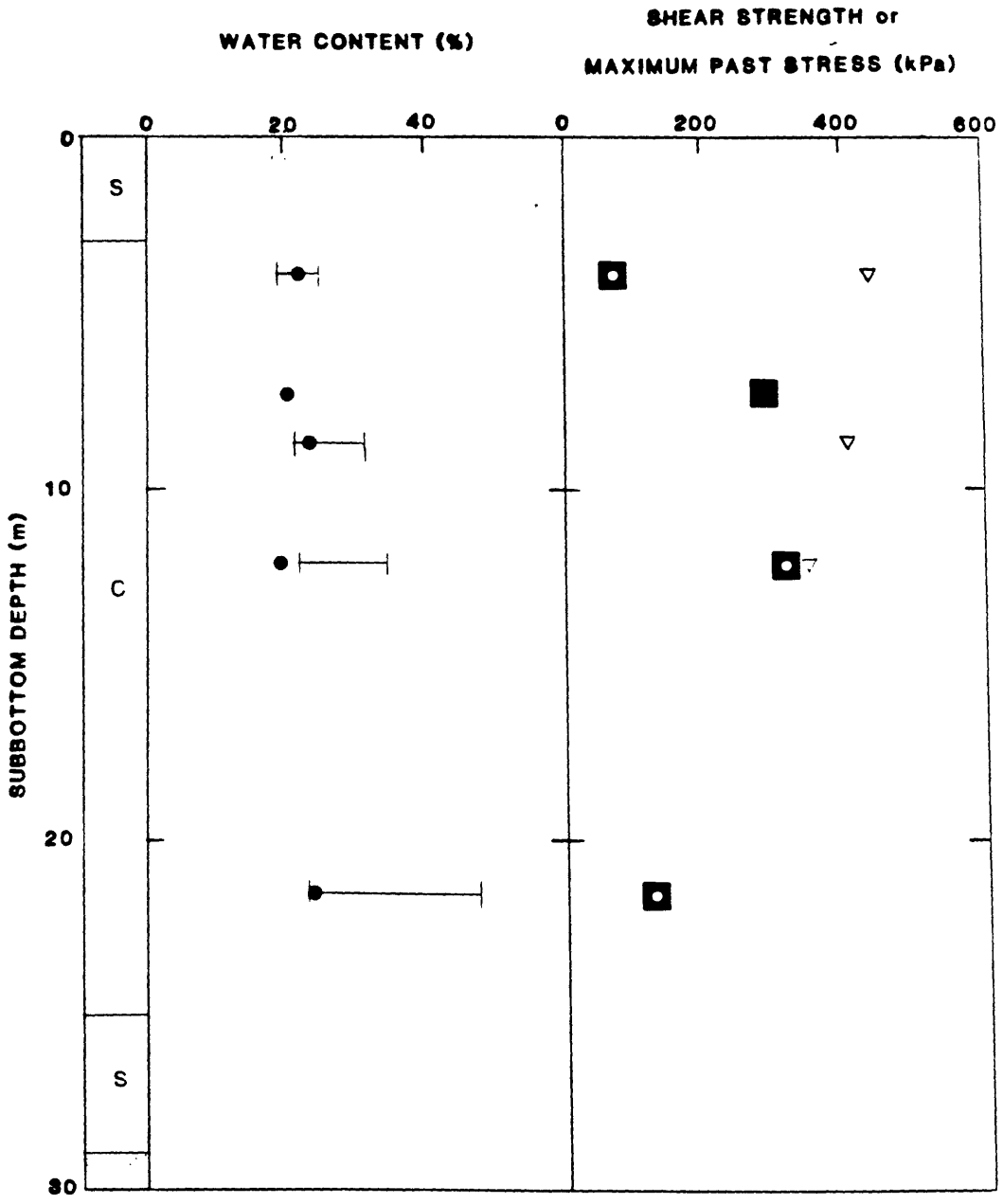

Figure 18. Physical properties and lithology profile for Boring HLA-11. See Figure 7 for legend.

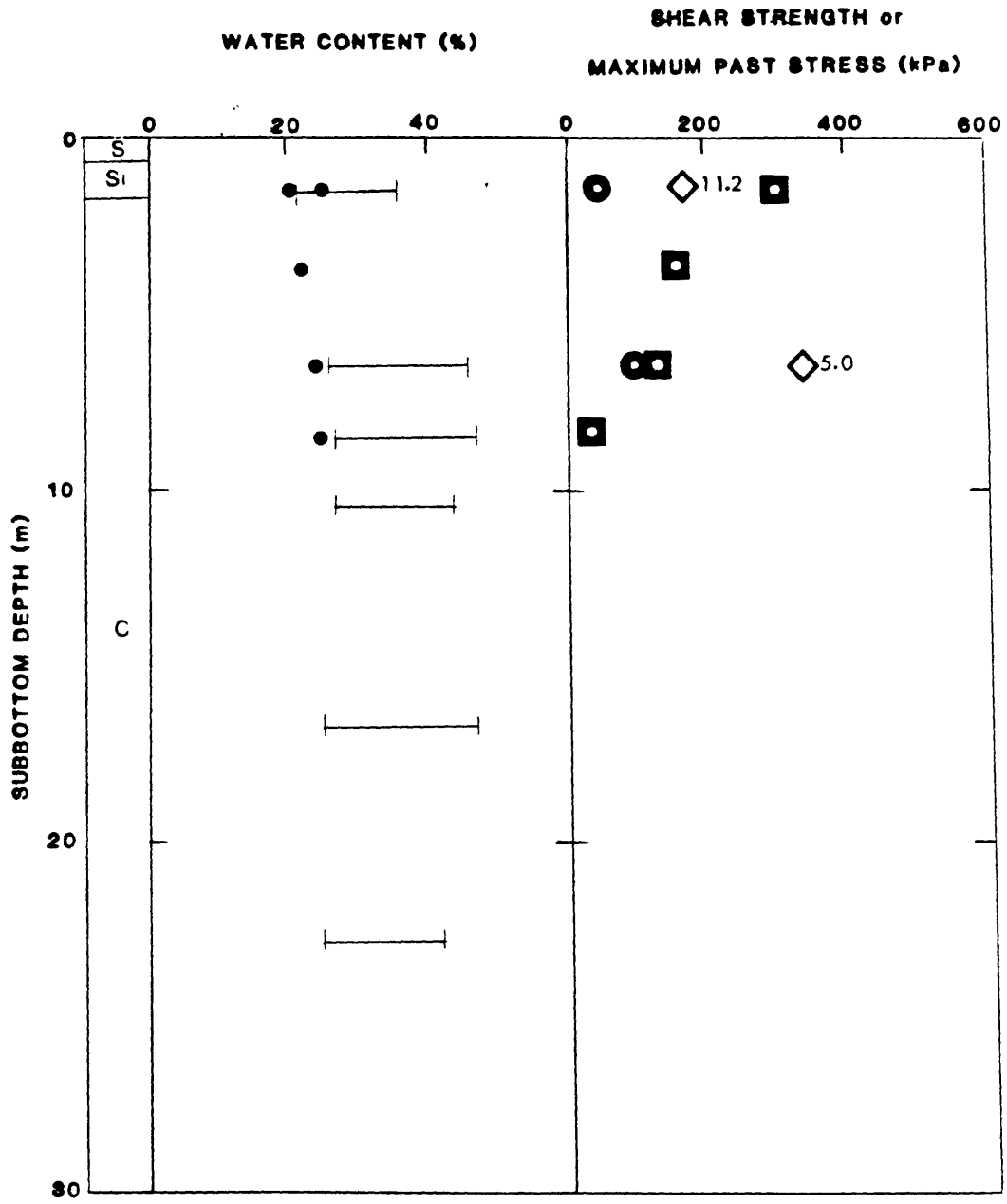

Figure 19. Physical properties and lithology profile for Boring HLA-12. See Figure 7 for legend.

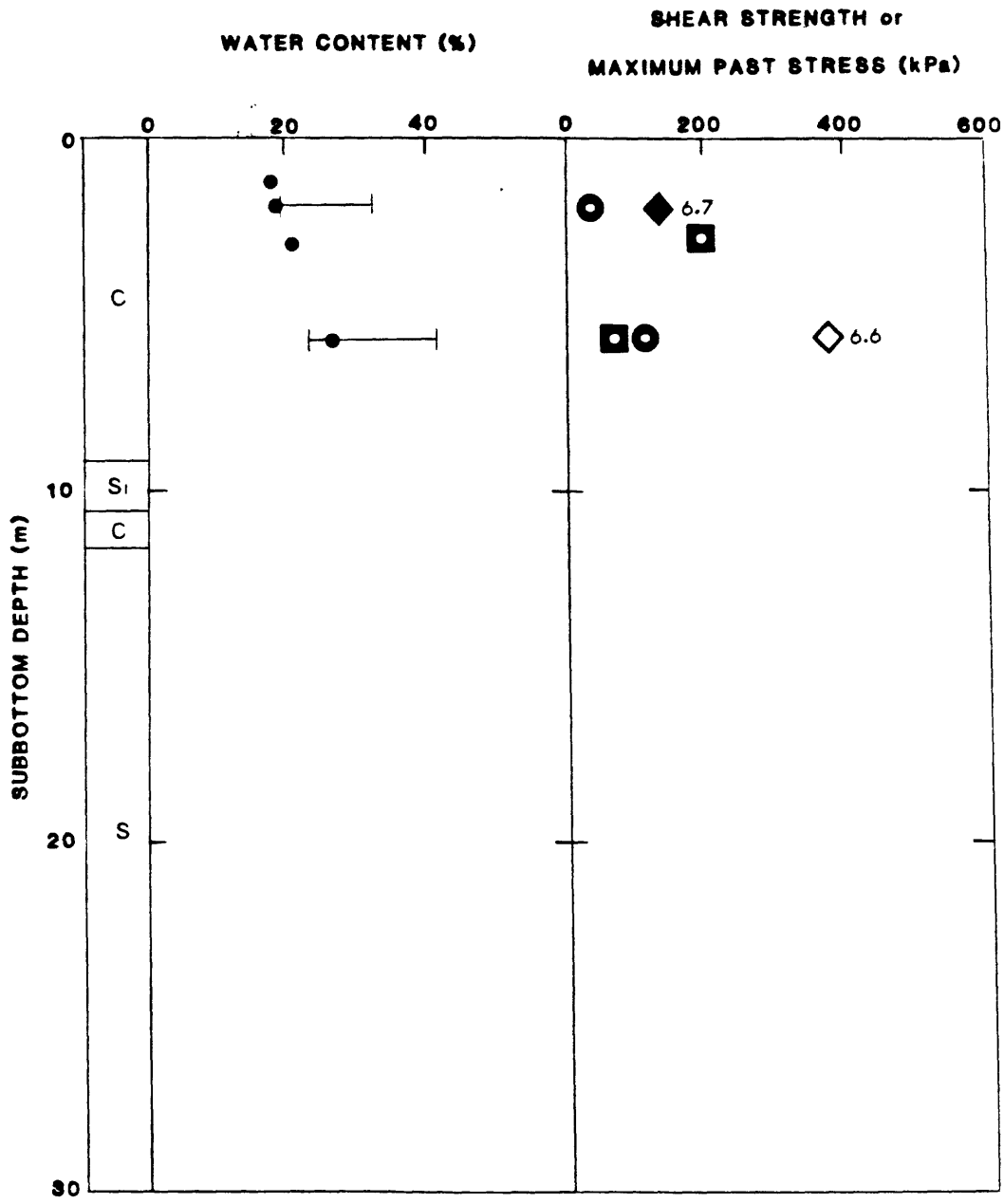

Figure 20. Physical properties and lithology profile for Boring HLA-13. See Figure 7 for legend.

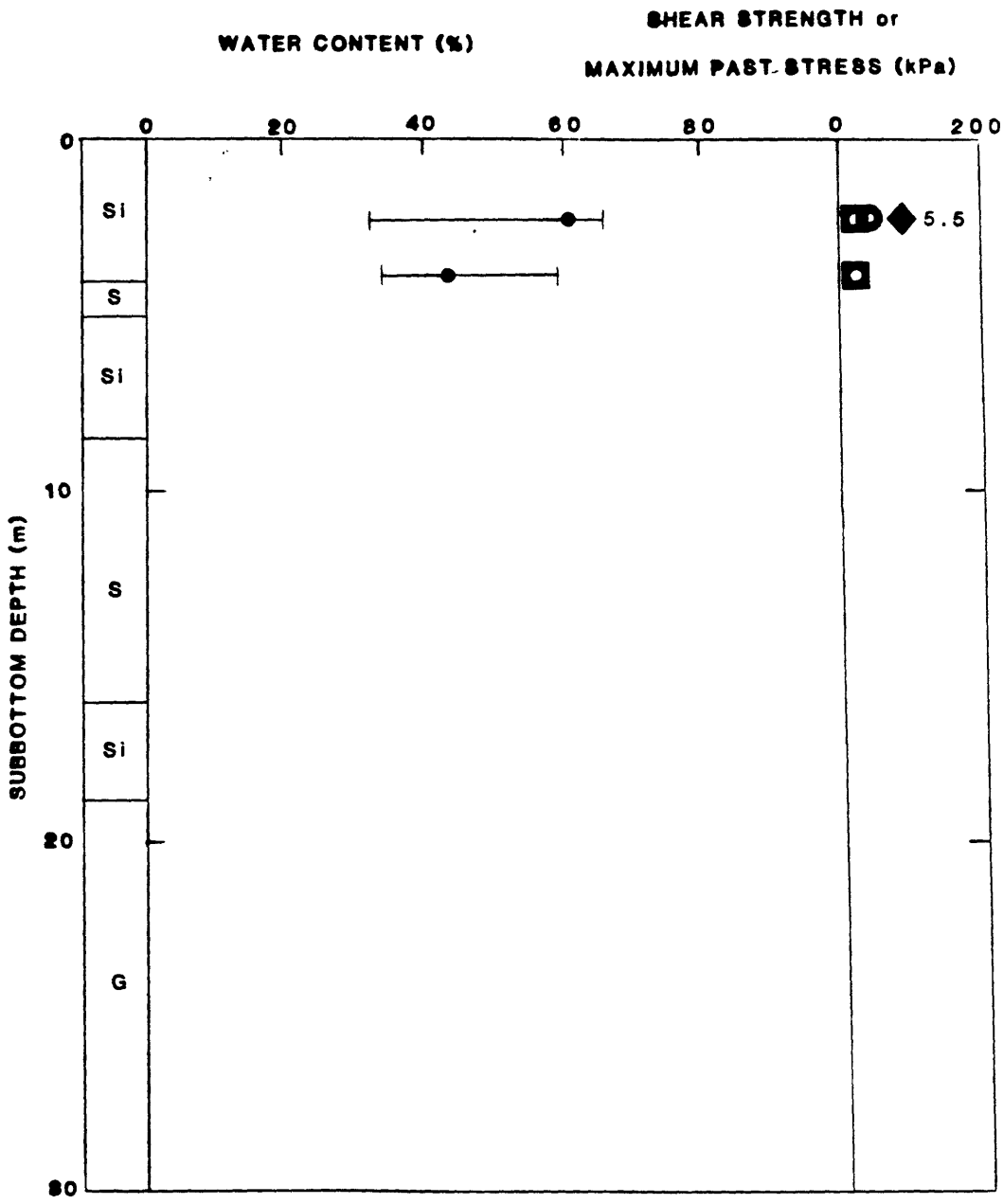

Figure 21. Physical properties and lithology profile for Boring HLA-14. See Figure 7 for legend.

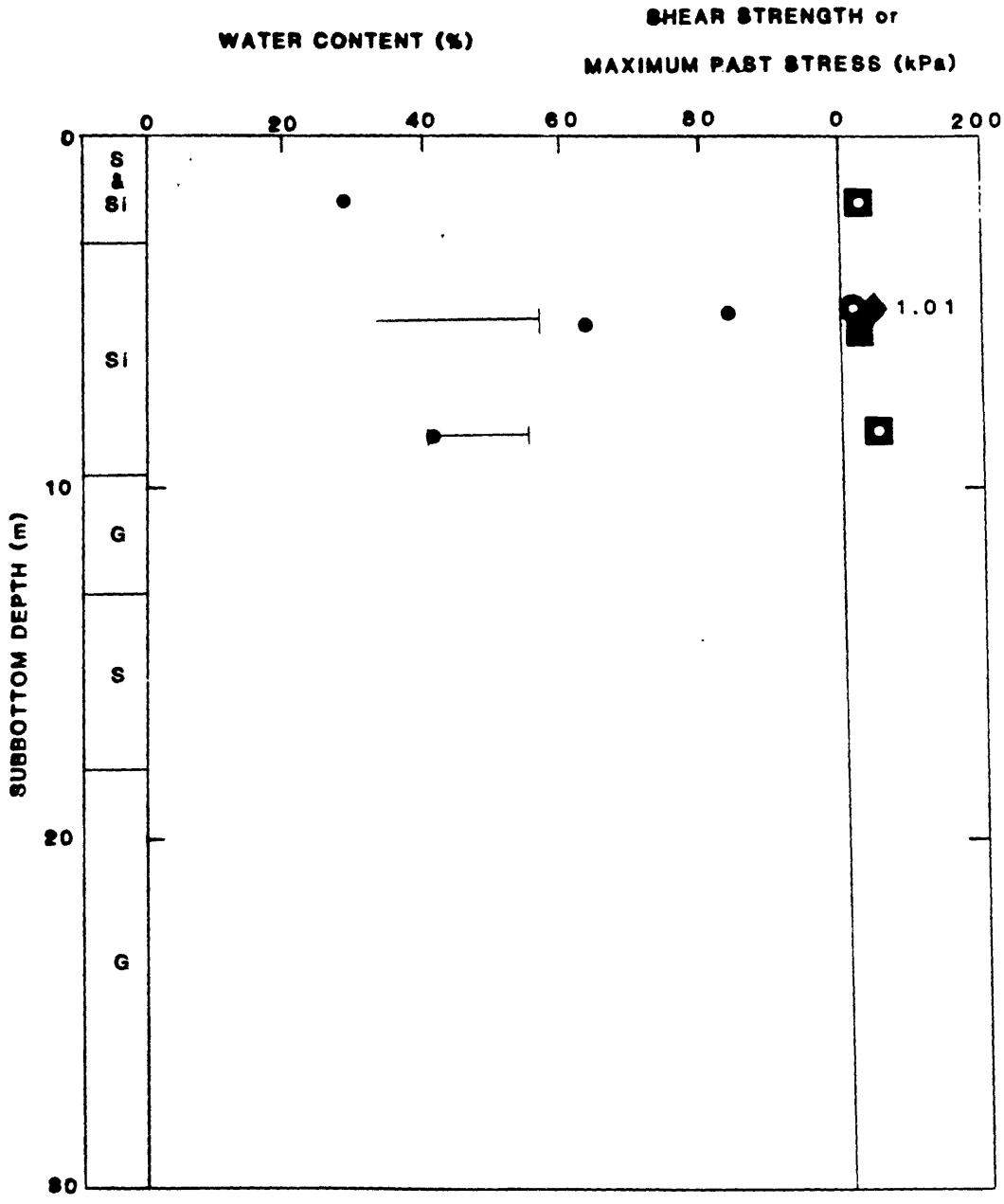

Figure 22. Physical properties and lithology profile for Boring HLA-15. See Figure 7 for legend.

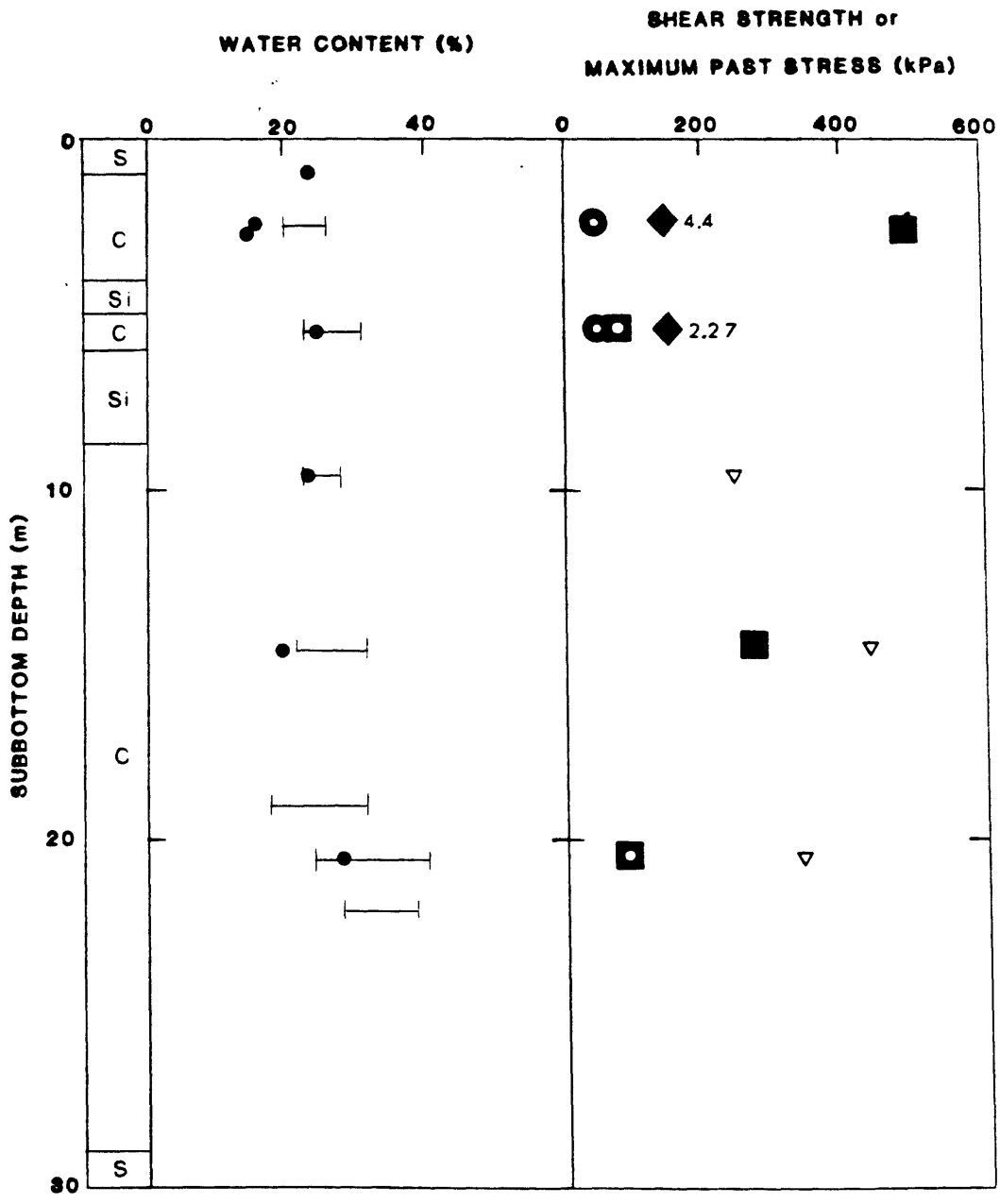

Figure 23. Physical properties and lithology profile for Boring HLA-16. See Figure 7 for legend.

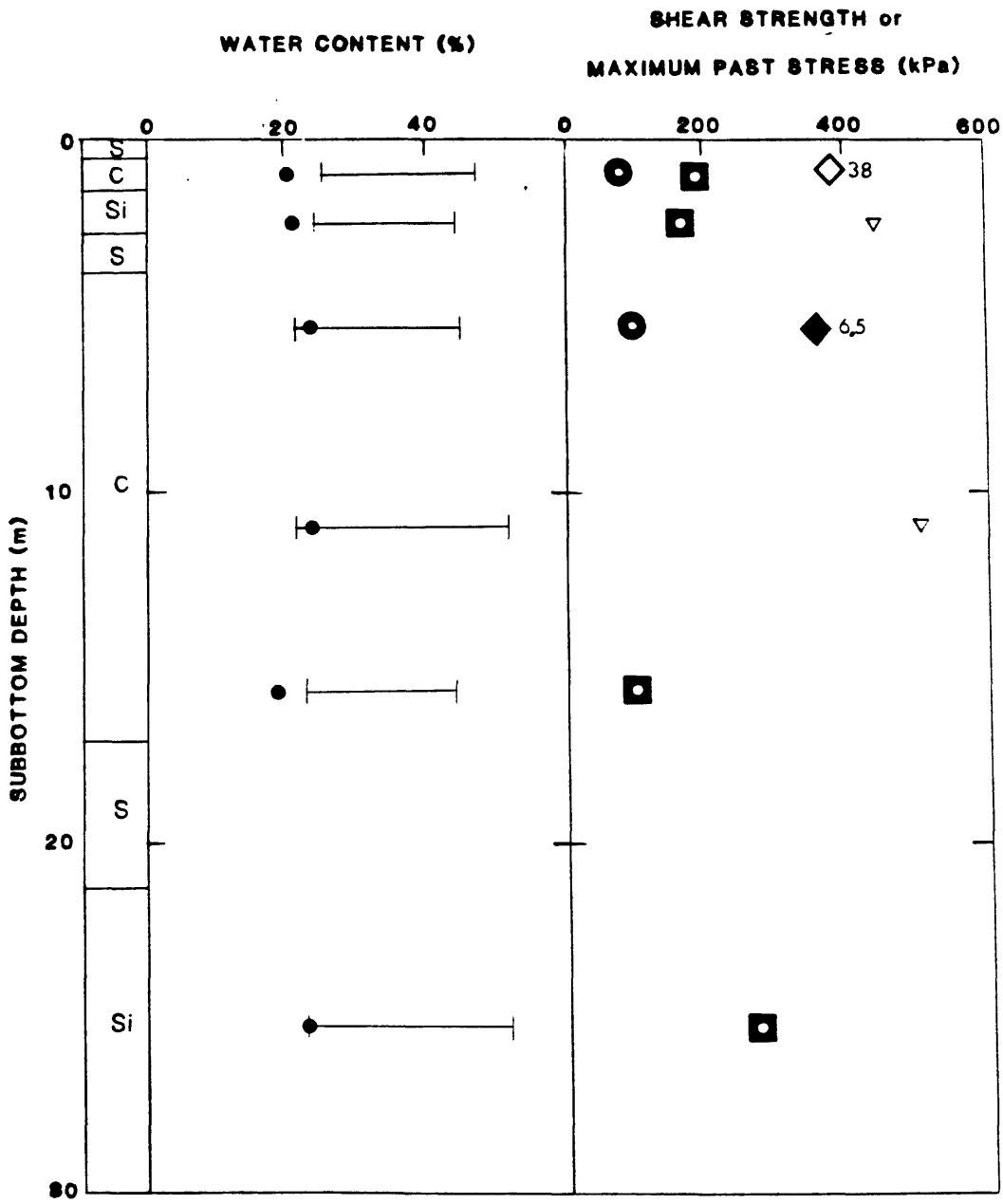

Figure 24. Physical properties and lithology profile for Boring HLA-17. See Figure 7 for legend.

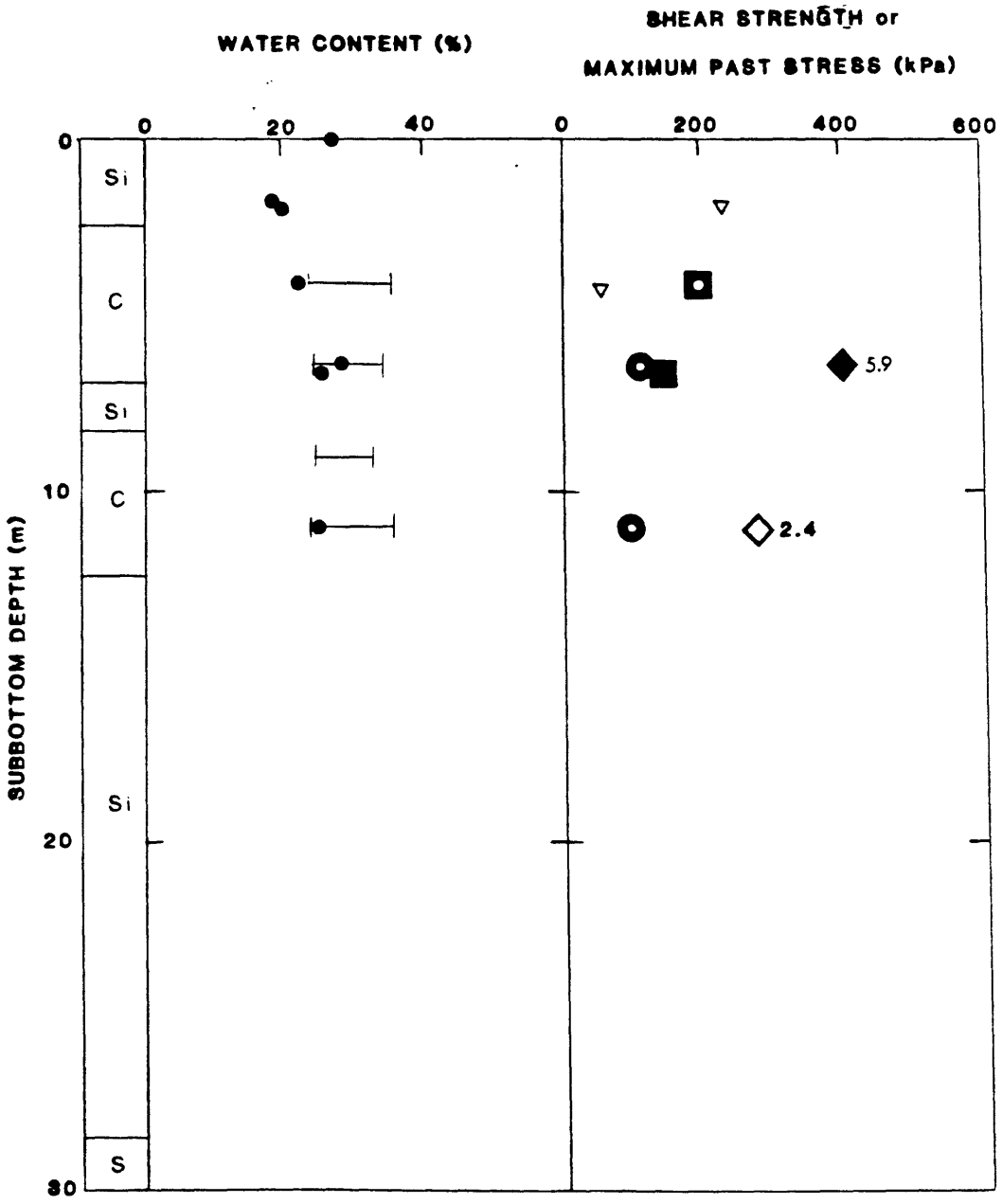

Figure 25. Physical properties and lithology profile for Boring HLA-18. See Figure 7 for legend.

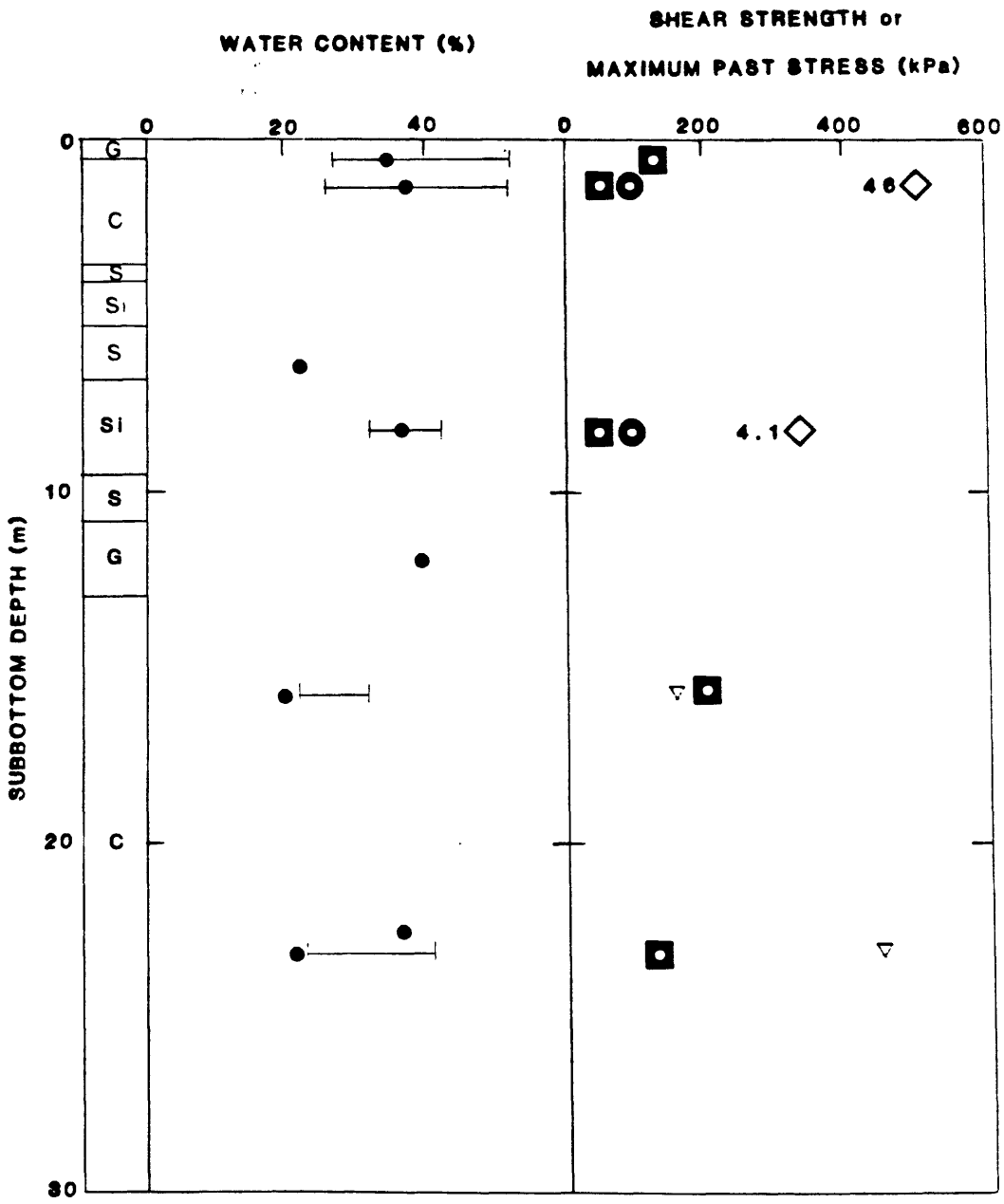

Figure 26. Physical properties and lithology profile for Boring HLA-19. See Figure 7 for legend.

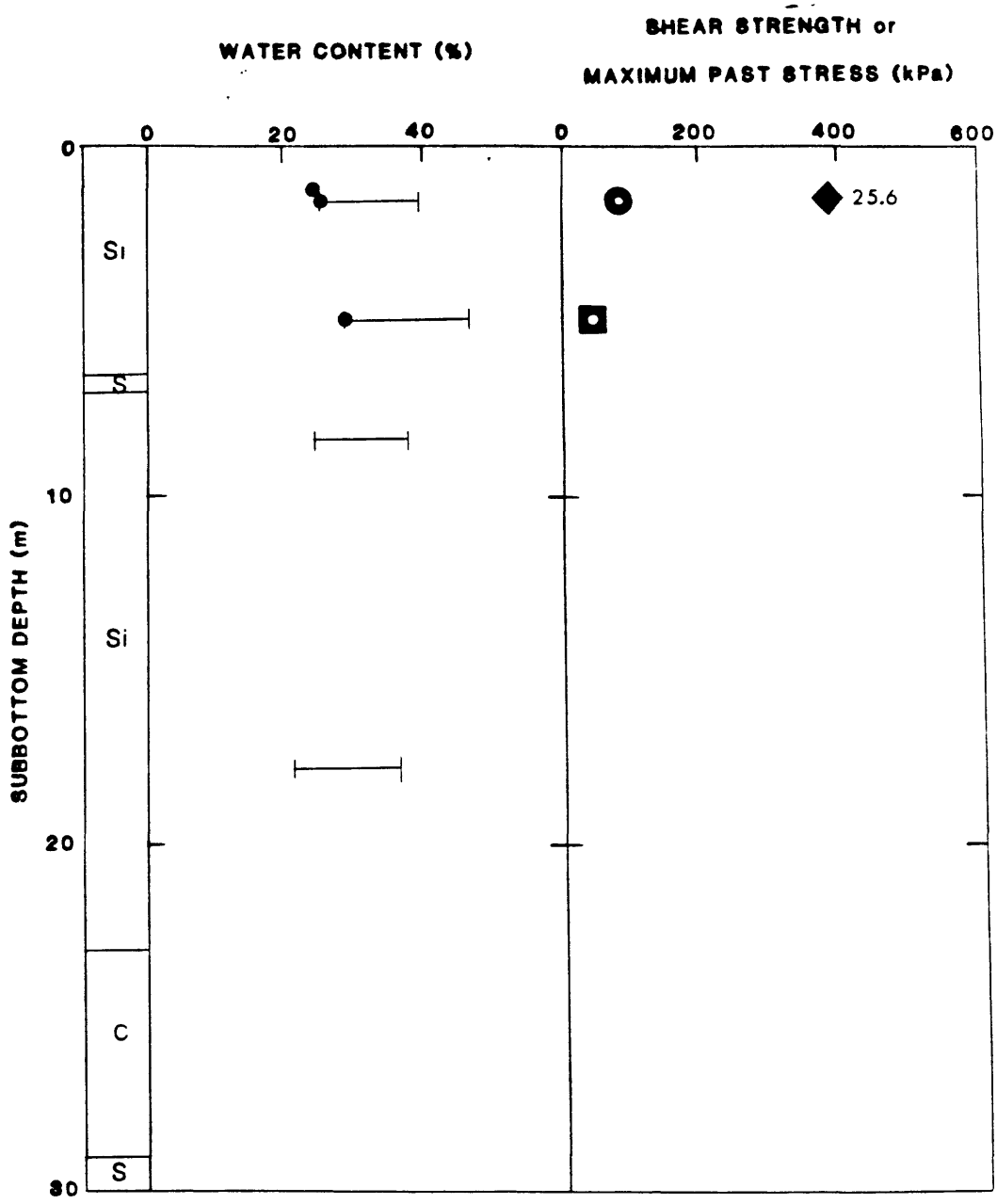

Figure 27. Physical properties and lithology profile for Boring HLA-20. See Figure 7 for legend.

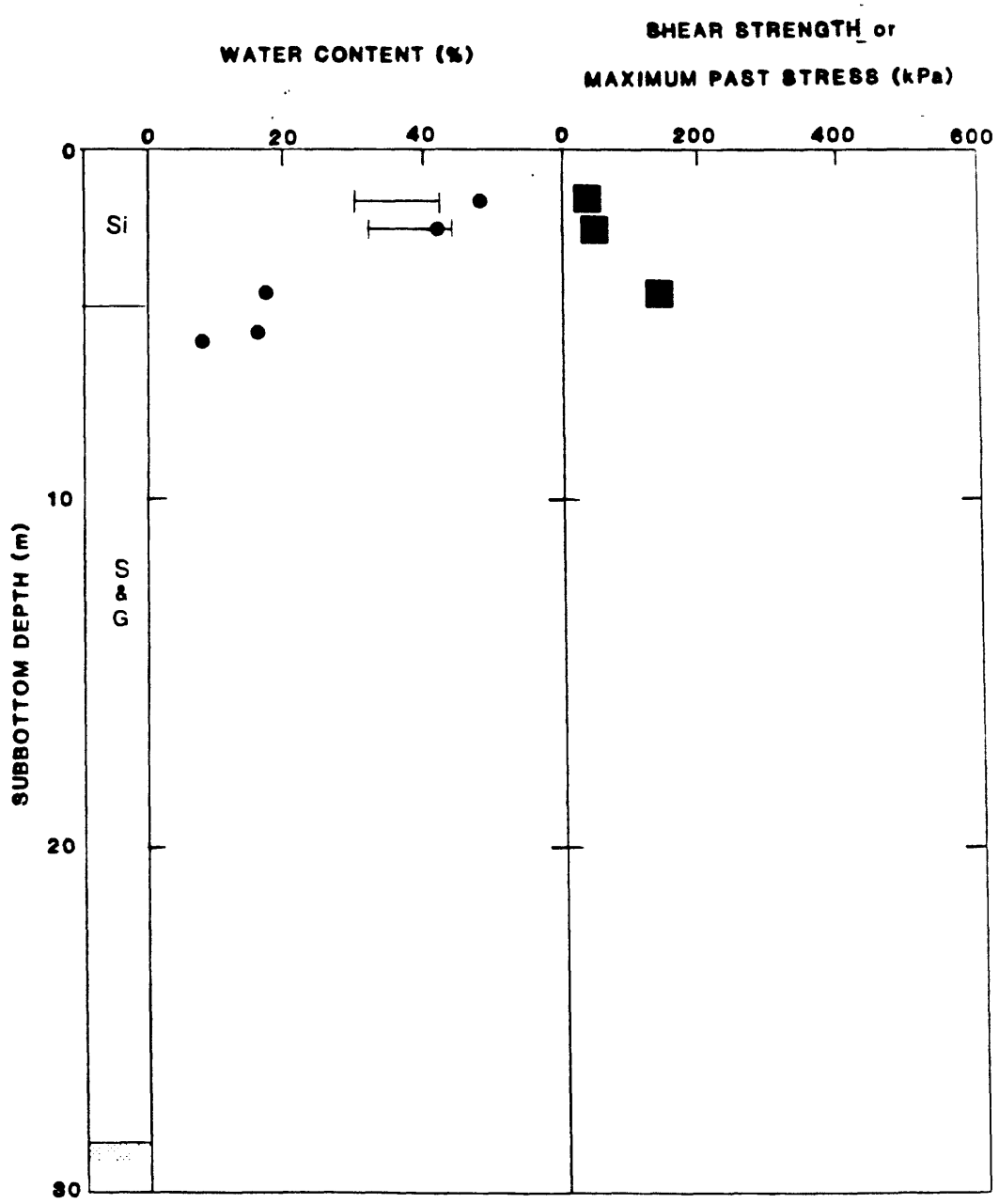

Figure 28. Physical properties and lithology profile for Boring PB-1. See Figure 7 for legend.

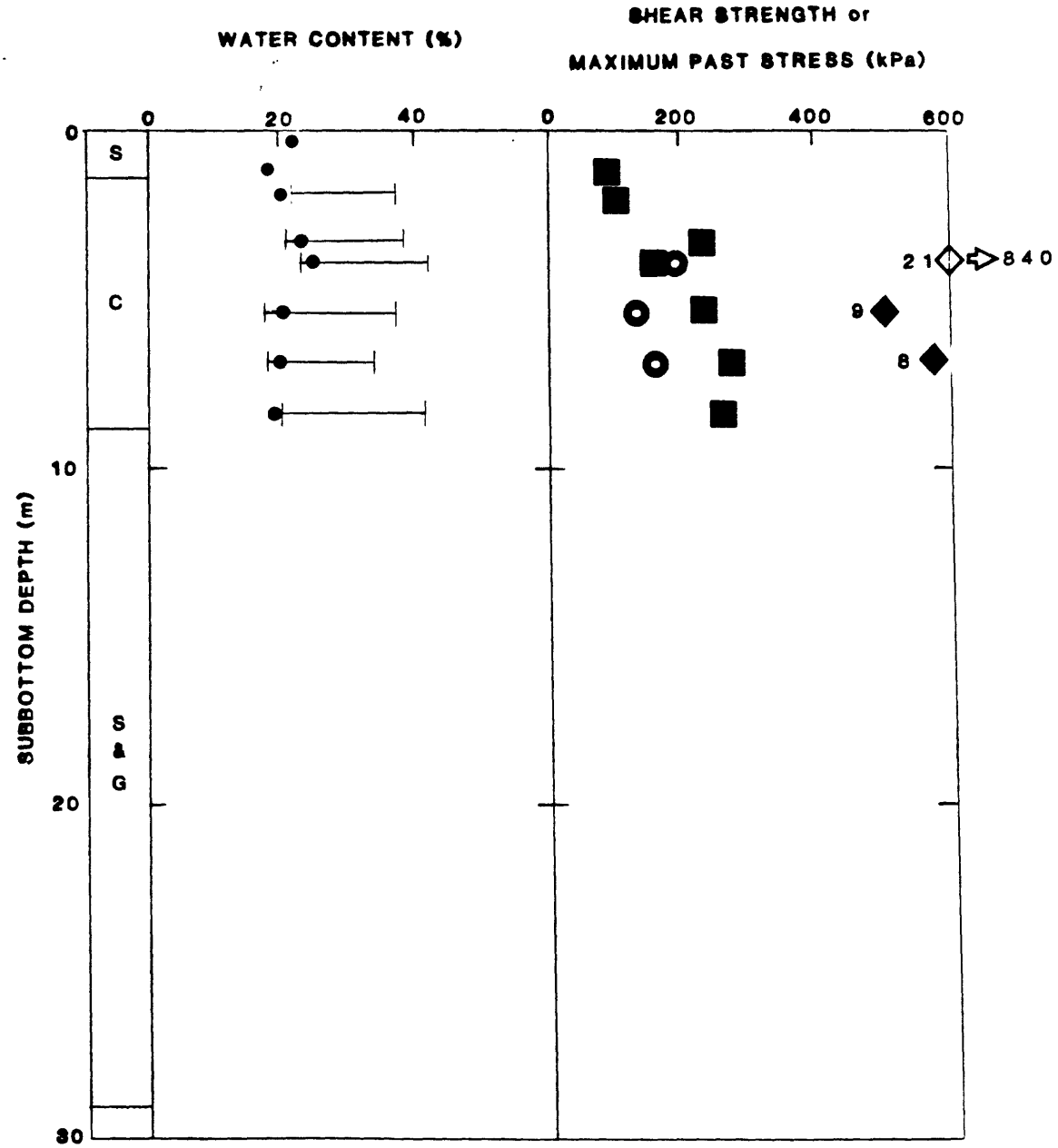

Figure 29. Physical properties and lithology profile for Boring PB-2. See Figure 7 for legend.

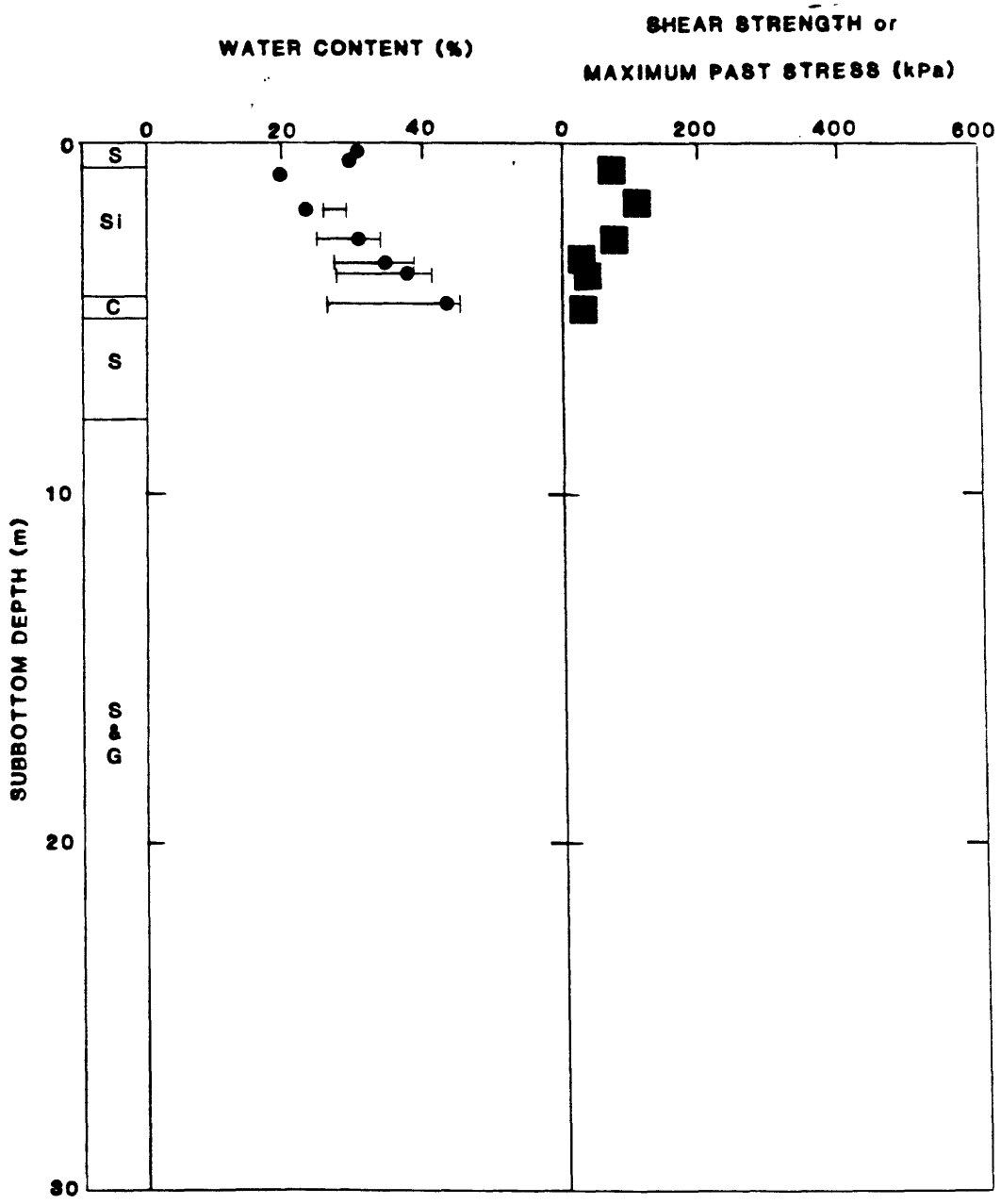

Figure 30. Physical properties and lithology profile for Boring PB-3. See Figure 7 for legend.

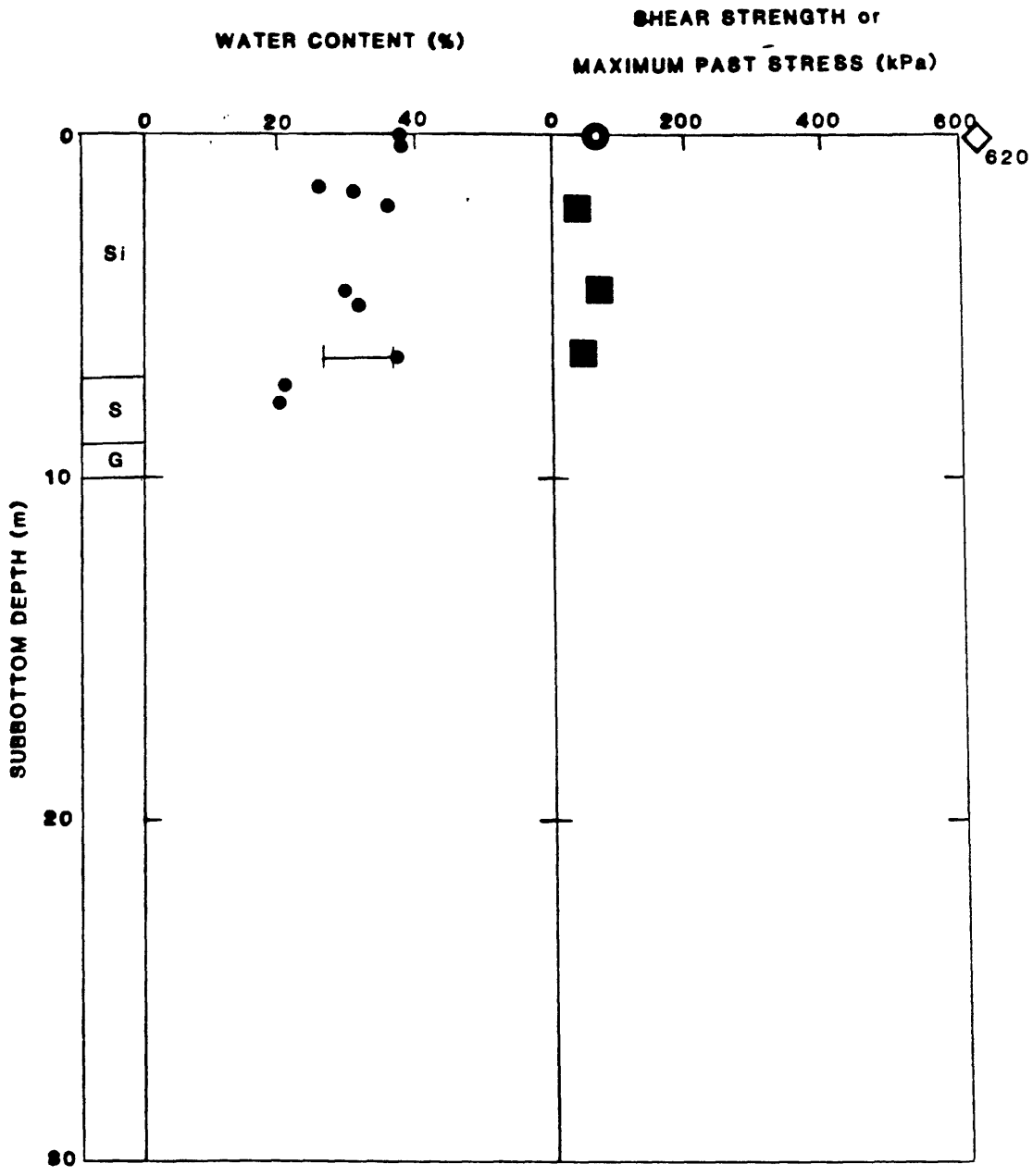

Figure 31. Physical properties and lithology profile for Boring PB-5. See Figure 7 for legend.

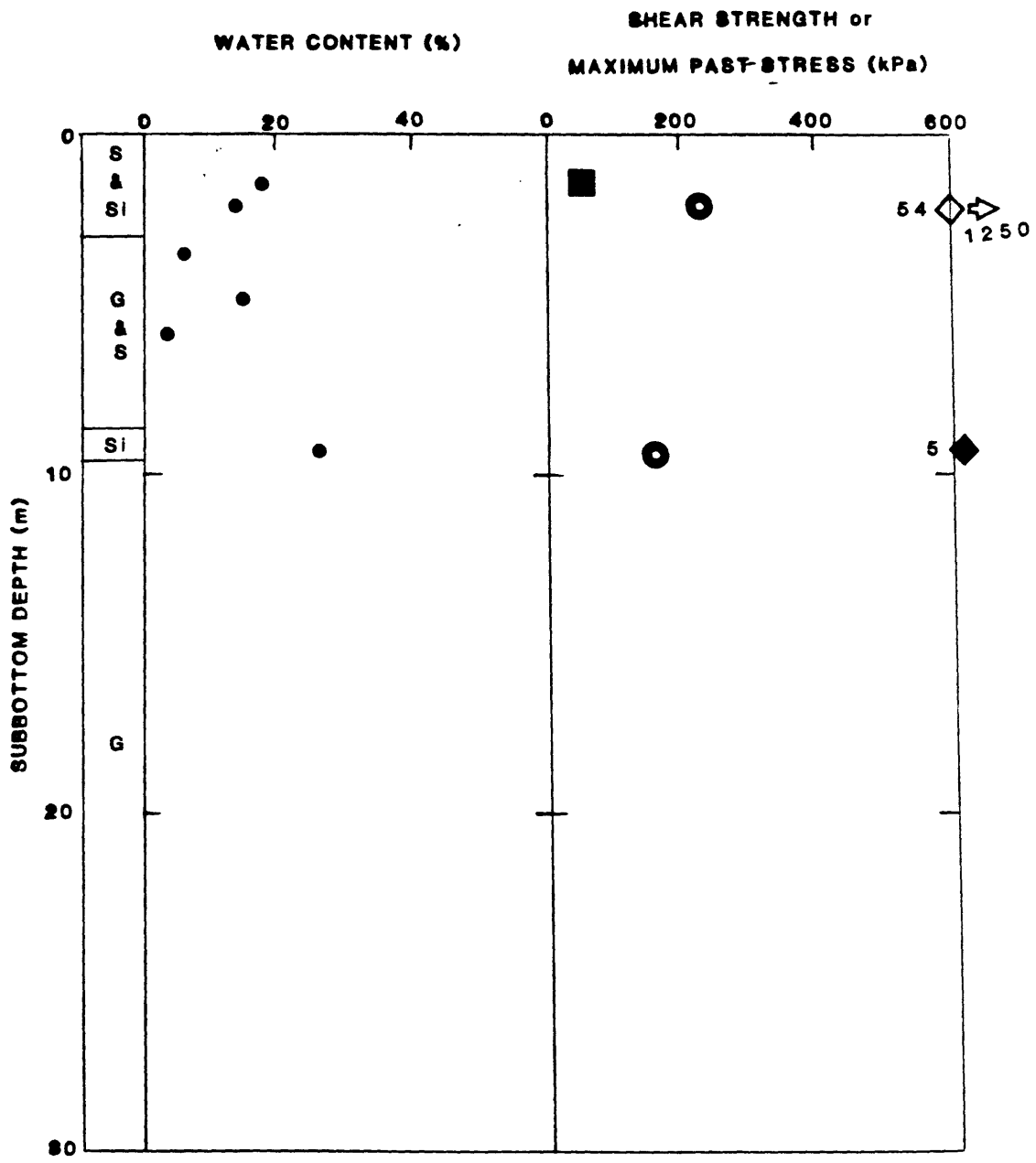

Figure 32. Physical properties and lithology profile for Boring PB-6. See Figure 7 for legend.

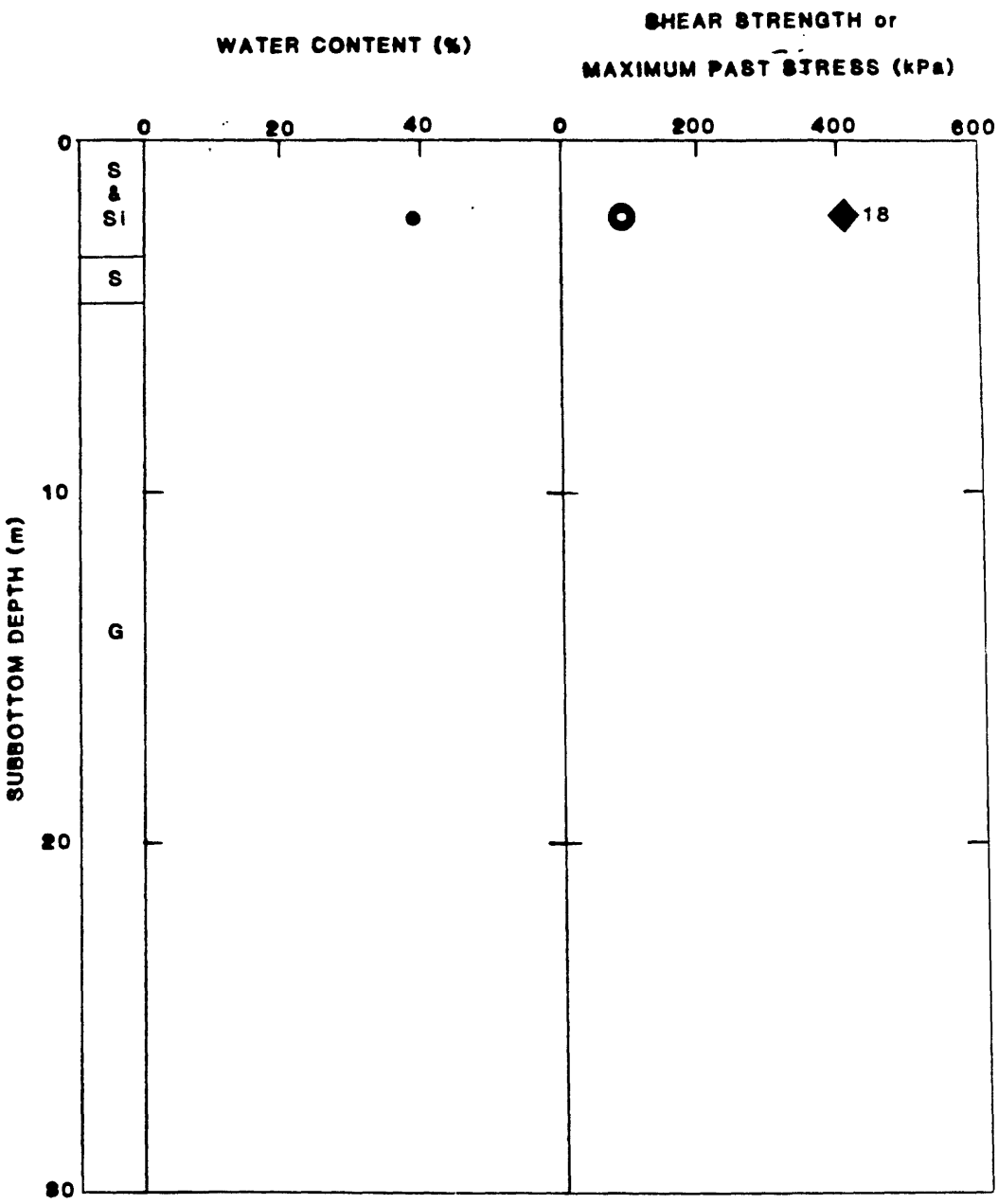

Figure 33. Physical properties and lithology profile for Boring PB-7. See Figure 7 for legend.

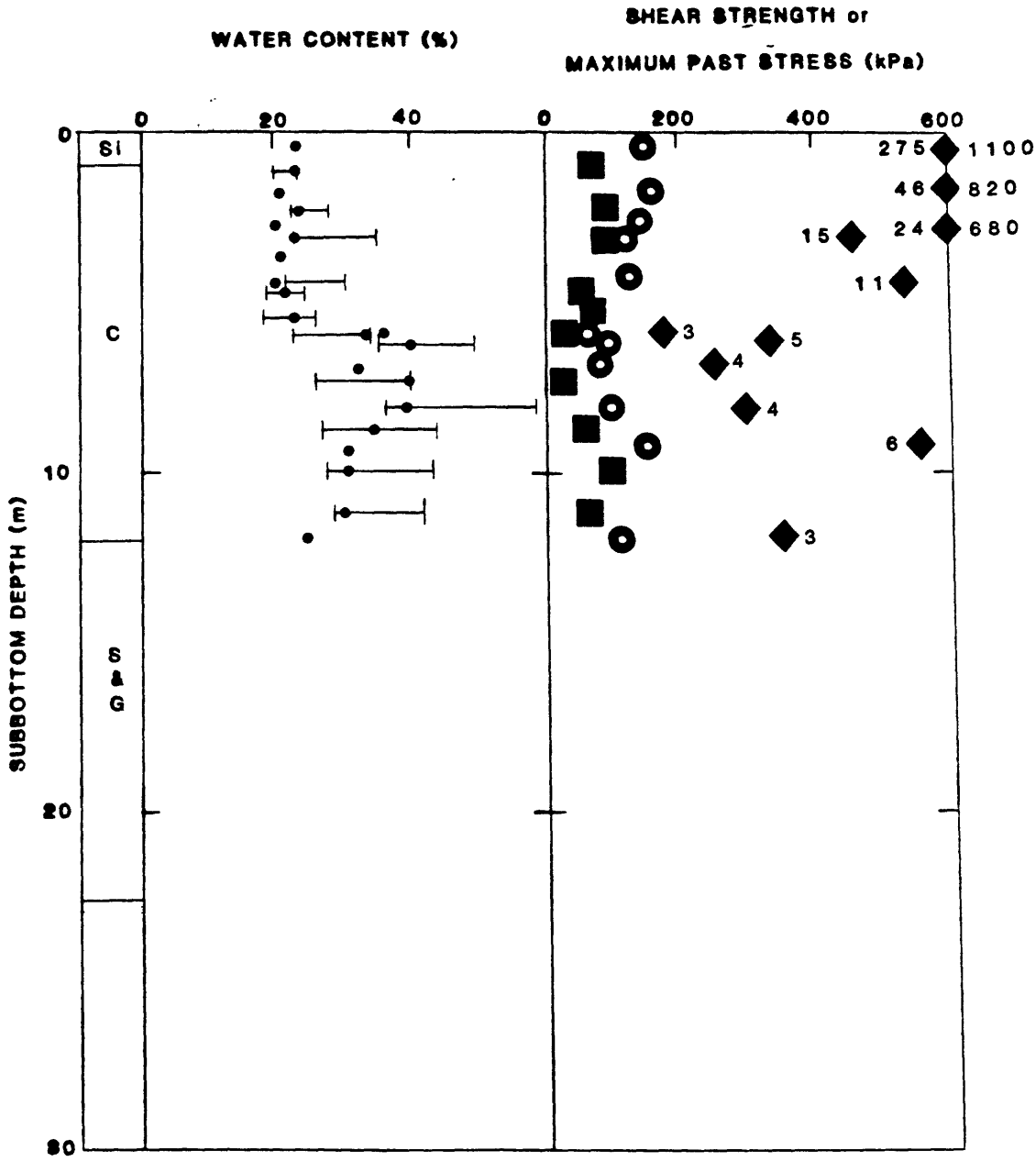

Figure 34. Physical properties and lithology profile for Boring PB-8. See Figure 7 for legend.

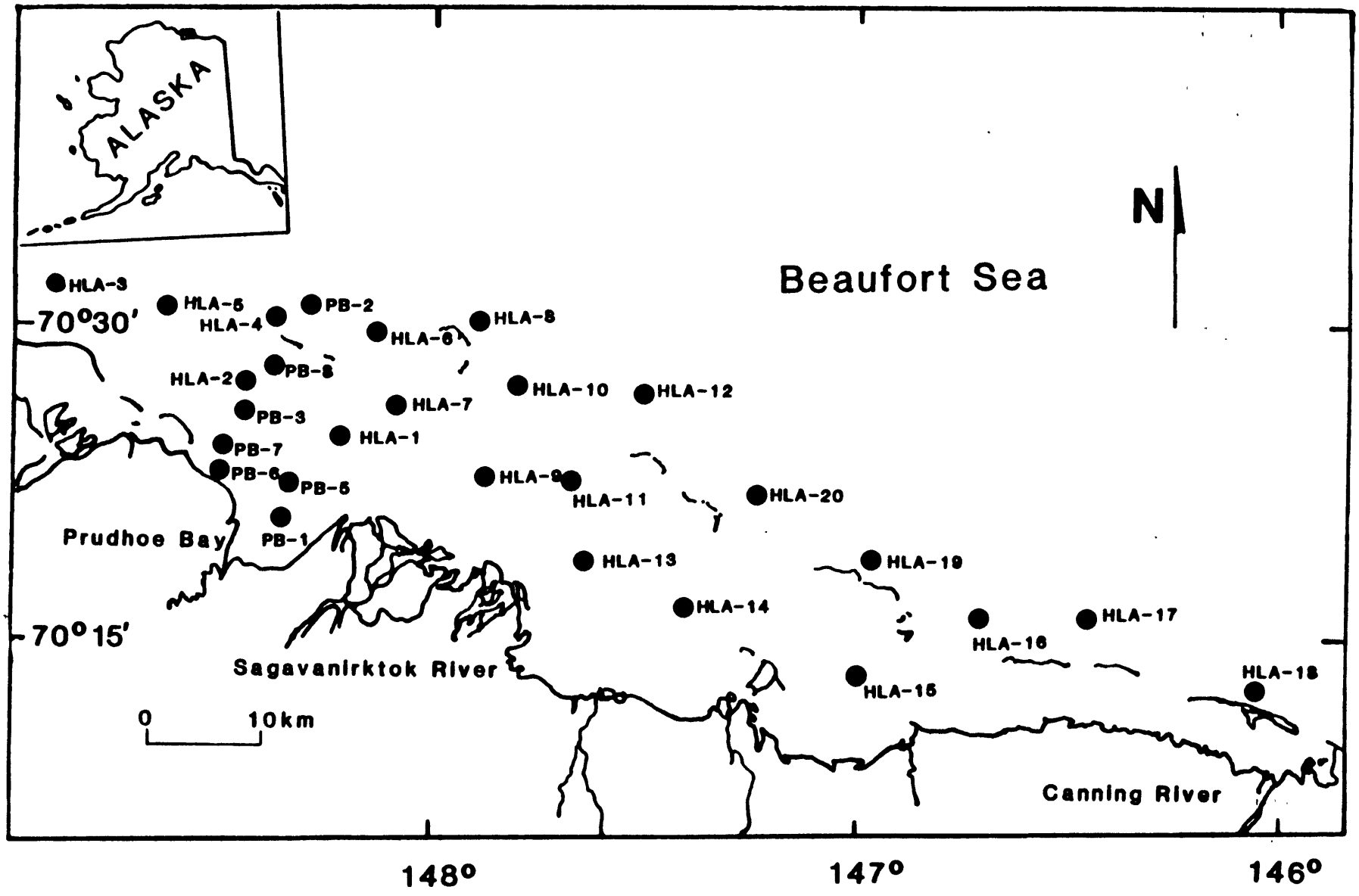

Figure 35. Location of borings.

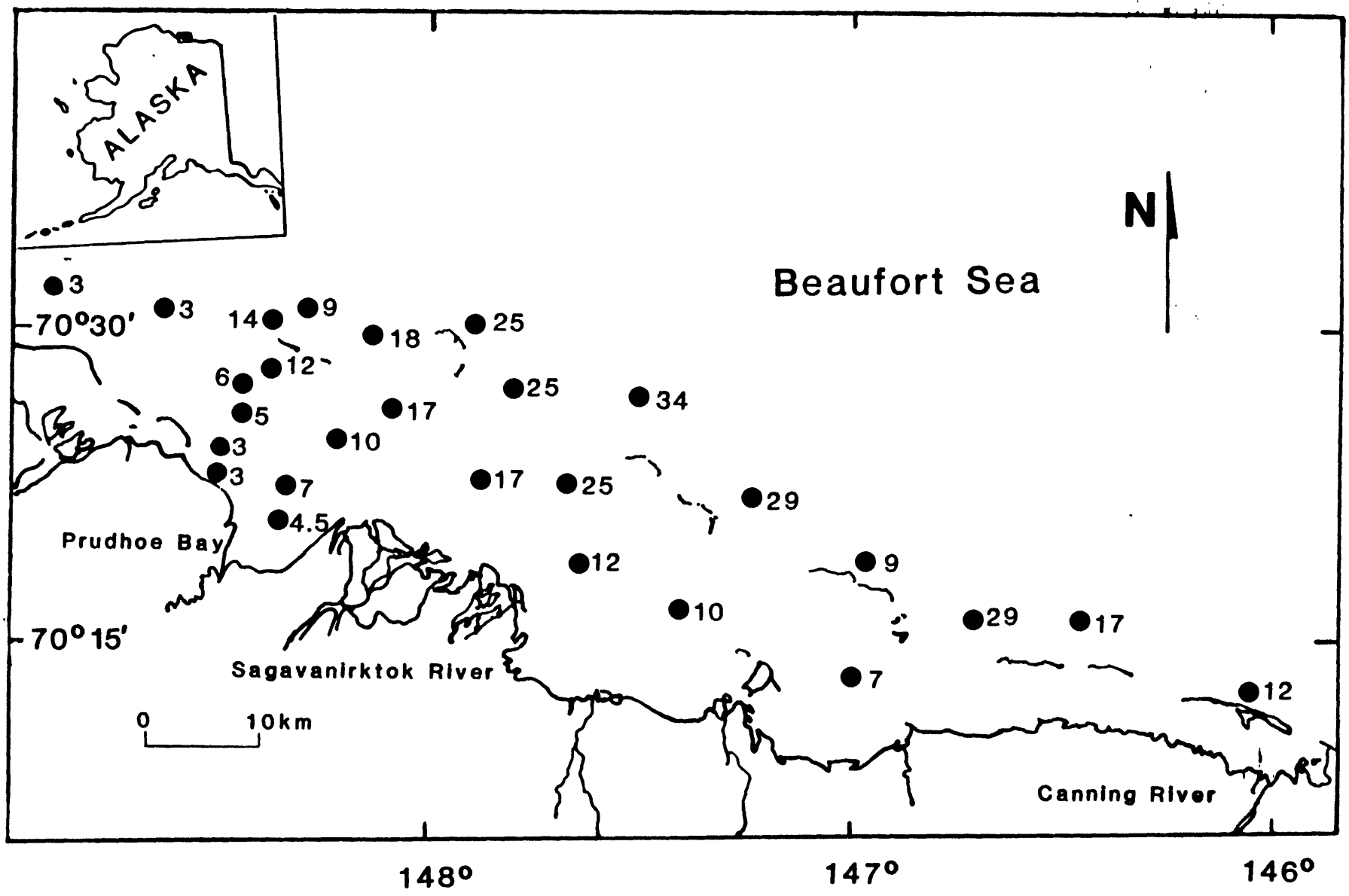

Figure 36. Variation in thickness (m) of upper fine grained layer.

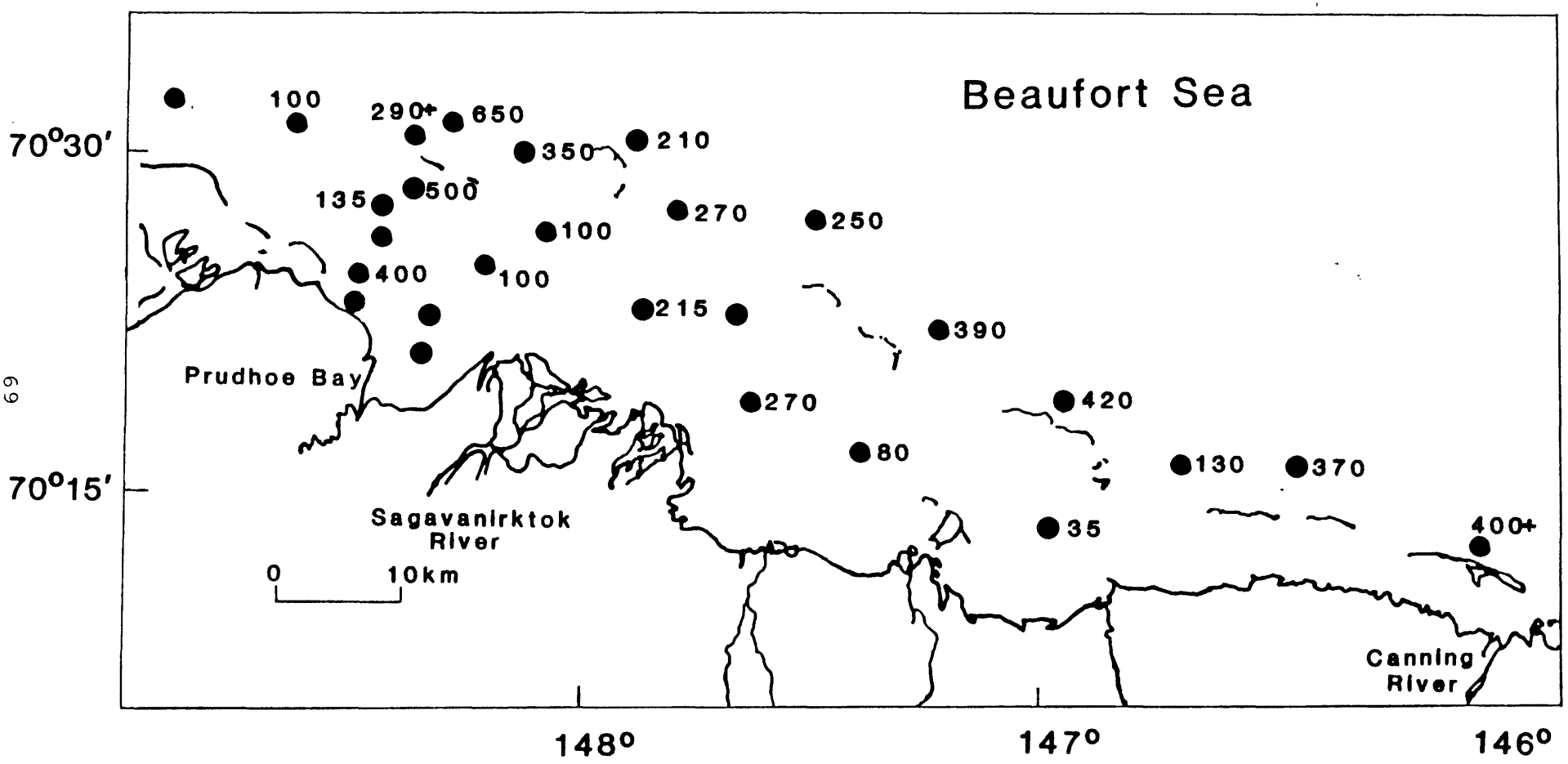

Figure 37. Estimated maximum past stress (kPa) at a subbottom depth of 4 m. See also Table 5.

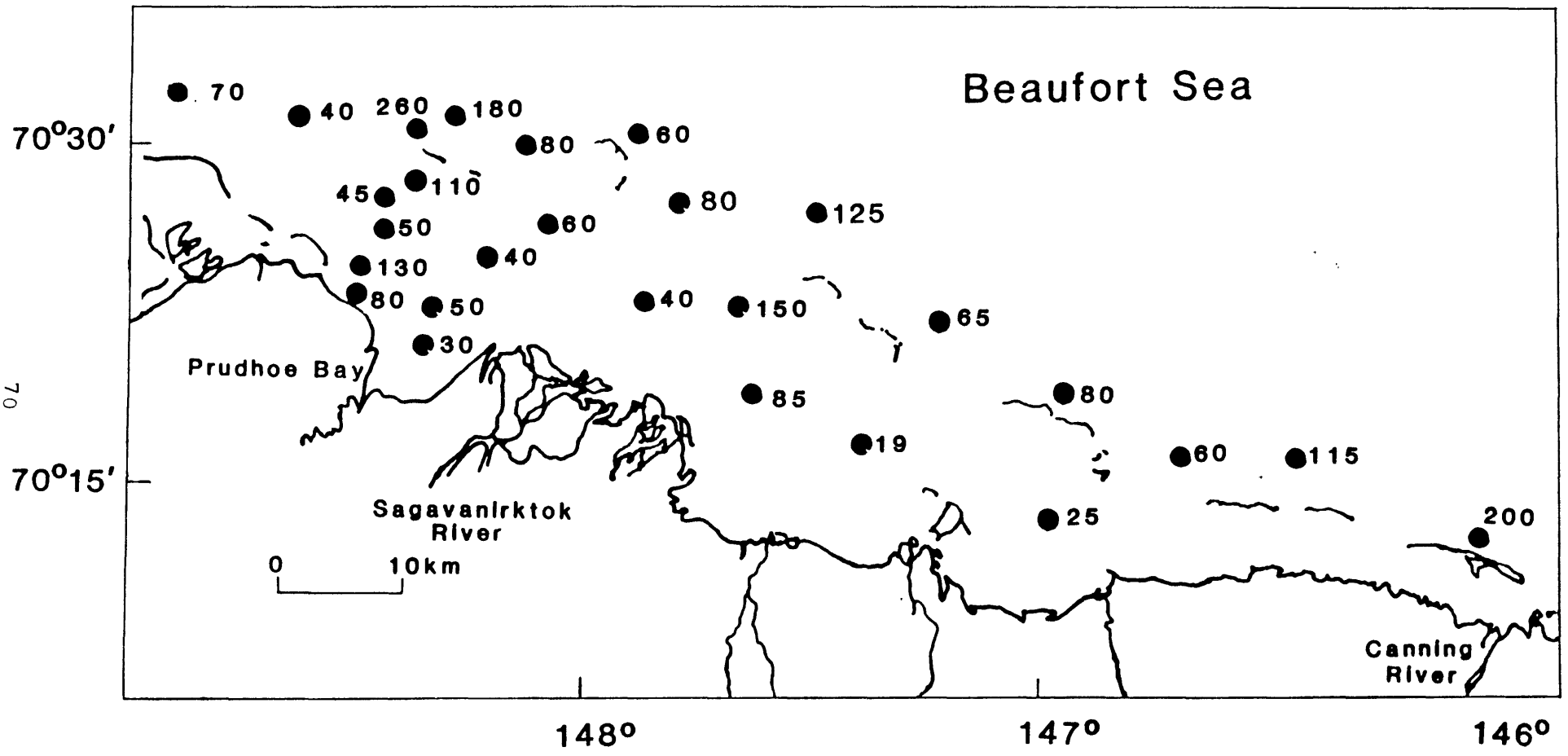

Figure 38. Estimated undrained shear strength (kPa) at a subbottom depth of 4 m. See also Table 5.

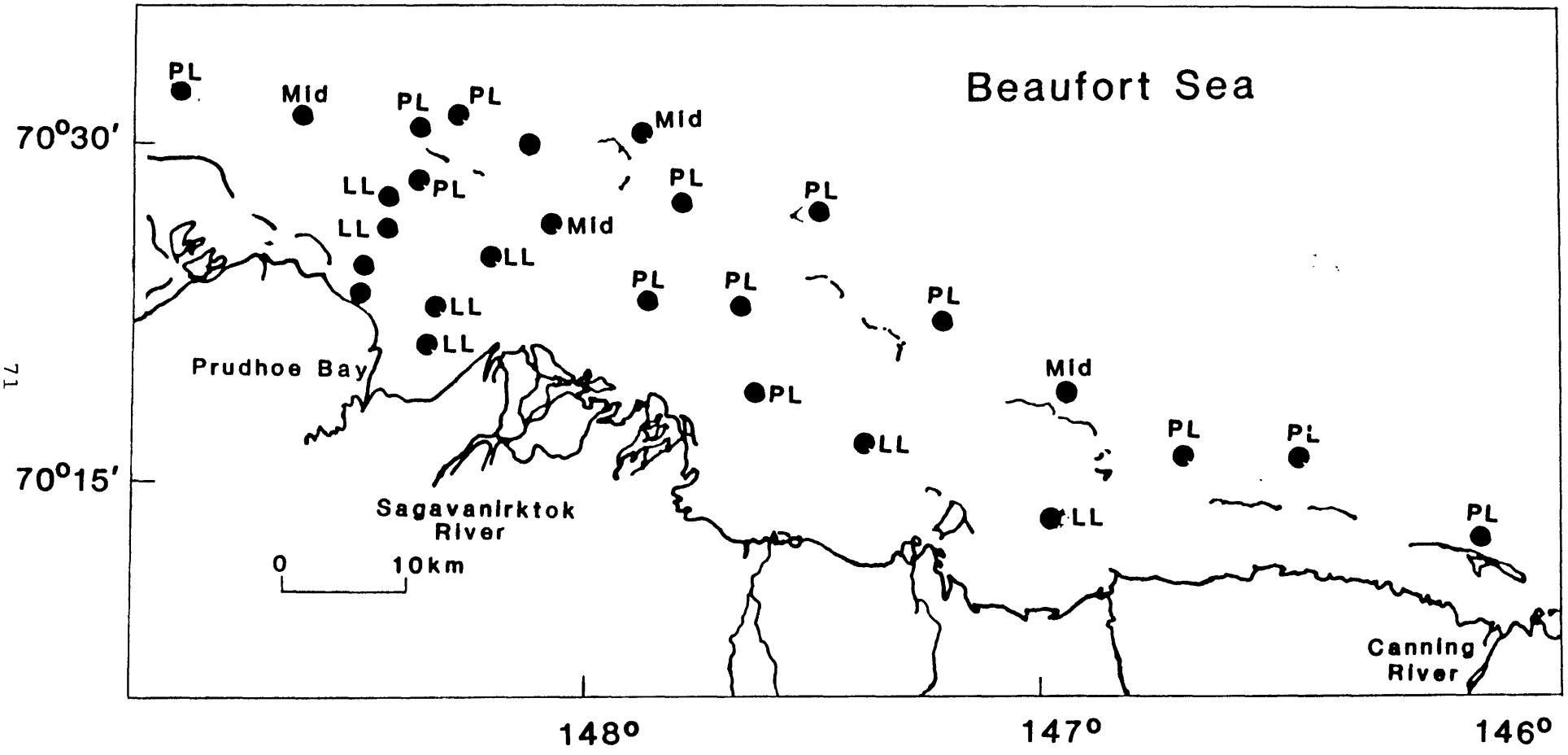

Figure 39. Qualitative estimate of whether the water content at 4 m typically lies near the liquid limit (LL), plastic limit (PL), or midway between (mid).

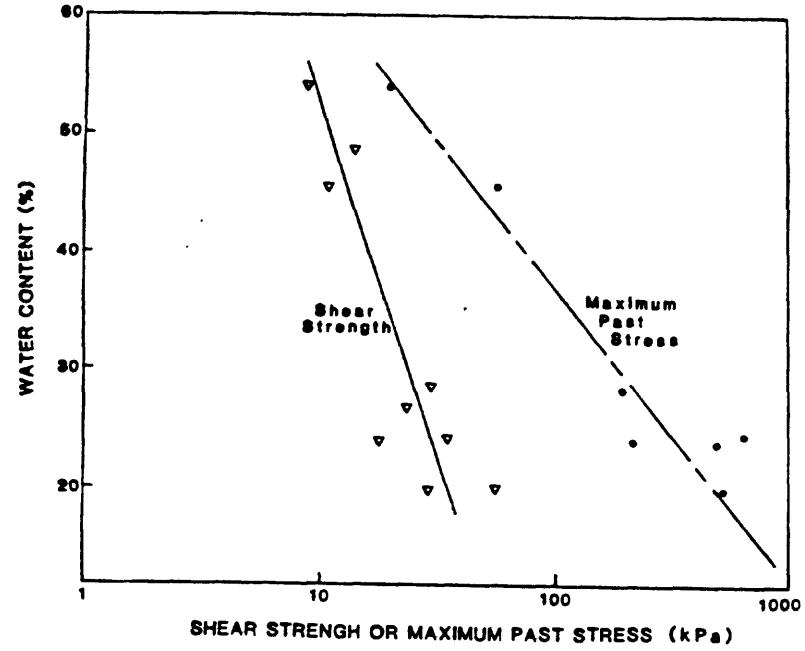

a) Block Samples

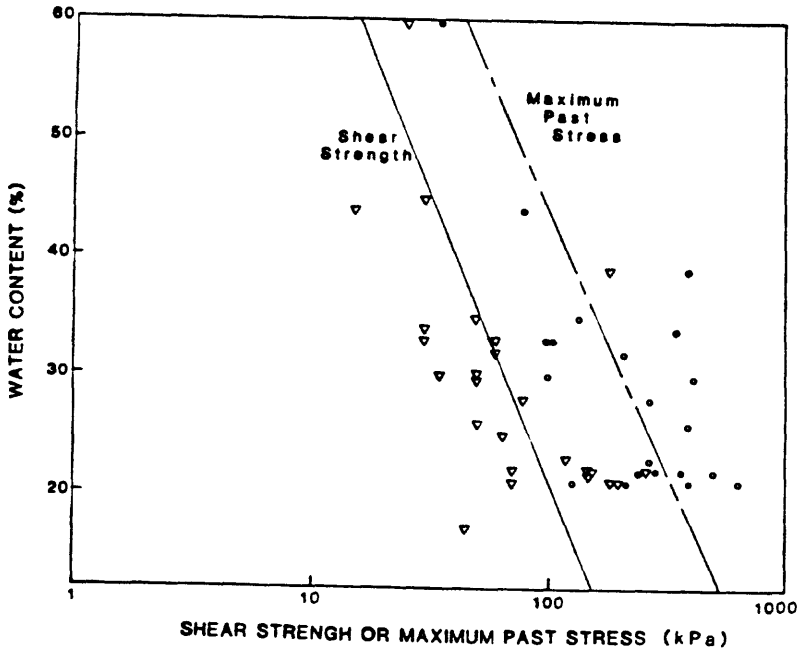

b) Samples from borings - estimate for 4m

Figure 40. Plots of shear strength and maximum past stress against water content. Regression lines for each set of data are shown. Triangles represent shear strength; circles represent maximum past stress. See also Table 2.

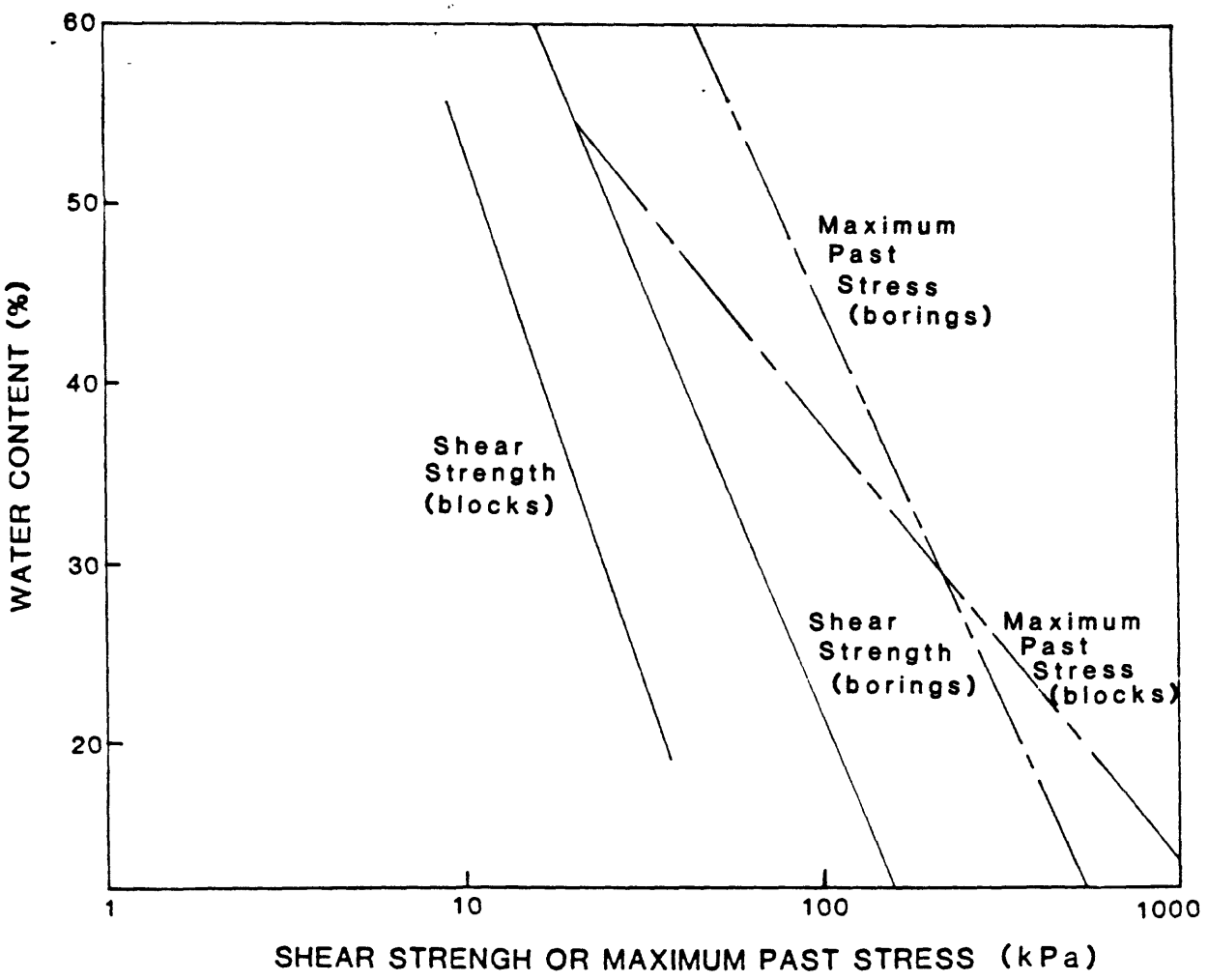

Figure 41. Comparison of the linear regressions of shear strength and maximum past stress against water content (both block samples and boring samples). Data points are shown in Figure 40.

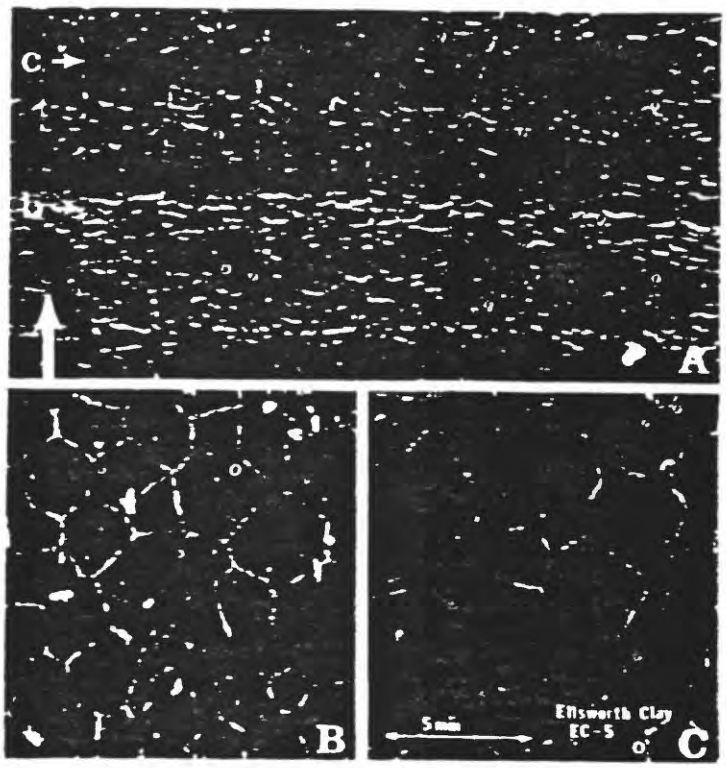

Figure 42. Frozen structure of a frozen clay (Chamberlain and Gow, 1979).

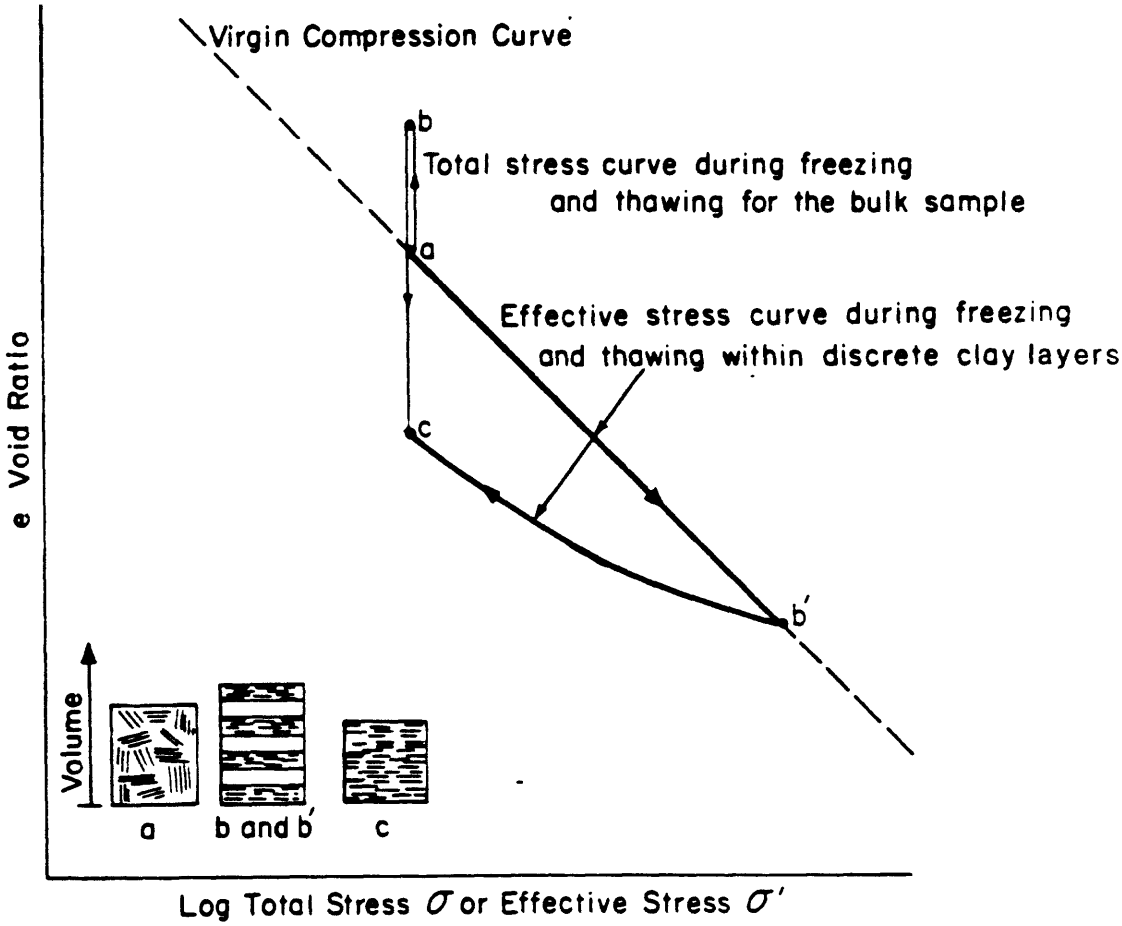

Figure 43. Theorized overconsolidation process by freezing and thawing (Chamberlain, 1978). Letters on the effective and total stress curves refer to the clay fabrics shown in the lower left corner.

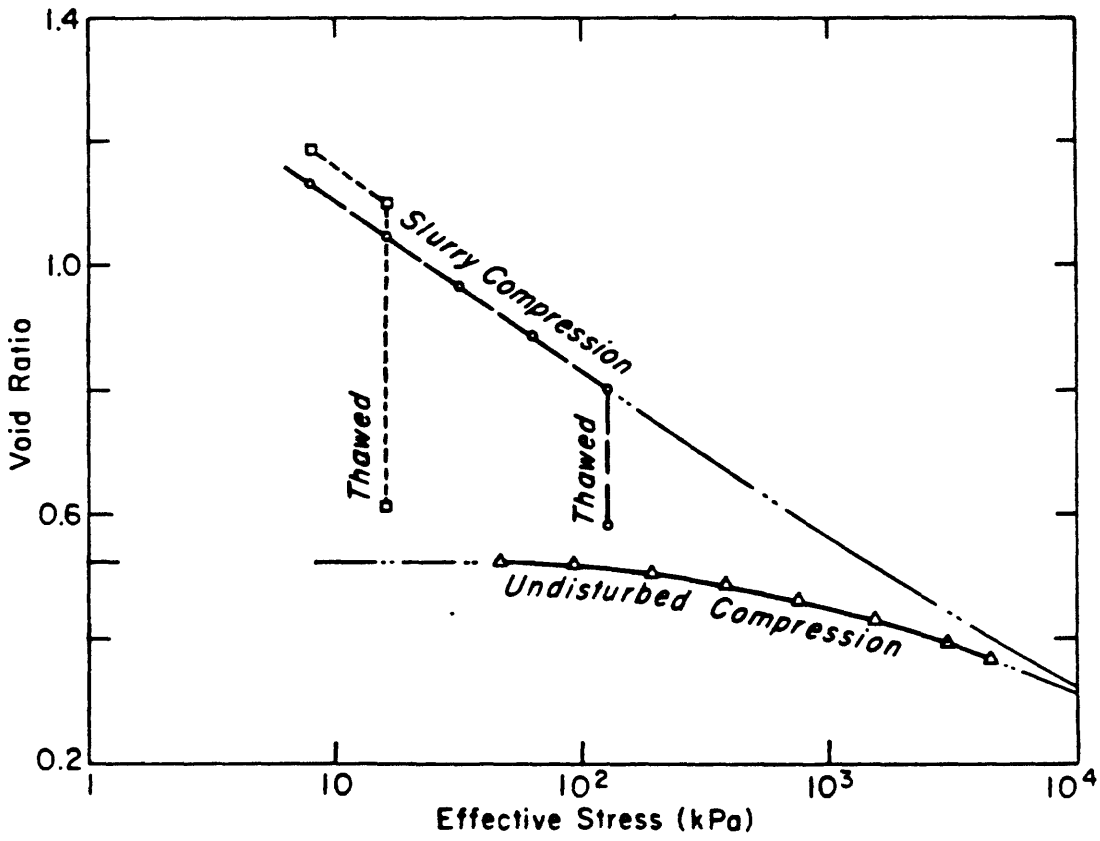

Figure 44. Comparison of free/thaw (squares and circles) and undisturbed consolidation (triangles) curves for a Beaufort Sea sediment sample (Chamberlain, 1978).

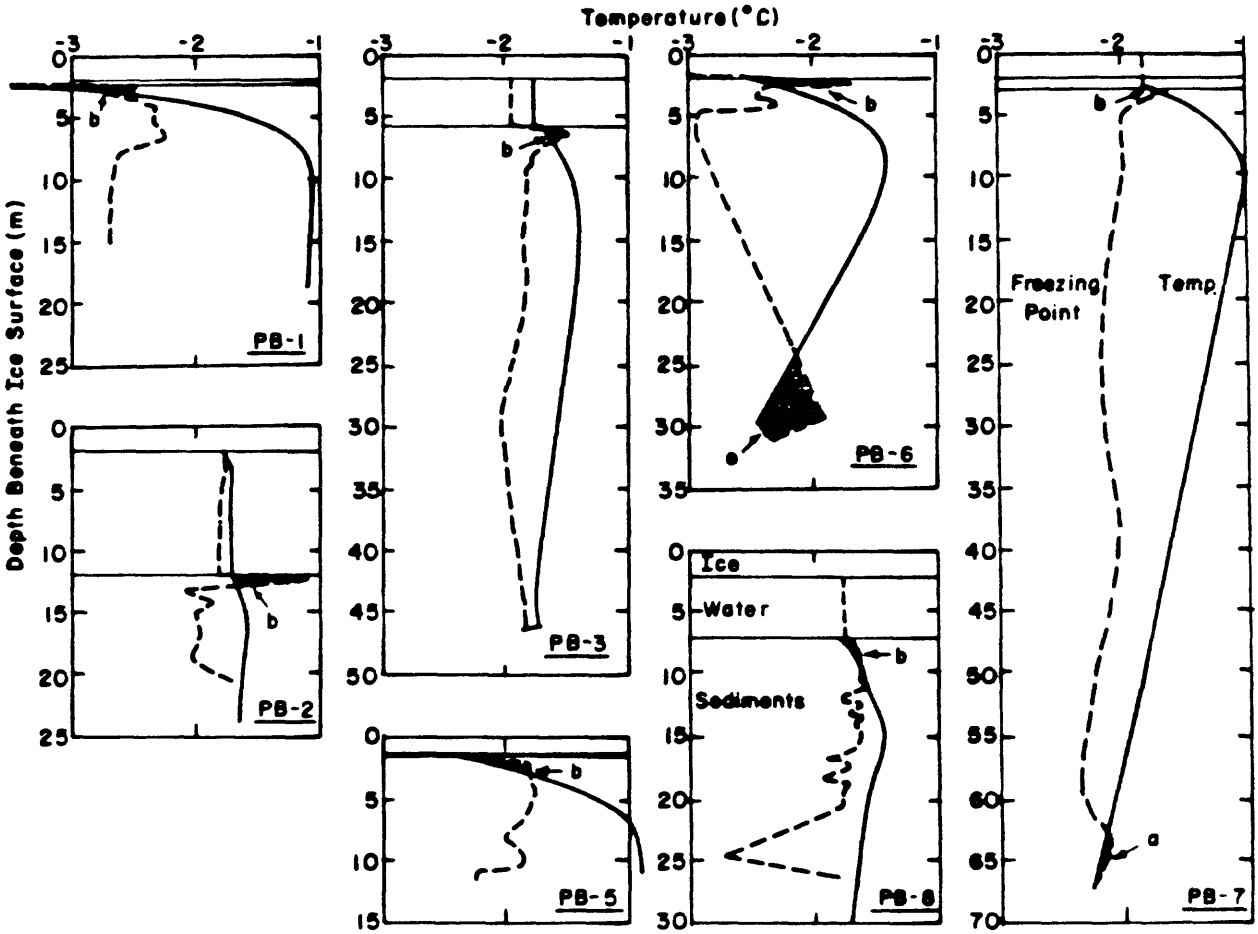

a. Temperature below freezing point of interstitial water (perennially frozen sediments?)

b. Temperature below freezing point of interstitial water (seasonally frozen sediments?)

Figure 45. Comparison of calculated freezing points and observed temperatures in seven Beaufort Sea boreholes (Sellman and Chamberlain, 1980).

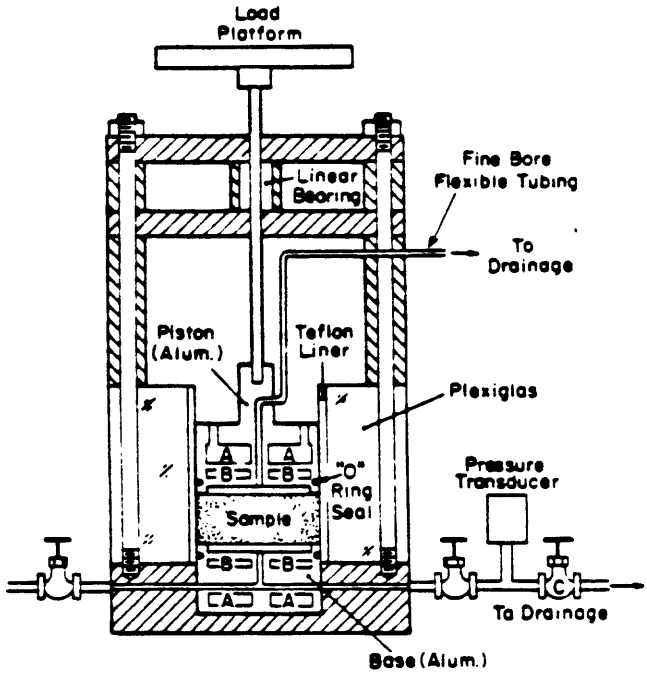

Figure 46. Laboratory freeze/thaw consolidation permeameter.

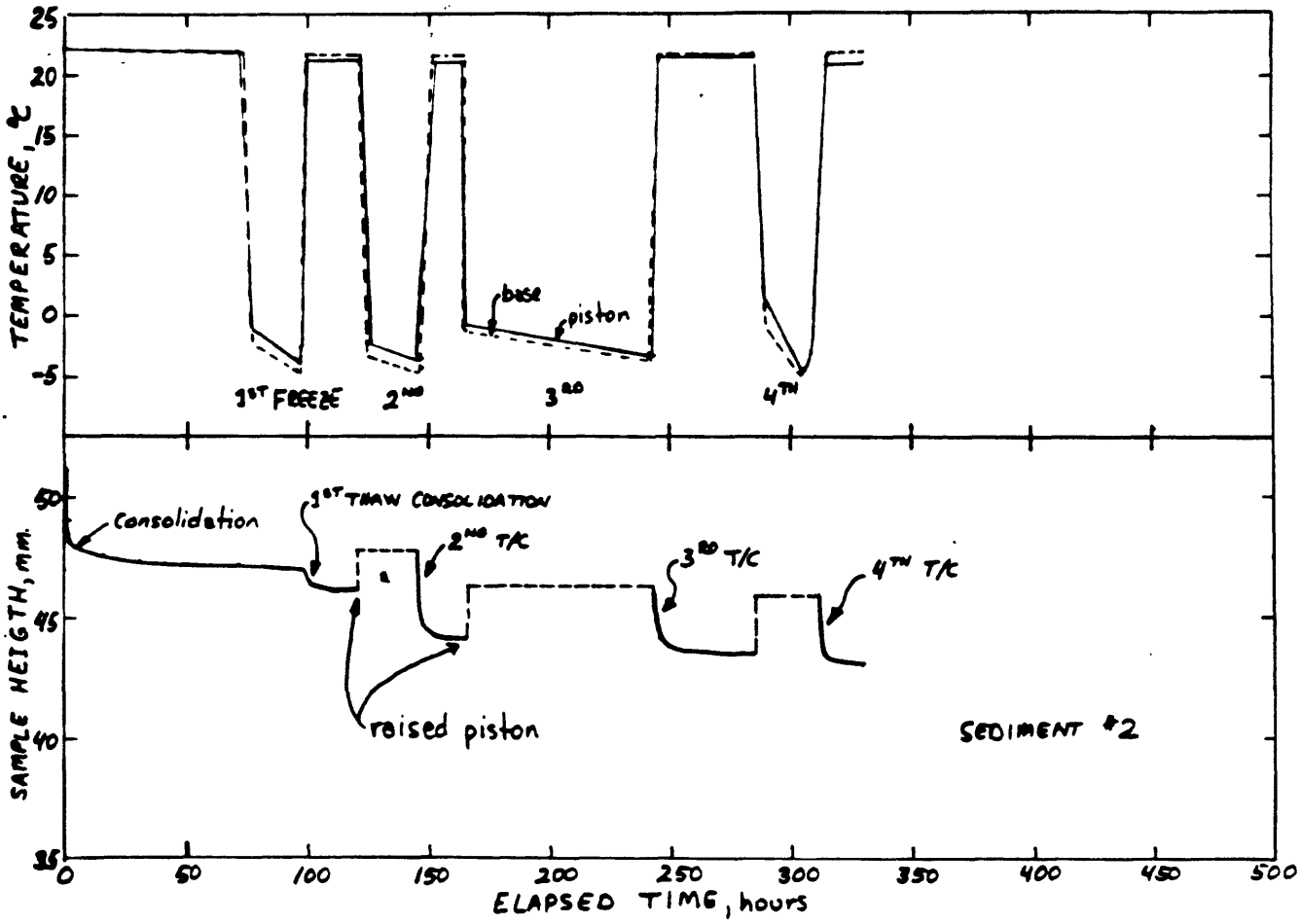

Figure 47. Freeze/thaw settlement of Sediment 2. Dashed line in lower figure derived from location of bottom of raised piston-not top of sediment.

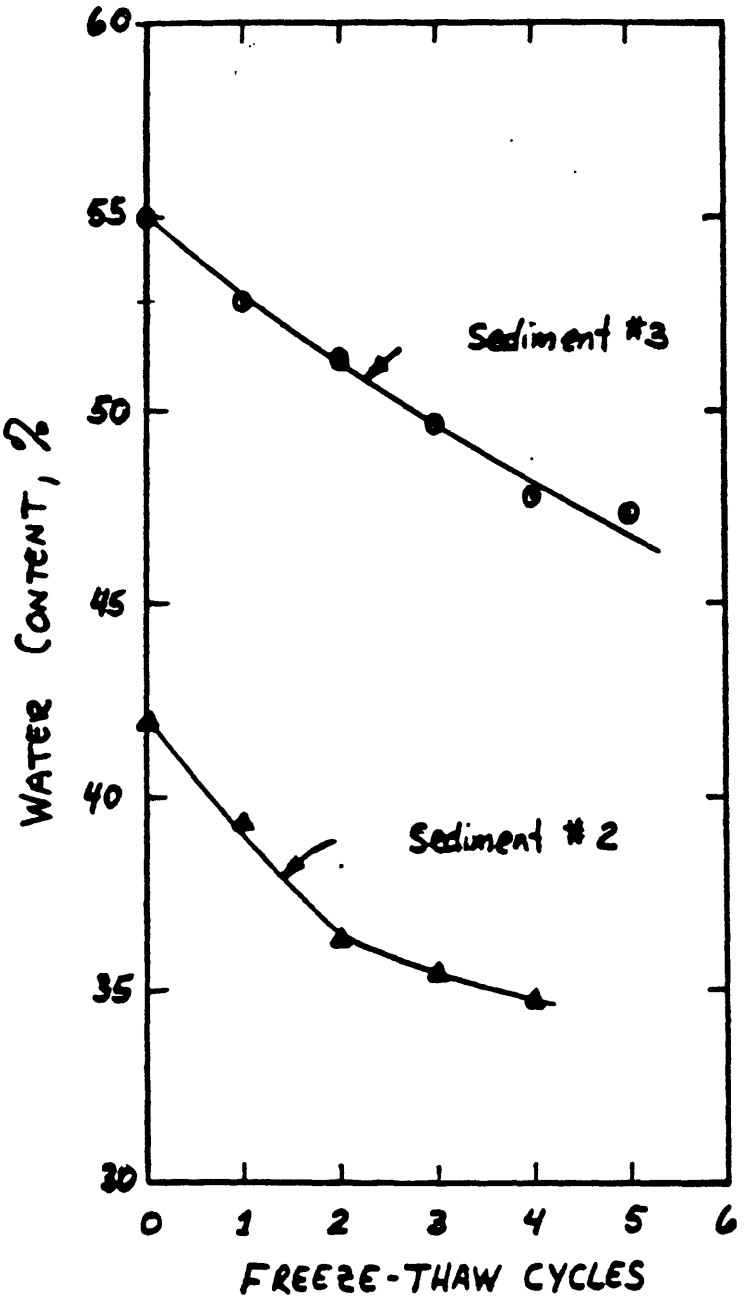

Figure 48. Reduction in water content of Sediments 2 and 3.

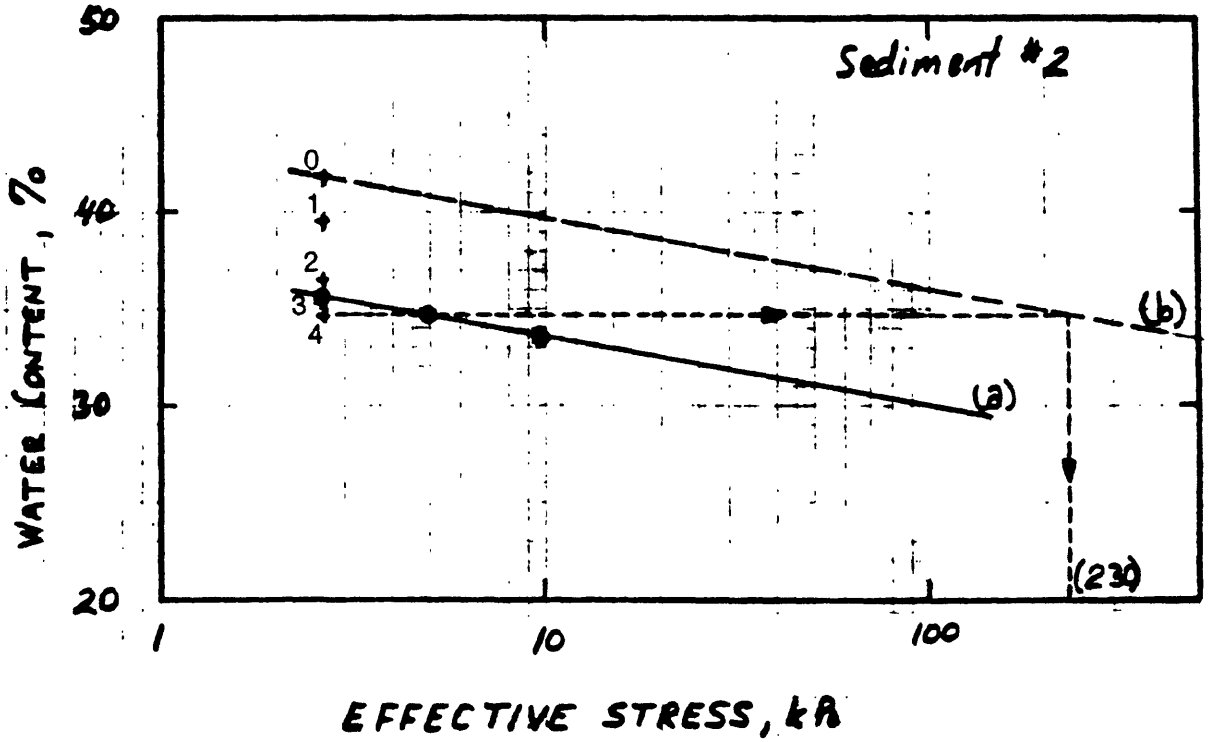

Figure 49. Comparison of freeze/thaw and normal consolidation curves for Sediment 2. Solid curve (a) shows the results of a conventional consolidation test with incremental loading. Dashed curve (b) is curve (a) transposed to pass through the starting conditions of a similar sample selected to be subjected to freeze/thaw cycles. The dashed curve represents the "normal" consolidation behavior of the freeze/thaw sample. Data points indicated by + signs are the endpoints of each freeze/thaw cycle. Values next to + signs define the freeze/thaw cycle number. A horizontal line through freeze/thaw cycle point 4 intersects the assumed "normal" consolidation curve at 230 kPa. This stress is the equivalent maximum past stress corresponding to 4 freeze/thaw cycles.

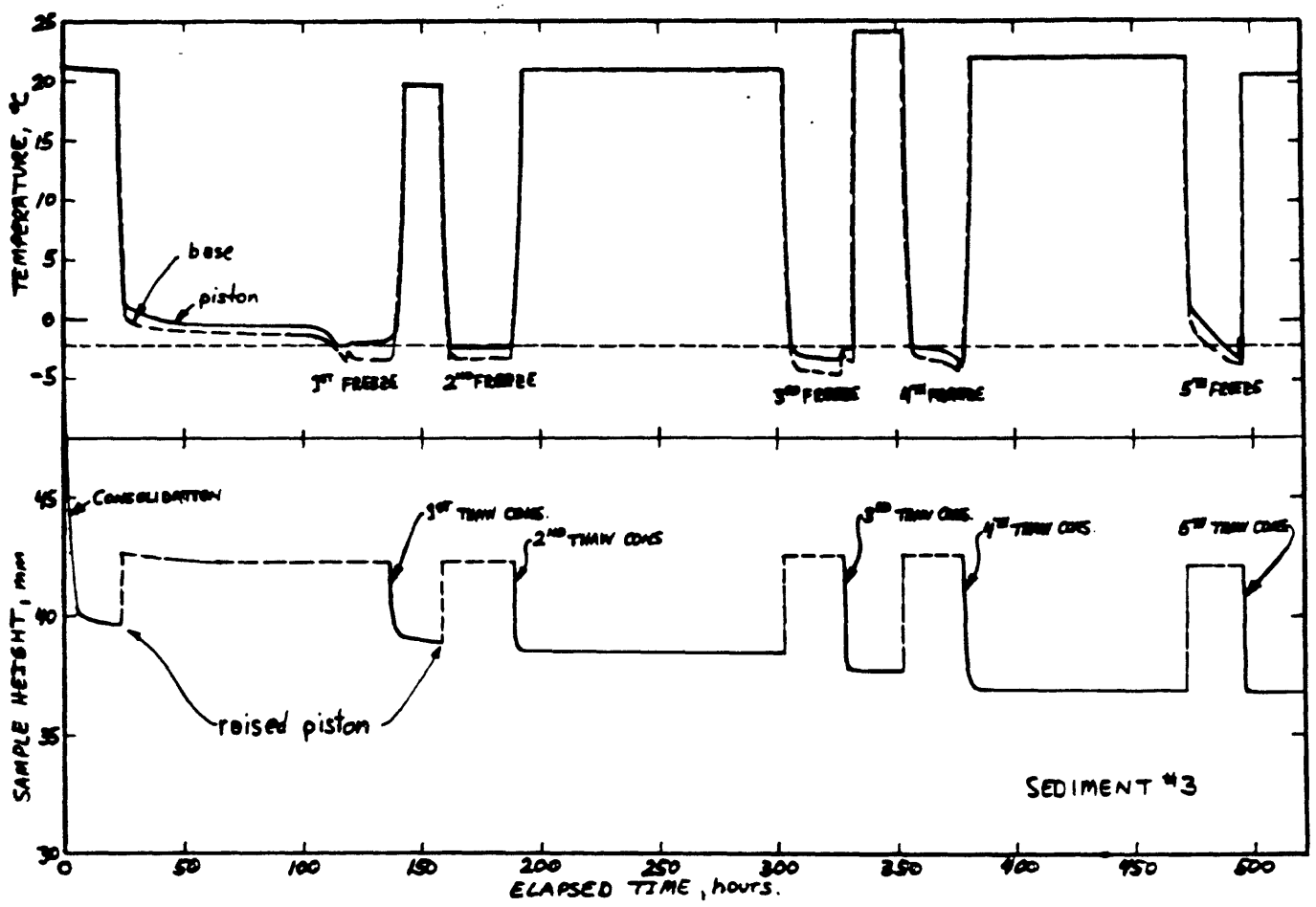

Figure 50. Freeze/thaw settlement of Sediment 3.

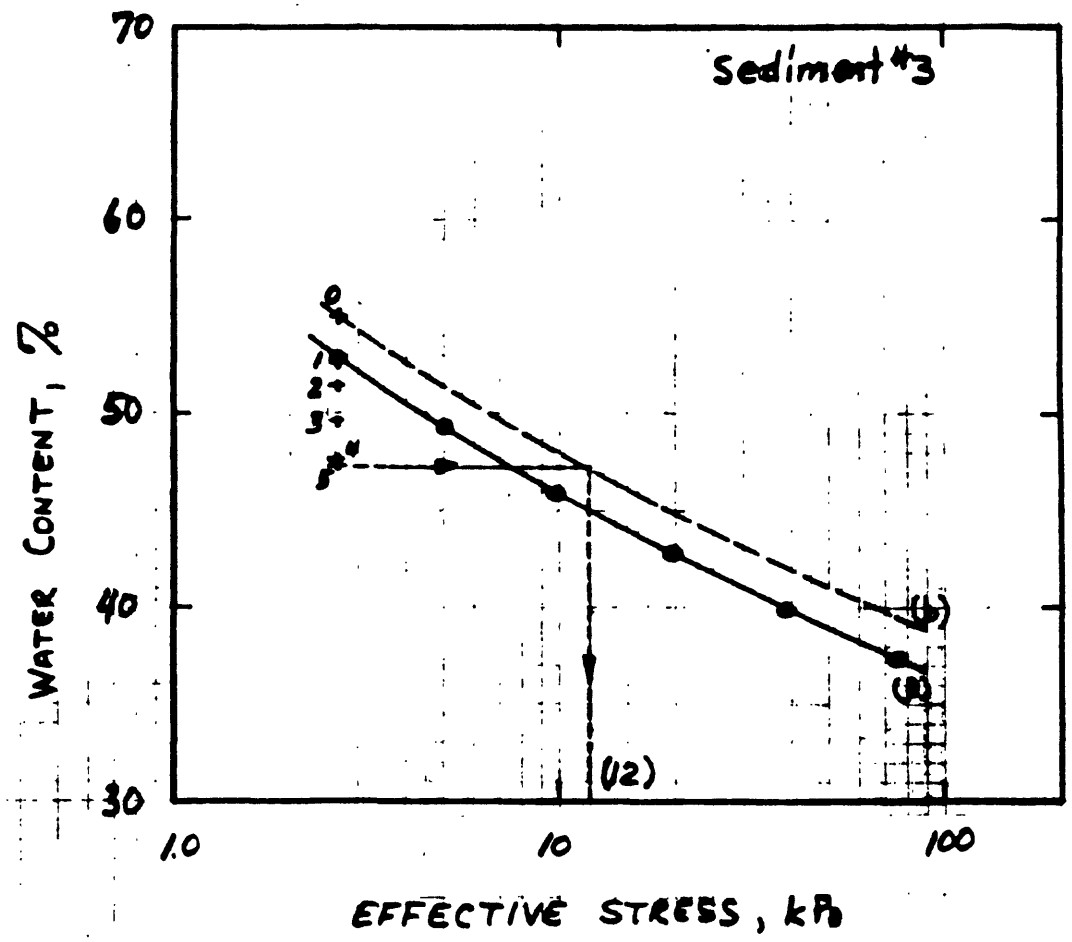

Figure 51. Comparison of freeze/thaw and normal consolidation curves for Sediment 3. Solid curve (a) shows the results of a conventional consolidation test with incremental loading. Dashed curve (b) is curve (a) transposed to pass through the starting conditions of a similar sample selected to be subjected to freeze/thaw cycles. The dashed curve represents the "normal" consolidation behavior of the freeze/thaw sample. Data points indicated by + signs are the endpoints of each freeze/thaw cycle. Values next to + signs define the freeze/thaw cycle number. A horizontal line through freeze/thaw cycle point 5 intersects the assumed "normal" consolidation curve at 12 kPa. This stress is the equivalent maximum past stress corresponding to 5 freeze/thaw cycles.